



Federal Reserve Bank of Cleveland Working Paper Series

Online Appendix

A Unified Framework to Estimate Macroeconomic Stars

Saeed Zaman

Working Paper No. 21-23R2

May 2024

Suggested citation: Zaman, Saeed. 2024. "A Unified Framework to Estimate Macroeconomic Stars." Working Paper No. 21-23R2. Federal Reserve Bank of Cleveland.
<https://doi.org/10.26509/frbc-wp-202123r2>.

Federal Reserve Bank of Cleveland Working Paper Series

ISSN: 2573-7953

Working papers of the Federal Reserve Bank of Cleveland are preliminary materials circulated to stimulate discussion and critical comment on research in progress. They may not have been subject to the formal editorial review accorded official Federal Reserve Bank of Cleveland publications.

See more working papers at: www.clevelandfed.org/research. Subscribe to email alerts to be notified when a new working paper is posted at: <https://www.clevelandfed.org/subscriptions>.

Online Appendix

A Unified Framework to Estimate Macroeconomic Stars

Saeed Zaman*

Federal Reserve Bank of Cleveland, USA

First draft: June 30, 2021

This version: May 28, 2024

I am extremely grateful to Joshua Chan, Todd Clark, Julia Darby, Ana Galvão, Benjamin Johannsen, Gary Koop (my advisor), Edward Knotek, Kurt Lunsford, Elmar Mertens, James Mitchell, Aubrey Poon, Ellis Tallman, Willem Van Zandweghe, Randal Verbrugge, and Ben Wong for valuable comments on the first draft. This research has benefited from discussions with Boragan Aruoba, Fabio Canova, Siddhartha Chib, Olivier Coibion, Sharada Davidson, Deepa Datta, Jesus Fernandez-Villaverde, Garo Garabedian, Paolo Gelain, Yuriy Gorodnichenko, James Hamilton, Ken Kuttner, Stuart McIntyre, Leonardo Melosi, Eric Sims, Simon van Norden, and Ping Wu. I also thank participants at the Society for Computational Economics 27th Conference 2021, NBER-NSF SBIES 2021, European Seminar on Bayesian Econometrics 2021, Computational and Financial Econometrics Conference 2021, 2022 North American Summer Meeting of the Econometric Society, 5th Vienna Workshop on High-Dimensional Time Series in Macroeconomics and Finance, Central Bank Macroeconomic Modeling Workshop 2022, Midwest Macroeconomics Spring 2022, Society for Nonlinear Dynamics and Econometrics 2022, ES-CoE Conference on Economic Measurement 2022, Society of Economic Measurement Conference 2022, American Economic Association-ASSA Annual Meeting 2024, and the Cleveland Fed Brown Bag. The latest and historical estimates of stars and other objects are available for download at <https://github.com/zamansaeed/macrostars>. The views expressed herein are those of the author and do not necessarily represent the views of the Federal Reserve Bank of Cleveland or the Federal Reserve System.

*Research department, Federal Reserve Bank of Cleveland, Ohio, USA; email: saeed.zaman@clev.frb.org

Contents

A0. Acknowledgments	4
A1. Related Literature	5
A2. Detailed Model Description	8
A3. Additional Base Model Variants	14
A4. Backcast: Survey R* from 1959-1982	16
A5. Bayesian Estimation Details	17
A5.a. Base model equations	17
A5.b. Prior elicitation	19
A5.c. MCMC algorithm	21
A5.d Marginal likelihood computation	55
A6. Posterior Parameter Estimates: Base Model	56
A7. Prior Sensitivity Analysis	57
A8. MCMC Convergence Diagnostics	61
A9. Prior and Posterior Distributions of the Parameters: Base Model	63
A10. Prior and Posterior Distributions: Deeper Dive	67
A11. Stars from Base Model: Zoomed In	70
A12. Base Model: Estimate of the Unemployment Gap	74
A13. W-star Decomposition: Base Model	75
A14. R-star Decomposition: Base Model and Variants	76
A15. Phillips curve slope (post-Pandemic): Base vs. External Studies	77
A16. Precision of Stars: Base Model vs. Variants of Base	78
A17. Base vs. External Models: Comparison of Stars and Output Gap	79
A19. Additional Real-Time Estimates of Stars	88
A20. Forecasting Results I: Base vs. Base Variants and Base vs. Benchmarks	91

A21. Forecasting Results II: Steady-State BVAR, Base Stars vs. Survey	95
A22. Assessment of Policy Stance: Base Model	98

A0. Acknowledgments

I am grateful to Joshua Chan, Todd Clark, Julia Darby, Ana Galvão, Benjamin Johannsen, Gary Koop (my advisor), Edward Knotek, Kurt Lunsford, Elmar Mertens, James Mitchell, Aubrey Poon, Ellis Tallman, Willem Van Zandweghe, Randal Verbrugge, and Ben Wong for valuable comments. This research has benefited from discussions with Boragan Aruoba, Fabio Canova, Siddhartha Chib, Sharada Davidson, Deepa Datta, Jesus Fernandez-Villaverde, Garo Garabedian, Paolo Gelain, Yuriy Gorodnichenko, James Hamilton, Ken Kuttner, Stuart McIntyre, Leonardo Melosi, Eric Sims, Simon van Norden, and Ping Wu. I also thank participants at the Society for Computational Economics 27th Conference 2021, NBER-NSF SBIES 2021, European Seminar on Bayesian Econometrics 2021, Computational and Financial Econometrics Conference 2021, 2022 North American Summer Meeting of the Econometric Society, 5th Vienna Workshop on High-Dimensional Time Series in Macroeconomics and Finance, Central Bank Macroeconomic Modeling Workshop 2022, Midwest Macroeconomics Spring 2022, Society for Nonlinear Dynamics and Econometrics 2022, ESCoE Conference on Economic Measurement 2022, Society of Economic Measurement Conference 2022, American Economic Association-ASSA Annual Meeting 2024, and the Cleveland Fed Brown Bag. The latest and historical estimates of stars and other objects are available for download at <https://github.com/zamansaeed/macrostars>. The views expressed herein are those of the author and do not necessarily represent the views of the Federal Reserve Bank of Cleveland or the Federal Reserve System.

A1. Related Literature

In recent years, advances in computational power and numerical methods have enabled researchers to estimate stars using UC models with more indicators and/or an expanded structure. For example, Johannsen and Mertens (2021)[JM], Pescatori and Turunen (2016), Del Negro et al. (2017), Brand and Mazelis (2019), Bauer and Rudebusch (2020), González-Astudillo and Laforte (2020), among others, have examined the roles of additional determinants in explaining r-star. With the exception of Pescatori and Turunen (2016), all others have highlighted the usefulness of exploiting information from both short-term and long-term interest rates in the identification of r-star. JM, González-Astudillo and Laforte (2020), and Brand and Mazelis (2019) document the usefulness of adding the TR equation to identify r-star. The latter two do not entertain SV, which JM has found to be empirically important. Pescatori and Turunen (2016) enrich the underlying structure to estimate r-star. In particular, to extract a reliable estimate of the output gap, they bring additional information from the Congressional Budget Office’s (CBO) estimate of the output gap by treating it as a noisy measure of the “true” output gap. None of these studies feature time-varying parameters, and only JM allow for SV, but their model size is significantly smaller than mine.

Chan et al. (2016) [henceforth CKP] illustrate the value of modeling u-star and pi-star as bounded random walk processes in a bivariate Phillips curve. The use of an unrestricted RW process has empirically been shown to work well, but CKP show that modeling u-star as a bounded RW process is even better. They use bounds because, by construction, the unemployment rate is a bounded variable, which implies that the long-run equilibrium in the labor market would restrict the movements in u-star within a bounded interval. CKP argue that economic forces that govern the movements in u-star are slow-moving and those forces would not cause the unemployment rate to fall to levels close to zero or to levels that are higher than the previous peaks caused by recessions. More recently, using fixed-parameter UC models, Crump et al. (2019) estimate u-star by combining a range of labor market indicators across demographic groups and survey expectations of inflation, and Hasenzagl et al. (2022) jointly estimate pi-star, u-star, gdp-star (and output gap). Feunou and Fontaine (2023) develop a UC model with SV (but not time-varying parameters) to examine the secular decline in bond yields by jointly modeling r-star, g-star, and pi-star.

Coibion et al. (2018) examine estimates of potential output from a variety of model-based (including small-scale UC models) and external sources, including the CBO and survey forecasts, and based on a range of shock measures, find that (in real-time) the estimates of potential output are unable to distinguish between transitory and permanent shocks effectively. Put differently, they find that their estimates of potential output respond “gradually and similarly” to both supply shocks and demand shocks that drive cyclical fluctuations in real GDP. This, they say, is unfortunate since, by definition, potential output (and g-star) should only adjust in response to permanent shocks. In the conclusion of their paper, they postulate whether a framework that jointly estimates the dynamics of potential output with other relevant stars (as theory implies)

would better distinguish between permanent and transitory components and hence lead to more credible estimates of potential output. Unfortunately, my UC model estimates of g-star suggest otherwise.

Morley and Wong (2020) and Chan (2019) propose an alternative modeling framework based on VARs to estimate the long-run equilibrium values. The advantage of the VAR-based framework is the ability to handle larger amounts of information conveniently and flexibly compared to UC models. On the other hand, the advantage of UC modeling, as emphasized by CKP, is the availability of the direct estimates of stars, which, in the case presented here, proves quite convenient to allow for direct modeling of the relationships between various stars.

Several papers have documented the essential role of long-run survey (and institutional) forecasts in helping refine the econometric estimation of model parameters, including the latent components (e.g., pi-star: Kozicki and Tinsley (2012); Mertens (2016); Mertens and Nason (2020); CCK; gdp-star: Pescatori and Turunen (2016)). Specifically, Mertens and Nason (2020), CCK, Mertens (2016), and Kozicki and Tinsley (2012), in using different methodologies (in combining survey data with model forecasts) to estimate the trend in US inflation, show that long-run survey forecasts of inflation deliver crucial additional information (beyond the recent inflation history) in refining trend estimates and improving model fit. In a similar vein, Pescatori and Turunen (2016) document the usefulness of the CBO's projection of the potential output gap in improving their model's output gap precision. It is this particular literature that motivates me to consider long-run survey forecasts in the proposed large-scale econometric model.

The advantage of survey (and institutional) forecasts stems from the fact that they could be viewed as hybrid forecasts, i.e., a combination of judgment and forecasts derived from various modeling approaches. The fact that human judgment enters into survey expectations is an important reason for their success. As discussed by Kozicki and Tinsley (2012) and others, the good forecasting properties are partly because survey participants have at their disposal a wide range of indicators, including central bank communications, and information about changes in the tax laws, etc. The patterns gleaned from this large information set can help shape opinions, including any perceived structural change, which can immediately influence expectations about the long run.

In recent years, a large body of research has shown the importance of allowing for stochastic volatility in macroeconomic models (e.g., Fernald and Wang (2016), Koop and Korobilis (2010), and Carriero et al. (2019)). Since the work of Stock and Watson (2007), when modeling price inflation dynamics using small-scale UC models, SV is commonly featured (e.g., Chan (2013), Chan et al. (2013), CKP, Mertens (2016), Chan (2017), Tallman and Zaman (2017), CCK). Few papers on estimating the output gap using small-scale UC models have highlighted the usefulness of SV (e.g., Mertens (2014), Berger et al. (2016), Antolin-Diaz et al. (2017)), and similarly for the unemployment gap (e.g., Mertens (2014), Stella and Stock (2015), Tallman and Zaman (2017)). Motivated by these studies and that of JM (SV in the nominal interest rate gap), in this paper, in addition to allowing for SV in the output gap, the unemployment gap,

price inflation gap, and interest-rate gap, I include SV in the equations defining the nominal wage inflation gap and productivity gap. The results strongly indicate the importance of SV in all of the gap measures.

A growing body of research has found the importance of jointly modeling output and unemployment to obtain credible and economically meaningful estimates of output gap (e.g., Sinclair (2009), Fleischman and Roberts (2011), Berger et al. (2016), Grant and Chan (2017a), Barbarino et al. (2020), Morley and Wong (2020)). Most researchers working with UC models assume a common cyclical component between the output and the unemployment gaps. However, Berger et al. (2016) provide empirical evidence that cyclical unemployment displays more persistence than the output gap, suggesting that modeling two separate cycles linked to each other via the Okun's law relationship may provide more credible estimates of the output gap. And they find that evidence of time-variation in the parameter linking the two separate cycles is weak. Indeed, I confirm this using supplementary exercises: in my Base model specification, which entertains two separate cycles (cyclical unemployment and the output gap), the data support a time-invariant parameter describing the Okun's law relationship. In contrast, a specification with a common cyclical component favored a time-varying Okun's law relationship (adding support to Knotek II (2007)). Because the Bayesian model comparison metric preferred the specification of separate cycles linked via a time-invariant parameter over the common cycle with a time-varying parameter, in my baseline setup I go with the former.

In recent years, a growing number of papers have documented evidence of the importance of allowing time-variation in macroeconomic relationships, especially when models are estimated with data spanning a long sample. For instance, Galí and van Rens (2021), using split sample estimation, illustrate empirically the significant weakening in the correlation between labor productivity and employment, especially post-1984. They find that the relationship has become countercyclical in the past three decades when using employment as the cyclical indicator. But it is slightly procyclical when using output as the cyclical indicator. There is ample empirical evidence on the instability of the Phillips curve in the US and euro area data lending support of a time-varying price Phillips curve (e.g., Stella and Stock (2015); CKP; Del Negro et al. (2020), Bańbura and Bobeica (2020), among many others). Similarly, for the wage Phillips curve, see Knotek II and Zaman (2014), Peneva and Rudd (2017), and Galí and Gambetti (2019), among others). Knotek II and Zaman (2014) and Peneva and Rudd (2017) also document a significant weakening in the empirical link between price inflation and nominal wage inflation since the 1980s. Evidence in support of time-variation in price inflation persistence has been shown in Cogley and Sbordone (2008), Cogley et al. (2010), Chan et al. (2013), CKP, CCK, among others. These studies motivate the inclusion of time-variation in parameters defining the price Phillips curve, wage Phillips curve, pass-through between prices and wages, inflation persistence, and cyclicity of labor productivity in my baseline model.

A2. Detailed Model Description

Unemployment block

To estimate u-star, I combine information from prices (including nominal wages and survey expectations) with the estimated Phillips curve relationship between price inflation and the aggregate unemployment rate.

Specifically, following CKP, I posit that the observed unemployment rate is decomposed into a (bounded) RW trend component (u-star) and a stationary cyclical component.

$$U_t = U_t^* + U_t^c \quad (1)$$

The cyclical component is modeled as an AR(2) process.¹ Because I am also modeling the output gap, I depart from CKP by augmenting the AR2 unemployment gap with the output gap (denoted *ogap*) as an additional explanatory variable.

$$U_t - U_t^* = \rho_1^u(U_{t-1} - U_{t-1}^*) + \rho_2^u(U_{t-2} - U_{t-2}^*) + \phi^u \text{ogap}_t + \varepsilon_t^u, \quad \varepsilon_t^u \sim N(0, e^{h_t^u}) \quad (2)$$

where, $\rho_1^u + \rho_2^u < 1$, $\rho_2^u - \rho_1^u < 1$, and $|\rho_2^u| < 1$.

The variance of the error term ε_t^u is allowed to change over time.² Similarly, as shown later, I add information from the unemployment gap when modeling the output gap. The joint modeling of both the output gap and the unemployment gap gives an indication about the strength of the relationship between the two cyclical components, popularly known as Okun's law. The estimate, $\frac{1-\rho_1^u-\rho_2^u}{\phi^u}$, could be interpreted as the Okun's law coefficient.³

U-star is modeled as a bounded RW, where the bounds' values are fixed at 3.5% (lower bound) and 7.5% (upper bound).⁴

$$U_t^* = U_{t-1}^* + \varepsilon_t^{u*}, \quad \varepsilon_t^{u*} \sim TN(a_u - U_{t-1}^*, b_u - U_{t-1}^*; 0, \sigma_{u*}^2) \quad (3)$$

where the notation $TN(a, b; \mu, \sigma^2)$ refers to normal distribution with mean μ and variance σ^2 but truncated in the interval (a, b) .

Output block

To feasibly estimate both the potential output (i.e., gdp^*) and the growth rate in potential output (i.e., g^*), I follow the commonly adopted approach, which decomposes the level of

¹The use of a parsimonious (time-invariant) AR2 process to identify the cyclical component of the unemployment rate is a commonly used assumption, e.g., Lee and Nelson (2007), CKP, and Galí and Gambetti (2019). CKP explore the empirical importance of allowing for time variation in the parameters of an AR2 process, and find that the data prefer the time-invariant AR2 process, hence validating the widely used assumption of a simple AR2 process.

²Mertens (2014), Stella and Stock (2015), and Berger et al. (2016) provide evidence in support of SV in the cyclical component of the unemployment rate.

³As shown in Berger et al. (2016), in a specification that entertains two separate cycles (cyclical unemployment and the output gap), the data support a time-invariant parameter describing the Okun's law relationship. In contrast, a specification with a common cyclical component favored a time-varying Okun's law relationship (adding support to Knotek II, 2007). I found similar evidence, i.e., the Bayesian model comparison assessment slightly preferred the approach of two separate cycles with a time-invariant Okun's law compared to a common cycle with a time-varying Okun's law parameter.

⁴These values are informed by estimating the CKP model over the estimation sample, and are close to values reported in CKP based on their estimation sample. As a further check, most estimates of the u-star reported in the commonly cited literature fall within the bounds used in this paper.

aggregate output into the level of potential output and a cyclical component (output gap). This simple decomposition has a long tradition going back to Clark (1987).

$$gdp_t = gdp_t^* + ogap_t \quad (4)$$

where $gdp \equiv \log(GDP)$ and gdp^* refers to potential output, which is unobserved.

Following Grant and Chan (2017b), gdp^* is assumed to follow a second-order Markov process.⁵

$$gdp_t^* = 2gdp_{t-1}^* - gdp_{t-2}^* + \varepsilon_t^{gdp^*}, \quad \varepsilon_t^{gdp^*} \sim N(0, \sigma_{gdp^*}^2) \quad (5)$$

Which can be re-written as

$$\Delta gdp_t^* = \Delta gdp_{t-1}^* + \varepsilon_t^{gdp^*}$$

Assuming, $g_t^* \equiv \Delta gdp_t^*$, where Δ is the first difference operator, then,

$$g_t^* = g_{t-1}^* + \varepsilon_t^{gdp^*} \quad (6)$$

The cyclical component, $ogap$, is assumed to be a stationary AR(2) process augmented with additional explanatory variables: the real interest rate gap and the unemployment gap,

$$ogap_t = \rho_1^g(ogap_{t-1}) + \rho_2^g(ogap_{t-2}) + a^r(r_t^L - r_t^* - tp_t^*) + \lambda^g(U_t - U_t^*) + \varepsilon_t^{ogap} \quad (7)$$

where, $\varepsilon_t^{ogap} \sim N(0, e^{h_t^g})$, $\rho_1^g + \rho_2^g < 1$, $\rho_2^g - \rho_1^g < 1$, and $|\rho_2^g| < 1$

Equation (14) could be interpreted as defining an IS-curve (as in LW and subsequent papers modeling r -star) that allows feedback (via parameter a^r) from the real interest rate gap to the output gap (i.e., the real interest rate gap responds to economic slack). The long-term real interest rate, r^L , is constructed as the difference between the nominal yield on a 10-year Treasury bond and the 10-year inflation expectations (i.e., the PTR series for PCE inflation).⁶ The long-run value of term premium, tp^* is treated as an exogenous variable and is constructed as the average of the differential between the long-term interest rate (i.e., 10-year Treasury bond) and the federal funds rate, similar to Johannsen and Mertens (2021).

To improve the econometric estimation of the output gap, I enrich the IS equation by bringing in information from the unemployment gap (from the unemployment block) as an explanatory variable.⁷ This latter addition is motivated by the approach taken in a long list of papers (e.g., Morley and Wong, 2020; Grant and Chan, 2017a; Fleischman and Roberts, 2011; Sinclair, 2009) that demonstrate the usefulness of the unemployment rate in improving

⁵This modeling assumption implies that all permanent shocks to output are attributed as shocks to g^* . Results are similar had I instead modeled gdp^* as a random walk with a time-varying drift term, where the time-varying drift term (interpreted as g^*) is assumed to follow a random walk process (to allow for a stochastic g^*). However, the metric of Bayesian model comparison slightly favors the assumption of second-order Markov process for gdp^* , which is consistent with the findings of Grant and Chan (2017b). An advantage of modeling g^* as a second-order Markov process compared to an RW with time-varying drift is that it requires estimating a single shock parameter ($\sigma_{gdp^*}^2$), as opposed to two for the latter (one for the shock to gdp^* and the other for the shock to the time-varying drift, aka g^*). It is worth noting that the assumption of gdp^* following a second-order Markov process is consistent with the Beveridge-Nelson trend described in section 2.1 (see Proietti, 1995).

⁶I also experimented with an alternative specification, in which the interest rate gap is constructed as the difference between the short-term federal funds rate and the first lag of four-quarter trailing PCE inflation, similar in spirit to LW. Based on model fit, this specification was slightly inferior. It is worth noting that had the longer history of long-term inflation expectations data been available at the time of the writing, LW would have constructed the interest rate gap using the long-term interest rate (see page 1064 in LW).

⁷Model fit, the precision metric for u -star and the output gap, and the plausibility of the estimates of output gap strongly support the joint modeling of the output gap and the unemployment gap.

the econometric estimation of the output gap.⁸

Productivity block

Productivity growth is a notoriously volatile series and is subject to extreme revisions from one vintage to another. So, distinguishing highly persistent fluctuations from truly permanent changes is a difficult job for professionals and models alike (see, e.g., Jacobs and van Norden (2016)). Accordingly, I adopt a parsimonious structure for the productivity block relative to other blocks of the model.

The productivity gap, which is defined as (nonfarm) labor productivity growth⁹ (quarterly annualized) less p-star, is modeled as a function of a one-quarter lag in the productivity gap and the contemporaneous cyclical unemployment gap.

$$P_t - P_t^* = \rho^p(P_{t-1} - P_{t-1}^*) + \lambda_t^p(U_t - U_t^*) + \varepsilon_t^p, \quad \varepsilon_t^p \sim N(0, e^{h_t^p}) \quad (8)$$

where, $|\rho^p| < 1$

The variance of the error term ε_t^p is allowed to change over time. The inclusion of the cyclical unemployment gap helps tease out movements in productivity associated with the business cycle.¹⁰

Galí and van Rens (2021) find weakening in the correlation between labor productivity and the cyclical indicator, which motivates time variation in the coefficient λ^p .

$$\lambda_t^p = \lambda_{t-1}^p + \varepsilon_t^{\lambda^p}, \quad \varepsilon_t^{\lambda^p} \sim N(0, \sigma_{\lambda^p}^2) \quad (9)$$

Allowing for the time variation in the cyclical relationship and the error term allows the model to better discriminate the cyclical movements and idiosyncratic movements in productivity from those associated with shifts in p-star.

P-star is modeled as a driftless random walk component, and the variance of the shocks to this component is assumed to be constant.

$$P_t^* = P_{t-1}^* + \varepsilon_t^{p*}, \quad \varepsilon_t^{p*} \sim N(0, \sigma_{p^*}^2) \quad (10)$$

⁸I note that innovations $\varepsilon_{gdp^*}^2$ and ε_{ogap}^2 are uncorrelated. In an important contribution, Morley et al. (2003), who assume a deterministic g-star, show that this assumption matters for estimating potential output. However, Grant and Chan (2017a) show that in their specification, once a stochastic g-star is allowed for, the correlation between $\varepsilon_{gdp^*}^2$ and ε_{ogap}^2 goes to zero. They also show that the model without correlation performs comparably to the model with correlated innovations based on Bayesian model comparison. Accordingly, to keep estimation tractable, I assume uncorrelated innovations.

⁹As discussed in Kahn and Rich (2007), the focus outside of the farm sector is primarily on avoiding short-term transitory volatility in the farm sector that is heavily driven by weather and other nontechnological factors.

¹⁰The growth in labor productivity (and more generally aggregate productivity) has been shown to be procyclical to some degree (e.g., Roberts, 2001); it typically increases sharply at the onset of recoveries and falls during recessions. However, empirical evidence on the strength and the direction of the cyclical relationship is mixed. This mixed evidence stems from the use of different estimation samples and or cyclical indicators (employment-based or output-based). For instance, Galí and van Rens (2021), using split sample estimation, illustrate empirically the significant weakening in the correlation between labor productivity and employment, especially post-1984. They find that the relationship has become countercyclical in the past three decades when using employment as the cyclical indicator. But it is slightly procyclical when using output as the cyclical indicator. In an alternative specification I replace cyclical unemployment with the output gap and obtain similar results. Galí and van Rens (2021) using a structural macro model attribute the weakening procyclicality of labor productivity in part to the increased flexibility of the US labor market post-1984, which has enabled firms to make adjustments at the extensive margin quickly and easily in response to shocks.

Economic theory posits that the long-run nominal wage inflation equals the sum of long-run productivity growth and long-run price inflation. As discussed later in the wage inflation block, this theoretical restriction defines the law of motion for w-star and constitutes an additional channel influencing the dynamics of p-star.

Price inflation block

I use price inflation as measured by the personal consumption expenditures (PCE) price index, the inflation measure that the Federal Reserve targets. The formulation for the price inflation block closely follows CKP and CCK, combining elements from both of these papers. Specifically, as in CKP, the stationary component, the inflation gap (defined as the deviation of inflation from pi-star), is modeled as a function of the one-quarter lagged inflation gap, unemployment gap, and an error term, whose variance is allowed to vary over time.

The coefficient, ρ^π on the lagged inflation gap, which captures persistence in inflation dynamics, is allowed to vary over time.¹¹

$$\pi_t - \pi_t^* = \rho_t^\pi (\pi_{t-1} - \pi_{t-1}^*) + \lambda_t^\pi (U_t - U_t^*) + \varepsilon_t^\pi, \quad \varepsilon_t^\pi \sim N(0, e^{h_t^\pi}) \quad (11)$$

$$\rho_t^\pi = \rho_{t-1}^\pi + \varepsilon_t^{\rho^\pi}, \quad \varepsilon_t^{\rho^\pi} \sim TN(0 - \rho_{t-1}^\pi, 1 - \rho_{t-1}^\pi; 0, \sigma_{\rho^\pi}^2) \quad (12)$$

The innovations to the AR(1) coefficient, ρ^π are truncated so that $0 < \rho_t^\pi < 1$, ensuring that the inflation gap (in equation 20) is stationary at each point in time t .

$$\lambda_t^\pi = \lambda_{t-1}^\pi + \varepsilon_t^{\lambda^\pi}, \quad \varepsilon_t^{\lambda^\pi} \sim TN(-1 - \lambda_{t-1}^\pi, 0 - \lambda_{t-1}^\pi; 0, \sigma_{\lambda^\pi}^2) \quad (13)$$

λ^π is the slope of the price Phillips curve and is constrained in the interval $(-1, 0)$.

There is ample evidence in support of a time-varying price Phillips curve (e.g., Stella and Stock, 2015; CKP), hence the choice of allowing for time-variation in the parameter λ^π .

Pi-star is modeled as a driftless random walk component, and the variance of the shocks to this component is assumed to be constant (as in CKP).¹²

$$\pi_t^* = \pi_{t-1}^* + \varepsilon_t^{\pi^*}, \quad \varepsilon_t^{\pi^*} \sim N(0, \sigma_{\pi^*}^2) \quad (14)$$

Lastly, as I show next (see equation 26), pi-star is restricted to satisfy the long-run restriction informed by theory.

Wage inflation block

The long-run equilibrium level of nominal wage inflation (w-star) is the nominal wage growth rate consistent with its fundamentals – p-star and pi-star. As noted earlier, in the long run, economic theory posits that the nominal wage inflation equals the sum of the long-run growth rate of labor productivity and the long-run level of price inflation. I impose this relationship to

¹¹Chan et al. (2013), CKP, and CCK have found strong empirical support for the time-variation in the coefficient of inflation gap. My results reinforce the empirical importance of allowing for time-variation in this coefficient.

¹²Allowing SV in the inflation gap component and not in the trend component is not without precedent. Besides CKP, Chan (2013) is a recent paper modeling SV only in the measurement equation (i.e., cyclical/transitory component). Berger et al. (2016) find support for SV in the inflation gap component but weak evidence for SV in the trend component. My preliminary results indicate similar findings: that adding SV to the pi-star equation neither helps nor hurts the model fit.

define w-star.

$$W_t^* = \pi_t^* + P_t^* + Wedge_t + \varepsilon_t^{w*}, \quad \varepsilon_t^{w*} \sim N(0, \sigma_{w*}^2) \quad (15)$$

$$Wedge_t = Wedge_{t-1} + \varepsilon_t^{wlr}, \quad \varepsilon_t^{wlr} \sim N(0, \sigma_{wlr}^2) \quad (16)$$

Because all three, nominal wage inflation, price inflation, and labor productivity growth data come from different sources and so differ in scope and coverage, a time-varying wedge, which is assumed to evolve as an RW process, is added to the above equation. The above equation implies that W^* adjusted for the wedge is approximately equal to sum of $\pi_t^* + P_t^*$.

Equation (28) relates the nominal wage inflation gap – defined as the difference between the nominal wage inflation and w-star – to its one-quarter lagged gap, the cyclical unemployment gap, and the price inflation gap. The variance of the error term, ε_t^w , is allowed to vary over time.

$$W_t - W_t^* = \rho_t^w (W_{t-1} - W_{t-1}^*) + \lambda_t^w (U_t - U_t^*) + \kappa_t^w (\pi_t - \pi_t^*) + \varepsilon_t^w, \quad \varepsilon_t^w \sim N(0, e^{h_t^w}) \quad (17)$$

The findings in Knotek II and Zaman (2014) motivate the inclusion of a one-quarter lagged nominal wage inflation gap, with time variation in the parameter ρ^w , which quantifies the persistence in wage inflation dynamics.

$$\rho_t^w = \rho_{t-1}^w + \varepsilon_t^{\rho w}, \quad \varepsilon_t^{\rho w} \sim TN(0 - \rho_{t-1}^w, 1 - \rho_{t-1}^w; 0, \sigma_{\rho w}^2) \quad (18)$$

The innovations to the AR(1) coefficient, ρ^w , are truncated so that $0 < \rho_t^w < 1$, to ensure that the wage gap (in equation 28) is stationary at each point in time t .

The parameter λ^w in equation (28) measures the strength of the cyclical relationship between the nominal wage gap and labor market slack (aka the slope of the wage Phillips curve). Many studies, both theoretical (e.g., Galí, 2011) and empirical (e.g., Peneva and Rudd, 2017; Galí and Gambetti, 2019), have demonstrated the instability of the wage Phillips curve, motivating the need for time-variation in the parameter λ^w .

$$\lambda_t^w = \lambda_{t-1}^w + \varepsilon_t^{\lambda w}, \quad \varepsilon_t^{\lambda w} \sim TN(-1 - \lambda_{t-1}^w, 0 - \lambda_{t-1}^w; 0, \sigma_{\lambda w}^2) \quad (19)$$

λ^w is constrained in the interval $(-1, 0)$.

Previous research has documented a significant weakening in the empirical link between price inflation and nominal wage inflation since the 1980s (e.g., Peneva and Rudd, 2017; Knotek II and Zaman, 2014), motivating time variation in the parameter κ^w . The expression $\frac{\kappa_t^w}{1 - \rho_t^w}$ could be interpreted as an estimate of the short-run pass-through from price inflation to wage inflation.

$$\kappa_t^w = \kappa_{t-1}^w + \varepsilon_t^{\kappa w}, \quad \varepsilon_t^{\kappa w} \sim N(0, \sigma_{\kappa w}^2) \quad (20)$$

Interest rate block

I close the model with the interest rate block characterizing the interest rate dynamics and the law of motion for r-star (the long-run equilibrium real short-term interest rate).

The first equation of the block brings information from the nominal short-term interest rate via a Taylor-type rule (TR) to aid in identifying r-star. Specifically, this equation characterizes the dynamics of the short-term nominal interest rate gap, where the gap is the difference between the nominal short-term interest rate i , and the long-run level of the nominal neutral rate of interest, i-star. (i-star = pi-star + r-star). To capture both conventional and unconventional

monetary policy effects when the (observed) nominal federal funds rate is constrained at the effective lower bound (ELB), I use the shadow interest rate measure of Wu and Xia (2016).¹³

Equation (32) relates the nominal interest rate gap (based on the shadow federal funds rate) to its one-period lag interest rate gap, the current quarter inflation gap (i.e., the deviation of inflation from pi-star), and the unemployment rate gap (i.e., the deviation of the unemployment rate from u-star). This equation roughly characterizes the monetary policy reaction function as defined by Taylor (2001).¹⁴ There is a broad consensus that policy adjustments outside of cyclical turning points are made very gradually. Hence, this motivates the inclusion of the lagged interest rate gap term.

$$i_t - \pi_t^* - r_t^* = \rho^i(i_{t-1} - \pi_{t-1}^* - r_{t-1}^*) + \lambda^i(U_t - U_t^*) + \kappa^i(\pi_t - \pi_t^*) + \varepsilon_t^i, \quad \varepsilon_t^i \sim N(0, e^{h_t^i}) \quad (21)$$

where ρ^i is truncated so that $0 < \rho^i < 1$.

Chan and Eisenstat (2018b,a) and JM document strong empirical support for constant parameters in the Taylor rule equation while allowing for stochastic volatility in the errors. Hence, I allow for SV in the interest rate equation.

The second equation motivated by LW heeds the economic theory suggesting the role of various real factors in influencing movements in r-star. These factors include long-run output growth (and long-run productivity growth), trend labor force growth (reflecting shifts in demographics and net migration), taxation structure, government expenditure shifts, and shifts in liquidity preferences. Accordingly, equation (33) expresses r-star as a linear function of g-star and a “catch-all” component D, which follows a random walk process similar to LW (and many other papers).¹⁵

$$r_t^* = \zeta g_t^* + D_t. \quad (22)$$

$$D_t = D_{t-1} + \varepsilon_t^d, \quad \varepsilon_t^d \sim N(0, \sigma_d^2) \quad (23)$$

¹³The nominal *shadow* federal funds rate is identical to the nominal federal funds rate when the effective lower bound is not binding. The estimates from Wu and Xia (2016) are publicly available and regularly updated. Treating the shadow rate as the measure of the short-term nominal rate in place of the federal funds rate is a common practise in the literature. I examine the robustness of my results to the shadow federal funds rate obtained from Jones et al. (2021), which is based on an estimated structural macroeconomic model. I also test the robustness of replacing the shadow federal funds rate with the actual federal funds rate, i.e., the federal funds rate of zero over the ZLB period. I find that the estimates of stars (including r-star) are fairly identical across different measures of the shadow interest rate (and the federal funds rate). The inclusion of the SV in the TR equation is the key reason for this robust finding, as differences in the shadow rates’ estimates are reflected in the SV estimates, leaving r-star and other stars unaffected.

¹⁴It is worth emphasizing that I denote this equation as a “Taylor-type rule” and not an exact Taylor-rule because in the equation, pi-star refers to the estimate of trend inflation, which may or may not be equal to central bank’s long-run inflation goal.

¹⁵The RW assumption for D is an appropriate one, given that the focus is the long-run r-star that should, in principle, be influenced over time by permanent shifts in aggregate supply and demand (Laubach and Williams, 2016). Researchers have also explored an AR process for component D, which would be consistent if the interest is in medium-term r-star (see Lewis and Vazquez-Grande, 2019), as this would allow r-star to be influenced by the transitory shocks to aggregate demand (via the AR process) and permanent shocks to aggregate supply (via the RW process for g-star). In studies focused on the long-run notion of r-star, such as LW, Laubach and Williams (2016), Clark and Kozicki (2005), and Kiley (2020), specification based on the RW assumption has been shown to be empirically favored by the data compared to AR assumption.

A3. Additional Base Model Variants

To assess the usefulness of various empirical features incorporated in the Base model, additional model specifications are estimated.

Base-W*RW. To assess the empirical support of the theoretical restriction defined by equation 26 (which defines w-star as the sum of pi-star and p-star), I estimate a variant of the baseline model that replaces equation 26 with a random walk assumption for w-star as defined by equation 20b.

$$W_t^* = W_{t-1}^* + \varepsilon_t^{w*}, \quad \varepsilon_t^{w*} \sim N(0, \sigma_{w*}^2) \quad (20b)$$

Base-R*RW. To assess the empirical support for the theoretical restriction defined by equation 33 (the link between g-star and r-star), I estimate a model specification that replaces equation 33 with a random walk assumption for r-star as defined by equation 27b.

$$r_t^* = r_{t-1}^* + \varepsilon_t^{r*}, \quad \varepsilon_t^{r*} \sim N(0, \sigma_{r*}^2) \quad (27b)$$

Base-NoLinkStars. To assess the empirical support of both theoretical restrictions defined by equations 26 and 33, I estimate a variant of the baseline model that combines *Base-W*RW* and *Base-R*RW*.

Base-G*LinkP*. To assess the empirical support for the theoretical link between g-star and p-star, I estimate a model specification that replaces equations 12 and 13 with equations 10b, 11b, and 11c.

$$gdp_t^* = gdp_{t-1}^* + g_t^* + \varepsilon_t^{gdp*}, \quad \varepsilon_t^{gdp*} \sim N(0, \sigma_{gdp*}^2) \quad (10b)$$

$$g_t^* = \psi p_t^* + g_t^{other*} \quad (11b)$$

$$g_t^{other*} = g_{t-1}^{other*} + \varepsilon_t^{gother*}, \quad \varepsilon_t^{gother*} \sim N(0, \sigma_{gother*}^2) \quad (11c)$$

Equation 11b expresses g-star as a linear function of p-star and a “catch-all” component g^{other*} , which captures the influence on g-star of all factors other than p-star. The parameter ψ captures the strength of the relationship between trend growth and trend productivity.

Base-NoBoundU*. To assess the empirical support for imposing bounds on the U*, I estimate a model specification without the bounds on the U* process defined in eq. 8.

Base-PT-Wages-to-Prices. To assess the empirical support of allowing for pass-through from wages to prices, I estimate a model specification that replaces eq. 20 with eq. 16b, which adds the nominal wage inflation gap as an explanatory variable in the equation describing the price inflation gap. The parameter γ^π captures the strength of the relationship between the two cyclical inflation measures. The expression $\frac{\gamma^\pi}{1-\rho^\pi}$ can be interpreted as the pass-through from cyclical wage inflation to cyclical price inflation.¹⁶

$$\pi_t - \pi_t^* = \rho_t^\pi (\pi_{t-1} - \pi_{t-1}^*) + \lambda_t^\pi (U_t - U_t^*) + \gamma^\pi (W_t - W_t^*) + \varepsilon_t^\pi, \quad \varepsilon_t^\pi \sim N(0, e^{h_t^\pi}) \quad (16b)$$

Base-NoPT. The Base model allows for pass-through from prices to wages. I assess the empirical support of this restriction by estimating a model specification that replaces eq. 28

¹⁶I explored the possibility of allowing for time-variation in γ^π but the estimation ran into difficulties hence I resort to a time-invariant γ^π .

with eq. 22b, which removes the price inflation gap in the equation describing nominal wage inflation gap.

$$W_t - W_t^* = \rho_t^w (W_{t-1} - W_{t-1}^*) + \lambda_t^w (U_t - U_t^*) + \varepsilon_t^w, \quad \varepsilon_t^w \sim N(0, e^{h_t^w}) \quad (22b)$$

Base-NoR*Survey. To assess the marginal value of survey expectations of r^* in fitting the interest rate data, I estimate a Base model specification that excludes survey expectations of r^* , but keeps survey data for other variables. I find that doing so worsens the model fit to the interest rate data and lowers the precision of the r -star estimate.

Base-NoR*Surv-NoTRule. To assess the marginal value of the Taylor-type rule equation to the model, I estimate a model specification from the previous step (Base-NoR*Survey) but without the TR equation. I compare this model's fit to the interest rate with that of Base-NoR*Survey. I find that removing the TR equation worsens the model fit to the interest rate data and significantly lowers the precision of the r -star estimate.

A4. R*: Backcast Survey R* from 1959-1982

The survey estimates of g-star, u-star, and pi-star are direct reads from the survey. In contrast, the r-star survey estimate is not a direct estimate. Instead, it is inferred from the Blue Chip survey long-run estimates of the GDP deflator and short-term interest rates (3-month Treasury bill) using the long-run Fisher equation, specifically, the long-run forecast of 3-month Treasury bills less the long-run forecast of the GDP deflator. To this differential, I add +0.3 to reflect the average differential between the federal funds rate and the 3-month Treasury bill (r-star refers to the long-run equilibrium federal funds rate).

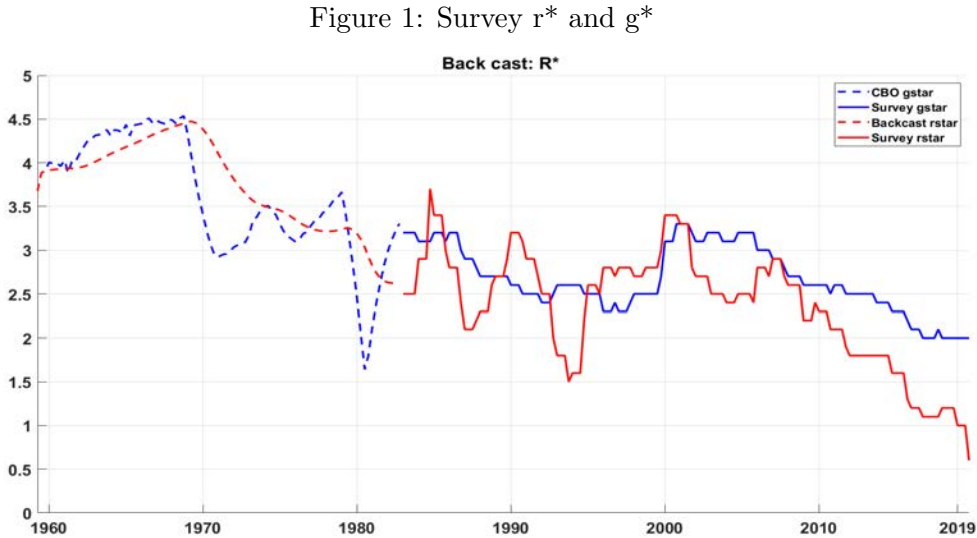
Survey projections are not available before 1983Q1. To fill in estimates for the survey variables between 1959Q4 and 1982Q4, I use the CBO long-run projections in the case of real GDP growth and the unemployment rate. In the case of inflation, I use the PTR series available from the Federal Reserve Board’s website; this series is used in many studies employing long-run expectations of inflation (e.g., CCK, Tallman and Zaman, 2020). We do not have a readily available historical source for long-run forecasts for interest rates (and r-star). So I backcast a particular time series of implied r-star using the CBO’s long-run projections of g-star. Specifically, I first fit a simple linear regression model over the post-1983 period that regresses survey r-star on a constant, its lags (2 lags), and a one-period lag “gap,” defined as the difference between survey r-star and survey g-star. We use the estimated model and the CBO’s long-run projections of g-star over the sample 1959Q4 through 1982Q4 to backcast the implied survey r-star estimates. (When backcasting, the initial values of r-star for 1959Q2 and 1959Q3 are assumed to be identical to the CBO’s g-star)

$$r_t^{*,Surv} = c + \beta_1 gap_{t-1}^{r^*,g^*,Surv} + \beta_2 r_{t-1}^{*,Surv} + \beta_3 r_{t-2}^{*,Surv} + \varepsilon_t^{*,Surv}, \quad \varepsilon_t^{*,Surv} \sim N(0, \sigma_{\varepsilon_t^{*,Surv}}^2) \quad (24)$$

$$\text{where, } gap_t^{r^*,g^*,Surv} = g_t^{*,Surv} - r_t^{*,Surv}$$

The OLS estimation yields $c = -0.0745$; $\beta_1 = 0.06$; $\beta_2 = 1.167$; $\beta_3 = -0.148$

Figure 1 plots the survey g-star and r-star estimates in solid lines, and the CBO’s g-star and the backcast r-star in dashed lines.



A5. Bayesian Estimation Details

A5.a. Base model equations

For convenience, I list all model equations keeping the numbering as in the main text.

$$U_t = U_t^* + U_t^c \quad (6)$$

$$U_t - U_t^* = \rho_1^u(U_{t-1} - U_{t-1}^*) + \rho_2^u(U_{t-2} - U_{t-2}^*) + \phi^u \text{ogap}_t + \varepsilon_t^u, \quad \varepsilon_t^u \sim N(0, e^{h_t^u}) \quad (7)$$

where, $\rho_1^u + \rho_2^u < 1$, $\rho_2^u - \rho_1^u < 1$, and $|\rho_2^u| < 1$; $\phi^u < 0$

$$U_t^* = U_{t-1}^* + \varepsilon_t^{u*}, \quad \varepsilon_t^{u*} \sim TN(a_u - U_{t-1}^*, b_u - U_{t-1}^*; 0, \sigma_{u*}^2) \quad (8)$$

$$Z_t^u = C_t^u + \beta^u U_t^* + \varepsilon_t^{zu}, \quad \varepsilon_t^{zu} \sim N(0, \sigma_{zu}^2) \quad (9)$$

$$C_t^u = C_{t-1}^u + \varepsilon_t^{cu}, \quad \varepsilon_t^{cu} \sim N(0, \sigma_{cu}^2) \quad (10)$$

$$\text{gdp}_t = \text{gdp}_t^* + \text{ogap}_t \quad (11)$$

$$\text{gdp}_t^* = 2\text{gdp}_{t-1}^* - \text{gdp}_{t-2}^* + \varepsilon_t^{\text{gdp}*}, \quad \varepsilon_t^{\text{gdp}*} \sim N(0, \sigma_{\text{gdp}*}^2) \quad (12)$$

$$g_t^* \equiv \Delta \text{gdp}_t^*$$

$$g_t^* = g_{t-1}^* + \varepsilon_t^{\text{gdp}*} \quad (13)$$

$$\text{ogap}_t = \rho_1^g(\text{ogap}_{t-1}) + \rho_2^g(\text{ogap}_{t-2}) + a^r(r_t^L - r_t^* - \text{tp}_t^*) + \lambda^g(U_t - U_t^*) + \varepsilon_t^{\text{ogap}} \quad (14)$$

where, $\varepsilon_t^{\text{ogap}} \sim N(0, e^{h_t^i})$, $\rho_1^g + \rho_2^g < 1$, $\rho_2^g - \rho_1^g < 1$, and $|\rho_2^g| < 1$; $\lambda^g < 0$

$$Z_t^g = C_t^g + \beta^g * 4 * g_t^* + \varepsilon_t^{zg}, \quad \varepsilon_t^{zg} \sim N(0, \sigma_{zg}^2) \quad (15)$$

$$C_t^g = C_{t-1}^g + \varepsilon_t^{cg}, \quad \varepsilon_t^{cg} \sim N(0, \sigma_{cg}^2) \quad (16)$$

$$P_t - P_t^* = \rho^p(P_{t-1} - P_{t-1}^*) + \lambda_t^p(U_t - U_t^*) + \varepsilon_t^p, \quad \varepsilon_t^p \sim N(0, e^{h_t^p}) \quad (17)$$

where, $|\rho^p| < 1$

$$\lambda_t^p = \lambda_{t-1}^p + \varepsilon_t^{\lambda p}, \quad \varepsilon_t^{\lambda p} \sim N(0, \sigma_{\lambda p}^2) \quad (18)$$

$$P_t^* = P_{t-1}^* + \varepsilon_t^{p*}, \quad \varepsilon_t^{p*} \sim N(0, \sigma_{p*}^2) \quad (19)$$

$$\pi_t - \pi_t^* = \rho_t^\pi(\pi_{t-1} - \pi_{t-1}^*) + \lambda_t^\pi(U_t - U_t^*) + \varepsilon_t^\pi, \quad \varepsilon_t^\pi \sim N(0, e^{h_t^\pi}) \quad (20)$$

$$\rho_t^\pi = \rho_{t-1}^\pi + \varepsilon_t^{\rho\pi}, \quad \varepsilon_t^{\rho\pi} \sim TN(0 - \rho_{t-1}^\pi, 1 - \rho_{t-1}^\pi; 0, \sigma_{\rho\pi}^2) \quad (21)$$

where, ρ^π is truncated so that $0 < \rho_t^\pi < 1$.

$$\lambda_t^\pi = \lambda_{t-1}^\pi + \varepsilon_t^{\lambda\pi}, \quad \varepsilon_t^{\lambda\pi} \sim TN(-1 - \lambda_{t-1}^\pi, 0 - \lambda_{t-1}^\pi; 0, \sigma_{\lambda\pi}^2) \quad (22)$$

λ^π is the slope of the price Phillips curve and is constrained in the interval (-1,0).

$$\pi_t^* = \pi_{t-1}^* + \varepsilon_t^{\pi*}, \quad \varepsilon_t^{\pi*} \sim N(0, \sigma_{\pi*}^2) \quad (23)$$

$$Z_t^\pi = C_t^\pi + \beta^\pi \pi_t^* + \varepsilon_t^{z\pi}, \quad \varepsilon_t^{z\pi} \sim N(0, \sigma_{z\pi}^2) \quad (24)$$

$$C_t^\pi = C_{t-1}^\pi + \varepsilon_t^{c\pi}, \quad \varepsilon_t^{c\pi} \sim N(0, \sigma_{c\pi}^2) \quad (25)$$

$$W_t^* = \pi_t^* + P_t^* + Wedge_t + \varepsilon_t^{w*}, \quad \varepsilon_t^{w*} \sim N(0, \sigma_{w*}^2) \quad (26)$$

$$Wedge_t = Wedge_{t-1} + \varepsilon_t^{wlr}, \quad \varepsilon_t^{wlr} \sim N(0, \sigma_{wlr}^2) \quad (27)$$

$$W_t - W_t^* = \rho_t^w (W_{t-1} - W_{t-1}^*) + \lambda_t^w (U_t - U_t^*) + \kappa_t^w (\pi_t - \pi_t^*) + \varepsilon_t^w, \quad \varepsilon_t^w \sim N(0, e^{h_t^w}) \quad (28)$$

$$\rho_t^w = \rho_{t-1}^w + \varepsilon_t^{\rho w}, \quad \varepsilon_t^{\rho w} \sim TN(0 - \rho_{t-1}^w, 1 - \rho_{t-1}^w; 0, \sigma_{\rho w}^2) \quad (29)$$

$$\lambda_t^w = \lambda_{t-1}^w + \varepsilon_t^{\lambda w}, \quad \varepsilon_t^{\lambda w} \sim TN(-1 - \lambda_{t-1}^w, 0 - \lambda_{t-1}^w; 0, \sigma_{\lambda w}^2) \quad (30)$$

λ^w is the slope of the wage Phillips curve and is constrained in the interval $(-1, 0)$.

$$\kappa_t^w = \kappa_{t-1}^w + \varepsilon_t^{\kappa w}, \quad \varepsilon_t^{\kappa w} \sim N(0, \sigma_{\kappa w}^2) \quad (31)$$

$$i_t - \pi_t^* - r_t^* = \rho^i (i_{t-1} - \pi_{t-1}^* - r_{t-1}^*) + \lambda^i (U_t - U_t^*) + \kappa^i (\pi_t - \pi_t^*) + \varepsilon_t^i, \quad \varepsilon_t^i \sim N(0, e^{h_t^i}) \quad (32)$$

where, ρ^i is truncated so that $0 < \rho^i < 1$.

$$r_t^* = \zeta g_t^* + D_t. \quad (33)$$

$$D_t = D_{t-1} + \varepsilon_t^d, \quad \varepsilon_t^d \sim N(0, \sigma_d^2) \quad (34)$$

$$Z_t^r = C_t^r + \beta^r r_t^* + \varepsilon_t^{zr}, \quad \varepsilon_t^{zr} \sim N(0, \sigma_{zr}^2) \quad (35)$$

$$C_t^r = C_{t-1}^r + \varepsilon_t^{cr}, \quad \varepsilon_t^{cr} \sim N(0, \sigma_{cr}^2) \quad (36)$$

$$h_t^{id} = h_{t-1}^{id} + \varepsilon_t^j, \quad \varepsilon_t^j \sim N(0, \sigma_j^2) \quad (37)$$

where $id = \{u, ogap, p, \pi, w, i\}$, and $j = \{hu, ho, hp, h\pi, hw, hi\}$

A5.b. Prior elicitation

The prior settings are similar to those used in Chan, Koop, and Potter (2016) [CKP], Chan, Clark, and Koop (2018) [CCK], and Gonzalez-Astudillo and Laforte (2020). As discussed in CCK, UC models with several unobserved variables, such as the one developed in this paper, require informative priors. That said, our priors settings for most variables are only slightly informative. The use of inequality restrictions on some parameters such as the Phillips curve, persistence, bounds on u-star could be viewed as additional sources of information that eliminates the need for tight priors, something also noted by CKP. The parameters for which there is a strong agreement in the empirical literature on their values, such as the Taylor-rule equation parameters, I use relatively tight priors, such that prior distributions are centered on prior means with small variance.

In the table below, the notation $N(a, b)$ denotes Normal distribution with mean a , and variance b ; and $IG(\nu, S)$ denotes Inverse Gamma distribution with degrees of freedom parameter ν , and scale parameter S .

Table 1: Prior settings

Parameter	Parameter Description	Prior
a^r	Coefficient on interest-rate gap in output gap equation	$N(0, 1)$
ρ_1^g	Persistence in output gap: lag 1	$N(1.3, 0.1^2)$
ρ_2^g	Persistence in output gap: lag 2	$N(-0.5, 0.1^2)$
ρ_1^u	Persistence in UR gap: lag 1	$N(1.3, 0.1^2)$
ρ_2^u	Persistence in UR gap: lag 2	$N(-0.5, 0.1^2)$
ρ^p	Persistence in productivity gap	$N(0.1, 1)$
ζ	Relationship between r^* and g^*	$N(1, 0.1)$
ρ^i	Persistence in interest-rate gap	$N(0.85, 0.1^2)$
λ^i	Interest rate sensitivity to UR gap: $(-2 * (1 - \rho^i))$	$N(-0.3, 0.1^2)$
κ^i	Interest rate sensitivity to inflation: $(0.5 * (1 - \rho^i))$	$N(0.075, 0.1^2)$
λ^g	Output gap response to UR gap	$N(-0.02, 1)$
ϕ^u	UR gap response to Output gap	$N(-0.02, 1)$
β^g	Link between g^* and survey	$N(1, 0.1^2)$
β^u	Link between u^* and survey	$N(1, 0.05^2)$
β^r	Link between r^* and survey	$N(1, 0.1^2)$
β^π	Link between π^* and survey	$N(1, 0.05^2)$
$\sigma_{\pi^*}^2$	Var. of the shocks to π^*	$IG(10, 0.1^2 \times 9)$
$\sigma_{p^*}^2$	Var. of the shocks to p^*	$IG(10, 0.142^2 \times 9)$
$\sigma_{u^*}^2$	Var. of the shocks to u^*	$IG(10, 0.1^2 \times 9)$
$\sigma_{gdp^*}^2$	Var. of the shocks to gdp^*	$IG(10, 0.01^2 \times 9)$
σ_d^2	Var. of the shocks to d	$IG(10, 0.1^2 \times 9)$
$\sigma_{w^*}^2$	Var. of the shocks to w^*	$IG(10, 0.03^2 \times 9)$
σ_{ho}^2	Var. of the volatility – Ogap eq.	$IG(10, 0.707^2 \times 9)$
σ_{hu}^2	Var. of the volatility – UR gap eq.	$IG(10, 0.707^2 \times 9)$
σ_{hp}^2	Var. of the volatility – Productivity eq.	$IG(10, 0.316^2 \times 9)$
σ_h^2	Var. of the volatility – Price Inf. eq.	$IG(10, 0.316^2 \times 9)$
σ_{hw}^2	Var. of the volatility – Wage Inf. eq.	$IG(10, 0.316^2 \times 9)$

Continued on next page

Table 1 – continued from previous page

Parameter	Parameter Description	Prior
σ_{hi}^2	Var. of the volatility – Interest rate eq.	$IG(10, 0.316^2 \times 9)$
$\sigma_{\lambda\pi}^2$	Var. of the shocks to TVP λ^π , Price Phillips curve	$IG(10, 0.04^2 \times 9)$
$\sigma_{\lambda w}^2$	Var. of the shocks to TVP λ^w , Wage Phillips curve	$IG(10, 0.04^2 \times 9)$
$\sigma_{\lambda p}^2$	Var. of the shocks to TVP λ^p , Cyc. Productivity	$IG(10, 0.04^2 \times 9)$
$\sigma_{\kappa w}^2$	Var. of the shocks to TVP κ^w , PT: π to Wages	$IG(10, 0.04^2 \times 9)$
$\sigma_{\rho w}^2$	Var. of the shocks to TVP ρ^w , Persist. Wage-gap	$IG(10, 0.04^2 \times 9)$
$\sigma_{\rho\pi}^2$	Var. of the shocks to TVP ρ^π , Persist. Inflation-gap	$IG(10, 0.04^2 \times 9)$
C_0^π	Time-varying Intercept in eq. linking survey to pi-star	$N(0, 0.1)$
C_0^u	Time-varying Intercept in eq. linking survey to u-star	$N(0, 0.1)$
C_0^g	Time-varying Intercept in eq. linking survey to g-star	$N(0, 0.1)$
C_0^r	Time-varying Intercept in eq. linking survey to r-star	$N(0, 0.1)$
$\sigma_{c\pi}^2$	Var. of the shocks to TVP C^π	$IG(10, 0.1^2 \times 9)$
σ_{cu}^2	Var. of the shocks to TVP C^u	$IG(10, 0.1^2 \times 9)$
σ_{cg}^2	Var. of the shocks to TVP C^g	$IG(10, 0.1^2 \times 9)$
σ_{cr}^2	Var. of the shocks to TVP C^r	$IG(10, 0.1^2 \times 9)$
σ_{wlr}^2	Var. of the shocks to TVP <i>Wedge</i>	$IG(10, 0.1^2 \times 9)$
$\sigma_{z\pi}^2$	Var. of the shocks in measurement eq. Z^π ,	$IG(10, 0.2 \times 9)$
σ_{zu}^2	Var. of the shocks in measurement eq. Z^u ,	$IG(10, 0.3 \times 9)$
σ_{zg}^2	Var. of the shocks in measurement eq. Z^g ,	$IG(10, 0.1 \times 9)$
σ_{zr}^2	Var. of the shocks in measurement eq. Z^r ,	$IG(10, 0.2 \times 9)$
π_0^*	Initial value of pi-star	$N(3, 5^2)$
u_0^*	Initial value of u-star, $t = 0$	$N(5, 5^2)$
u_{-1}^*	Initial value of u-star, $t = -1$	$N(5, 5^2)$
p_0^*	Initial value of p-star	$N(3, 5^2)$
w_0^*	Initial value of w-star, $E(p_0^*) + E(\pi_0^*) = 6$	$N(6, 5^2)$
D_0	Initial value of D, "catch-all" component of r-star	$N(0, 0.3162^2)$
gdp_0^*	Initial value of gdp-star, $t = 0$	$N(750, 10^2)$
gdp_{-1}^*	Initial value of gdp-star, $t = -1$	$N(750, 10^2)$

A5.c. MCMC algorithm

The estimation of my complex UC model and sampling from its joint posterior distribution reduces to sequentially drawing from a set of conditional posterior densities, some of which are standard and some that are non-standard.

Collect all the time-invariant model parameters into θ :

$$\theta = (\rho_1^u, \rho_2^u, \sigma_{hu}^2, \phi_u, \sigma_{u*}^2, \beta^u, \sigma_{zu}^2, \sigma_{cu}^2, \sigma_{gdp*}^2, \rho_1^g, \rho_2^g, a^r, \lambda^g, \sigma_{ho}^2, \sigma_{zg}^2, \sigma_{cg}^2, \beta^g, \rho^p, \sigma_{hp}^2, \sigma_{p*}^2, \sigma_{\lambda\pi}^2, \dots, \sigma_{\rho\pi}^2, \sigma_{h\pi}^2, \sigma_{\pi*}^2, \sigma_{z\pi}^2, \sigma_{c\pi}^2, \beta^\pi, \sigma_{w*}^2, \sigma_{hw}^2, \sigma_{\rho w}^2, \sigma_{\lambda w}^2, \sigma_{\kappa w}^2, \rho^i, \lambda^i, \kappa^i, \sigma_{hi}^2, \sigma_{zr}^2, \sigma_{cr}^2, \sigma_{wlr}^2, \beta^r, \sigma_d^2)$$

We denote \bullet as representing all other model parameters.

1. $p(U^*|Y, \bullet)$
2. $p(gdp^*|Y, \bullet)$
3. $p(P^*|Y, \bullet)$
4. $p(\pi^*|Y, \bullet)$
5. $p(w^*|Y, \bullet)$
6. $p(r^*|Y, \bullet)$
7. $p(\lambda^p|Y, \bullet)$
8. $p(\rho^\pi|Y, \bullet)$
9. $p(\lambda^\pi|Y, \bullet)$
10. $p(\rho^w|Y, \bullet)$
11. $p(\lambda^w|Y, \bullet)$
12. $p(\kappa^w|Y, \bullet)$
13. $p(h^p, h^\pi, h^w, h^i|Y, \bullet)$
14. $p(C^u, C^g, C^\pi, C^r, Wedge|Y, \bullet)$
15. $p(D|Y, \bullet)$
16. $p(\theta|Y, \bullet)$

Step 1. Derive the conditional distribution $p(U^*|Y, \bullet)$

The derivation of this distribution is most complex because the information about U^* comes from eight sources (i.e., model equations). Below, I derive an expression for each of the eight sources.

The first source is the state equation of U^* . We rewrite it in a matrix notation as follows,

$$HU^* = \alpha_u + \varepsilon^{u*} \quad \varepsilon^{u*} \sim N(0, \Omega_{u*}), \quad \text{where } \Omega_{u*} = \text{diag}(\omega_{u*}^2, \sigma_{u*}^2, \dots, \sigma_{u*}^2) \quad (38)$$

where,

$$\alpha_u = \begin{pmatrix} U_0^* \\ 0 \\ 0 \\ \vdots \\ 0 \end{pmatrix}, \quad H = \begin{pmatrix} 1 & 0 & 0 & \dots & 0 \\ -1 & 1 & 0 & \dots & 0 \\ 0 & -1 & 1 & \dots & 0 \\ \vdots & & & \ddots & \vdots \\ 0 & 0 & \dots & -1 & 1 \end{pmatrix}$$

That is, the prior density for U^* is given by

$$p(U^*|\sigma_{U^*}^2) \propto -\frac{1}{2}(U^* - H^{-1}\alpha_u)' H' \Omega_{u*}^{-1} H (U^* - H^{-1}\alpha_u) + g_{u*}(U^*, \sigma_{u*}^2)$$

where,

$a_u < U^* < b_u$ for $t = 1, \dots, T$, and

$$g_{u*}(U^*, \sigma_{u*}^2) = -\log \left(\Phi \left(\frac{b_u}{\omega_{u*}} \right) - \Phi \left(\frac{a_u}{\omega_{u*}} \right) \right) - \sum_{t=2}^T \log \left(\Phi \left(\frac{b_u - U_{t-1}^*}{\sigma_{u*}} \right) - \Phi \left(\frac{a_u - U_{t-1}^*}{\sigma_{u*}} \right) \right)$$

The second source of information comes from the unemployment measurement equation. Rewrite

the equation in a matrix notation,

$$K_u U = \mu^u + K_u U^* + \varepsilon^u \quad \varepsilon^u \sim N(0, \Omega_u), \quad \text{where } \Omega_u = \text{diag}(e^{h_1^u}, e^{h_2^u}, \dots, e^{h_T^u}) \quad (39)$$

and,

$$\mu_u = \begin{pmatrix} \rho_1^u(U_0 - U_0^*) + \rho_2^u(U_{-1} - U_{-1}^*) \\ \rho_2^u(U_0 - U_0^*) \\ 0 \\ \vdots \\ 0 \end{pmatrix}, \quad K_u = \begin{pmatrix} 1 & 0 & 0 & \cdots & 0 \\ -\rho_1^u & 1 & 0 & \cdots & 0 \\ -\rho_2^u & -\rho_1^u & 1 & \cdots & 0 \\ \vdots & & & \ddots & \vdots \\ 0 & \cdots & -\rho_2^u & -\rho_1^u & 1 \end{pmatrix}$$

Ignoring any terms not involving U^* , I have

$$\log p(U|U^*, \bullet) \propto -\frac{1}{2}(U - K_u^{-1}\mu_u - U^*)' K_u' \Omega_u^{-1} K_u (U - K_u^{-1}\mu_u - U^*)$$

The third source of information comes from the inflation measurement equation. Rewrite the equation in a matrix notation,

$$Z = \Lambda^\pi U^* + \varepsilon^\pi \quad \varepsilon^\pi \sim N(0, \Omega_\pi), \quad \text{where } \Omega_\pi = \text{diag}(e^{h_1^\pi}, e^{h_2^\pi}, \dots, e^{h_T^\pi}) \quad (40)$$

where,

$$z_t = (\pi_t - \pi_t^*) - \rho_t^\pi(\pi_{t-1} - \pi_{t-1}^*) - \lambda_t^\pi U_t,$$

$$Z = (z_1, \dots, z_T)' \text{ and } \Lambda^\pi = \text{diag}(-\lambda_1^\pi, \dots, -\lambda_T^\pi)$$

Ignoring any terms not involving U^* , we have

$$\log p(\pi|U^*, U, \pi^*, h^\pi, \rho^p, \bullet) \propto -\frac{1}{2}(Z - \Lambda^\pi U^*)' \Omega_\pi^{-1} (Z - \Lambda^\pi U^*)$$

The fourth source of information comes from the productivity measurement equation. Rewrite the equation in a matrix notation,

$$M^P = \Lambda^P U^* + \varepsilon^P \quad \varepsilon^P \sim N(0, \Omega_P), \quad \text{where } \Omega_P = \text{diag}(e^{h_1^P}, e^{h_2^P}, \dots, e^{h_T^P}) \quad (41)$$

where,

$$m_t = (P_t - P_t^*) - \rho^P(P_{t-1} - P_{t-1}^*) - \lambda_t^P U_t,$$

$$M^P = (m_1, \dots, m_T)' \text{ and } \Lambda^P = \text{diag}(-\lambda_1^P, \dots, -\lambda_T^P)$$

Ignoring any terms not involving U^* , we have

$$\log p(P|U^*, U, P^*, h^p, \rho^p, \bullet) \propto -\frac{1}{2}(M^P - \Lambda^P U^*)' \Omega_P^{-1} (M^P - \Lambda^P U^*)$$

The fifth source of information comes from the wage measurement equation. Rewrite the equation in a matrix notation,

$$M^w = \Lambda^w U^* + \varepsilon^w \quad \varepsilon^w \sim N(0, \Omega_w), \quad \text{where } \Omega_w = \text{diag}(e^{h_1^w}, e^{h_2^w}, \dots, e^{h_T^w}) \quad (42)$$

where,

$$m_t^w = (W_t - W_t^*) - \rho_t^W (W_{t-1} - W_{t-1}^*) - \lambda_t^W U_t - \kappa_t^W (\pi_t - \pi_t^*),$$

$$M^w = (m_1^w, \dots, m_T^w)' \text{ and } \Lambda^w = \text{diag}(-\lambda_1^W, \dots, -\lambda_T^W)$$

Ignoring any terms not involving U^* , we have

$$\log p(W|U^*, W, W^*, h^w, \rho^W, \bullet) \propto -\frac{1}{2}(M^w - \Lambda^w U^*)' \Omega_w^{-1} (M^w - \Lambda^w U^*)$$

The sixth source of information comes from the output gap measurement equation. Rewrite the equation in a matrix notation,

$$M^g = \Lambda^g U^* + \varepsilon^g \quad \varepsilon^g \sim N(0, \Omega_{ogap}), \quad \text{where } \Omega_{ogap} = \text{diag}(e^{h_1^o}, e^{h_2^o}, \dots, e^{h_T^o}) \quad (43)$$

where,

$$m_t^g = ogap_t - \rho_1^g (ogap_{t-1}) - \rho_2^g (ogap_{t-2}) - \lambda^g U_t - a^r (r_t - r_t^*),$$

$$M^g = (m_1^g, \dots, m_T^g)' \text{ and } \Lambda^g = \text{diag}(-\lambda^g, \dots, -\lambda^g)$$

Ignoring any terms not involving U^* , we have

$$\log p(ogap|U^*, U, \bullet) \propto -\frac{1}{2}(M^g - \Lambda^g U^*)' \Omega_{ogap}^{-1} (M^g - \Lambda^g U^*)$$

The seventh source of information comes from the Taylor-type rule measurement equation. Rewrite the equation in a matrix notation,

$$M^{ui} = \Gamma^{ui} U^* + \varepsilon^i \quad \varepsilon^i \sim N(0, \Omega_i), \quad \text{where } \Omega_i = \text{diag}(e^{h_1^i}, e^{h_2^i}, \dots, e^{h_T^i}) \quad (44)$$

where,

$$m_t^{ui} = i_t - \pi_t^* - r_t^* - \rho^i (i_{t-1} - \pi_{t-1}^* - r_{t-1}^*) - \kappa^i (\pi_t - \pi_t^*) - \lambda^i U_t,$$

$$M^{ui} = (m_1^{ui}, \dots, m_T^{ui})' \text{ and } \Gamma^{ui} = \text{diag}(-\lambda^i, \dots, -\lambda^i)$$

Ignoring any terms not involving U^* , we have

$$\log p(i|U^*, U, \pi, \bullet) \propto -\frac{1}{2}(M^{ui} - \Gamma^{ui} U^*)' \Omega_i^{-1} (M^{ui} - \Gamma^{ui} U^*)$$

The eighth source of information comes from the measurement equation that links surveys

to U^* . Rewrite the equation in a matrix notation,

$$F^u = \beta^u U^* + \varepsilon^{zu} \quad \varepsilon^{zu} \sim N(0, \Omega_{zu}), \quad \text{where } \Omega_{zu} = \text{diag}(\sigma_{zu}^2, \dots, \sigma_{zu}^2) \quad (45)$$

where,

$$f_t^u = Z_t^u - C_t^u,$$

$$F^u = (f_1^u, \dots, f_T^u)'$$

Ignoring any terms not involving U^* , we have

$$\log p(Z^u|U^*, U, \pi, \bullet) \propto -\frac{1}{2}(F^u - \beta^u U^*)' \Omega_{zu}^{-1} (F^u - \beta^u U^*)$$

Combining the above eight conditional densities we obtain,

$$\log p(U^*|Y, \bullet) \propto -\frac{1}{2}(U^* - \hat{U}^*)' D_{U^*}^{-1} (U^* - \hat{U}^*) + g_{u^*}(U^*, \sigma_{u^*}^2)$$

where,

$$D_{U^*} = (H' \Omega_{U^*}^{-1} H + K_u' \Omega_u^{-1} K_u + \Lambda \pi' \Omega_\pi^{-1} \Lambda \pi + \Lambda^{w'} \Omega_w^{-1} \Lambda^w + \Lambda^{g'} \Omega_{ogap}^{-1} \Lambda^g + \Gamma^{ui'} \Omega_i^{-1} \Gamma^{ui} + \Lambda^{P'} \Omega_P^{-1} \Lambda^P + (\beta^u)^2 \Omega_{zu}^{-1})^{-1}$$

$$\hat{U}^* = D_{U^*} (H' \Omega_{U^*}^{-1} \alpha_u + K_u' \Omega_u^{-1} K_u (U - K_u^{-1} \mu_u) + \Lambda \pi' \Omega_\pi^{-1} Z + \Lambda^{w'} M^w + \Lambda^w + \Lambda^{g'} \Omega_{ogap}^{-1} M^g + \Gamma^{ui'} \Omega_i^{-1} M^{ui} + \Lambda^{P'} \Omega_P^{-1} M^P + \beta^u \Omega_{zu}^{-1} F^u)$$

The addition of the term $g_{u^*}(U^*, \sigma_{u^*}^2)$ leads to a non-standard density. Accordingly, I sample U^* using an independence-chain Metropolis-Hastings (MH) procedure. This involves first generating candidate draws from $N(\hat{U}^*, D_{U^*})$ using the precision-based algorithm (of Chan and Jeliazkov, 2009) that are then accepted or rejected based on the accept-reject Metropolis-Hastings (ARMH) algorithm (discussed in Chan and Strachan, 2012).

Step 2. Derive the conditional distribution $p(gdp^*|Y, \bullet)$

The information about gdp^* comes from five sources. Below, I derive an expression for each of these sources.

The first source is the state equation of gdp^* . We rewrite it in a matrix notation as follows,

$$H_2 gdp^* = \alpha_{gdp^*} + \varepsilon^{gdp^*} \quad \varepsilon^{gdp^*} \sim N(0, \Omega_{gdp^*}), \quad \text{where } \Omega_{gdp^*} = \text{diag}(\omega_{gdp^*}^2, \sigma_{gdp^*}^2, \dots, \sigma_{gdp^*}^2) \quad (46)$$

where,

$$\alpha_{gdp^*} = \begin{pmatrix} gdp_0^* + \Delta gdp_0^* \\ -gdp_0^* \\ 0 \\ \vdots \\ 0 \end{pmatrix}, \quad H_2 = \begin{pmatrix} 1 & 0 & 0 & 0 & \cdots & 0 \\ -2 & 1 & 0 & 0 & \cdots & 0 \\ 1 & -2 & 1 & 0 & \cdots & 0 \\ 0 & 1 & -2 & 1 & \cdots & 0 \\ \vdots & & & & \ddots & \vdots \\ 0 & \cdots & 0 & 1 & -2 & 1 \end{pmatrix}$$

H_2 is a band matrix with unit determinant and hence is invertible.

The prior density for gdp^* is given by

$$p(gdp^* | \sigma_{gdp^*}^2) \propto -\frac{1}{2}(gdp^* - H_2^{-1}\alpha_{gdp^*})' H_2' \Omega_{gdp^*}^{-1} H_2 (gdp^* - H_2^{-1}\alpha_{gdp^*})$$

The second source of information about gdp^* is from the output gap measurement equation. Rewrite in matrix form,

$$H_{rhog} gdp = H_{rhog} gdp^* + a^r \tilde{r} + \lambda^g \tilde{u} + \alpha_{gmore} + \varepsilon^{ogap} \quad \varepsilon^{ogap} \sim N(0, \Omega_{ogap}), \quad \text{where } \Omega_{ogap} = \text{diag}(e^{h_1^o}, e^{h_2^o}, \dots, e^{h_T^o}) \quad (47)$$

where,

$$\alpha_{gmore} = \begin{pmatrix} \rho_1^g(gdp_0 - gdp_0^*) + \rho_2^g(gdp_{-1} - gdp_{-1}^*) \\ \rho_2^g(gdp_0 - gdp_0^*) \\ 0 \\ \vdots \\ 0 \end{pmatrix}, \quad H_{rhog} = \begin{pmatrix} 1 & 0 & 0 & 0 & \cdots & 0 \\ -\rho_1^g & 1 & 0 & 0 & \cdots & 0 \\ -\rho_2^g & -\rho_1^g & 1 & 0 & \cdots & 0 \\ 0 & -\rho_2^g & -\rho_1^g & 1 & \cdots & 0 \\ \vdots & \ddots & \ddots & \ddots & \ddots & 0 \\ 0 & \cdots & 0 & -\rho_2^g & -\rho_1^g & 1 \end{pmatrix},$$

$$\tilde{r} = \begin{pmatrix} r_1 - r_1^* \\ r_2 - r_2^* \\ r_3 - r_3^* \\ \vdots \\ r_T - r_T^* \end{pmatrix} \quad \tilde{u} = \begin{pmatrix} U_1 - U_1^* \\ U_2 - U_2^* \\ U_3 - U_3^* \\ \vdots \\ U_T - U_T^* \end{pmatrix}$$

$$\log p(gdp | gdp^*, \bullet) \propto -\frac{1}{2}(gdp - H_{rhog}^{-1}(H_{rhog} gdp^* + a^r \tilde{r} + \lambda^g \tilde{u} + \alpha_{gmore}))' H_{rhog}' \Omega_{ogap}^{-1} H_{rhog} (gdp - H_{rhog}^{-1}(H_{rhog} gdp^* + a^r \tilde{r} + \lambda^g \tilde{u} + \alpha_{gmore}))$$

The third source of information comes from the unemployment gap measurement equation. Rewrite that equation in matrix notation,

$$Y^{ugdp} = \Gamma^u gdp^* + \varepsilon^u \quad \varepsilon^u \sim N(0, \Omega_u), \quad \text{where } \Omega_u = \text{diag}(e^{h_1^u}, e^{h_2^u}, \dots, e^{h_T^u}) \quad (48)$$

where,

$$y_t^{ugdp} = \tilde{u}_t - \rho_1^u u_{t-1} - \rho_2^u u_{t-2} - \phi^u gdp, \quad \text{where } \tilde{u}_t = (U_t - U_t^*)$$

$$Y^{ugd}p = (y_1^{ugd}p, \dots, y_T^{ugd}p)'$$

Ignoring any terms not involving gdp^* , we have

$$\log p(U|gdp^*, \bullet) \propto -\frac{1}{2}(Y^{ugd}p - \Gamma^u gdp^*)' \Omega_u^{-1} (Y^{ugd}p - \Gamma^u gdp^*)$$

The fourth source of information comes from the equation linking r-star to g-star, i.e.,

$$r_t^* = \zeta(gdp_t^* - gdp_{t-1}^*) + D_t \quad (49)$$

Rewrite this equation in matrix notation,

$$r^* = \zeta H gdp^* + \alpha_{gr} + D \quad (50)$$

where,

$$\alpha_{gr} = (-\zeta gdp_0^*, 0, 0, \dots, 0)'$$

Ignoring any terms not involving gdp^* , we have

$$\log p(r^*|gdp^*, D, \bullet) \propto -\frac{1}{2}(r^* - (\zeta H gdp^* + \alpha_{gr} + D))' (r^* - (\zeta H gdp^* + \alpha_{gr} + D))$$

The fifth source of information comes from the measurement equation that links surveys to g^* . Rewrite the equation in a matrix notation,

$$F^g = \beta^g (H gdp^* - \alpha_g) + \varepsilon^{zg} \quad \varepsilon^{zg} \sim N(0, \Omega_{zg}), \quad \text{where } \Omega_{zg} = \text{diag}(\sigma_{zg}^2, \dots, \sigma_{zg}^2) \quad (51)$$

where,

$$f_t^g = Z_t^g - C_t^g, \quad F^g = (f_1^g, \dots, f_T^g)'$$

$$\alpha_g = (gdp_0^*, 0, 0, \dots, 0)' \text{ is a } T \times 1 \text{ vector.}$$

Ignoring any terms not involving gdp^* , we have

$$\log p(Z^g|gdp^*, \bullet) \propto -\frac{1}{2}(F^g - \beta^g (H gdp^* - \alpha_g))' \Omega_{zg}^{-1} (F^g - \beta^g (H gdp^* - \alpha_g))$$

Combining the above five conditional densities we obtain,

$$\log p(gdp^*|Y, \bullet) \propto -\frac{1}{2}(gdp^* - \hat{g}dp^*)' D_{gdp^*}^{-1} (gdp^* - \hat{g}dp^*)$$

where,

$$D_{gdp^*} = (H_2' \Omega_{gdp^*}^{-1} H_2 + H_{rhog}' \Omega_{ogap}^{-1} H_{rhog} + \Gamma^{u'} \Omega_u^{-1} \Gamma^u + (\zeta H)' (\zeta H) + \beta^g H' \Omega_{zg}^{-1} \beta^g H)^{-1}$$

$$\hat{g}dp^* = D_{gdp^*} (H_2' \Omega_{gdp^*}^{-1} H_2 \alpha_{gdp^*} + H_{rhog}' \Omega_{ogap}^{-1} (H_{rhog} gdp - a^r \tilde{r} - \lambda^g \tilde{u} - \alpha_{gmore}) + \Gamma^{u'} \Omega_u^{-1} Y^{ugd}p + (\zeta H)' (r^* - \alpha_{gr} + D) + \beta^g H' \Omega_{zg}^{-1} F^g)$$

Step 3. Derive the conditional distribution $p(P^*|Y, \bullet)$

First, rewrite the productivity measurement eq. as

$$K_P P = \mu_P + K_P P^* + \varepsilon^P \quad \varepsilon^P \sim N(0, \Omega_P), \quad \text{where } \Omega_P = \text{diag}(e^{h_1^P}, e^{h_2^P}, \dots, e^{h_T^P}) \quad (52)$$

$$\mu_P = \begin{pmatrix} \rho_1^P(P_0 - P_0^*) + \lambda_1^P(U_1 - U_1^*) \\ \lambda_2^P(U_2 - U_2^*) \\ \lambda_3^P(U_3 - U_3^*) \\ \vdots \\ \lambda_T^P(U_T - U_T^*) \end{pmatrix}, \quad K_P = \begin{pmatrix} 1 & 0 & 0 & \cdots & 0 \\ -\rho_2^P & 1 & 0 & \cdots & 0 \\ 0 & -\rho_3^P & 1 & \cdots & 0 \\ \vdots & & & \ddots & \vdots \\ 0 & 0 & \cdots & -\rho_T^P & 1 \end{pmatrix}, \quad P^* = \begin{pmatrix} P_1^* \\ P_2^* \\ P_3^* \\ \vdots \\ P_T^* \end{pmatrix}$$

Since $|K_P| = 1$ for any ρ_P , K_P is invertible. Therefore, the likelihood is

$$p(P|P^*, U, \bullet) \sim N(K_P^{-1}\mu_P + P^*, (K_P' \Omega_P^{-1} K_P)^{-1})$$

i.e.,

$$\log p(P|U, \bullet) \propto -\frac{1}{2} \iota_T' h^P - \frac{1}{2} (P - K_P^{-1}\mu_P - P^*)' K_P' \Omega_P^{-1} K_P (P - K_P^{-1}\mu_P - P^*),$$

where ι_T is a $T \times 1$ column of ones.

Similarly, rewrite the state equation for P^* as

$$H P^* = \alpha_P + \varepsilon^{P^*} \quad \varepsilon^{P^*} \sim N(0, \Omega_{P^*}), \quad \text{where } \Omega_{P^*} = \text{diag}(\omega_{P^*}^2, \sigma_{P^*}^2, \dots, \sigma_{P^*}^2) \quad (53)$$

where,

$$\alpha_P = \begin{pmatrix} P_0^* \\ 0 \\ 0 \\ \vdots \\ 0 \end{pmatrix}, \quad K_P = \begin{pmatrix} 1 & 0 & 0 & \cdots & 0 \\ -1 & 1 & 0 & \cdots & 0 \\ 0 & -1 & 1 & \cdots & 0 \\ \vdots & & & \ddots & \vdots \\ 0 & 0 & \cdots & -1 & 1 \end{pmatrix}$$

That is, the prior density for P^* is given by

$$p(P^*|\sigma_{P^*}^2) \propto -\frac{1}{2} (P^* - H^{-1}\alpha_P)' H' \Omega_{P^*}^{-1} H (P^* - H^{-1}\alpha_P)$$

Now account for the third source of information about P^* in the equation $W^* = P^* + \pi^* + \text{Wedge} + \varepsilon^{W^*}$,

$$p(P^*|W^*, \pi^*, \sigma_{W^*}^2) \propto -\frac{1}{2} (P^* - (W^* - \pi^* - \text{Wedge}))' \Omega_{W^*}^{-1} (P^* - (W^* - \pi^* - \text{Wedge}))$$

where,

$$\Omega_{W^*} = \text{diag}(\sigma_{W^*}^2, \sigma_{W^*}^2, \dots, \sigma_{W^*}^2), \quad W^* = (W_1^*, \dots, W_T^*)', \quad \pi^* = (\pi_1^*, \dots, \pi_T^*)', \quad \text{Wedge} = (\text{Wedge}_1, \dots, \text{Wedge}_T)'$$

Combining the above three conditional densities we obtain,

$$\log p(P^*|Y, \bullet) \propto -\frac{1}{2}(P^* - \hat{P}^*)' D_{P^*}^{-1} (P^* - \hat{P}^*)$$

where,

$$D_{P^*} = (H' \Omega_{P^*}^{-1} H + K_P' \Omega_P^{-1} K_P + \Omega_{W^*}^{-1})^{-1}$$

$$\hat{P}^* = D_{P^*} (H^{-1} \Omega_{P^*}^{-1} \alpha_p + K_P' \Omega_P^{-1} K_P (P - K_P^{-1} \mu_P) + \Omega_{W^*}^{-1} (W^* - \pi^*))$$

The candidate draws are sampled from $N(\hat{P}^*, D_{P^*})$ using the precision-based algorithm.

Step 4. Derive the conditional distribution $p(\pi^*|Y, \bullet)$

The information about π^* comes from six sources. Below, I derive an expression for each of these sources.

The first source is the inflation measurement equation. Rewrite it in a matrix notation as,

$$K_\pi \pi = \mu_\pi + K_\pi \pi^* + \varepsilon^\pi \quad \varepsilon^\pi \sim N(0, \Omega_\pi), \quad \text{where } \Omega_\pi = \text{diag}(e^{h_1^\pi}, e^{h_2^\pi}, \dots, e^{h_T^\pi}) \quad (54)$$

where,

$$\mu_\pi = \begin{pmatrix} \rho_1^\pi (\pi_0 - \pi_0^*) + \lambda_1^\pi (U_1 - U_1^*) \\ \lambda_2^\pi (U_2 - U_2^*) \\ \lambda_3^\pi (U_3 - U_3^*) \\ \vdots \\ \lambda_T^\pi (U_T - U_T^*) \end{pmatrix}, \quad K_\pi = \begin{pmatrix} 1 & 0 & 0 & \dots & 0 \\ -\rho_2^\pi & 1 & 0 & \dots & 0 \\ 0 & -\rho_3^\pi & 1 & \dots & 0 \\ \vdots & & & \ddots & \vdots \\ 0 & 0 & \dots & -\rho_T^\pi & 1 \end{pmatrix}$$

Since $|K_\pi| = 1$ for any ρ_π , K_π is invertible. Therefore, the likelihood is

$$\log p(\pi|U, U^*, \bullet) \propto -\frac{1}{2} \iota_T h^\pi - \frac{1}{2} (\pi - (K_\pi^{-1} \mu_\pi + \pi^*))' K_\pi' \Omega_\pi^{-1} K_\pi (\pi - (K_\pi^{-1} \mu_\pi + \pi^*))$$

The second source of information is from the state equation of π^* . Rewrite it in a matrix notation,

$$H\pi^* = \alpha_\pi + \varepsilon^{\pi^*} \quad \varepsilon^{\pi^*} \sim N(0, \Omega_{\pi^*}), \quad \text{where } \Omega_{\pi^*} = \text{diag}(\omega_{\pi^*}^2, \sigma_{\pi^*}^2, \dots, \sigma_{\pi^*}^2) \quad (55)$$

where,

$$\alpha_\pi = \begin{pmatrix} \pi_0^* \\ 0 \\ 0 \\ \vdots \\ 0 \end{pmatrix}$$

That is, the prior density for π^* is given by

$$p(\pi^* | \sigma_{\pi^*}^2) \propto -\frac{1}{2}(\pi^* - H^{-1}\alpha_\pi)' H' \Omega_{\pi^*}^{-1} H (\pi^* - H^{-1}\alpha_\pi)$$

Now account for the third source of information about π^* in the equation $W^* = P^* + \pi^* + \text{Wedge} + \varepsilon^{w^*}$,

$$p(\pi^* | W^*, P^*, \sigma_{W^*}^2) \propto -\frac{1}{2}(\pi^* - (W^* - P^* - \text{Wedge}))' \Omega_{W^*}^{-1} (\pi^* - (W^* - P^* - \text{Wedge}))$$

where,

$$\Omega_{W^*} = \text{diag}(\sigma_{W^*}^2, \sigma_{W^*}^2, \dots, \sigma_{W^*}^2), \quad W^* = (W_1^*, \dots, W_T^*)', \quad P^* = (P_1^*, \dots, P_T^*)', \quad \text{Wedge} = (\text{Wedge}_1, \dots, \text{Wedge}_T)'$$

The fourth source of information is from the wage measurement equation. Rewrite in matrix notation,

$$M^{w\pi} = X_{w\pi} \pi^* + \varepsilon^w \quad \varepsilon^w \sim N(0, \Omega_w), \quad \text{where } \Omega_w = \text{diag}(e^{h_1^w}, e^{h_2^w}, \dots, e^{h_T^w}) \quad (56)$$

where,

$$m_t^{w\pi} = w_t - w_t^* - \rho_t^w (w_{t-1} - w_{t-1}^*) - \lambda_t^w (U_t - U_t^*) - \kappa_t^w \pi_t$$

$$M^{w\pi} = (m_1^{w\pi}, m_2^{w\pi}, \dots, m_T^{w\pi})$$

$$X_{w\pi} = \begin{pmatrix} -\kappa_1^w & 0 & 0 & \dots & 0 \\ 0 & -\kappa_2^w & 0 & \dots & 0 \\ 0 & 0 & -\kappa_3^w & \dots & 0 \\ \vdots & & & \ddots & \vdots \\ 0 & 0 & \dots & 0 & -\kappa_T^w \end{pmatrix}$$

$$\log p(W | \pi^*, \bullet) \propto -\frac{1}{2}(M^{w\pi} - X_{w\pi} \pi^*)' \Omega_w^{-1} (M^{w\pi} - X_{w\pi} \pi^*)$$

The fifth source is the Taylor-rule equation. Rewrite the equation in the matrix notation,

$$M^{\pi i} = \alpha_{\pi i} + (K_{\pi i} + \Gamma_\pi) \pi^* + \varepsilon^i \quad \varepsilon^i \sim N(0, \Omega_i), \quad \text{where } \Omega_i = \text{diag}(e^{h_1^i}, e^{h_2^i}, \dots, e^{h_T^i}) \quad (57)$$

where,

$$m_t^{\pi i} = i_t - \rho^i i_{t-1} - r_t^* + \rho^i r_{t-1}^* - \lambda^i (U_t - U_t^*) - \kappa^i \pi_t$$

$$M^{\pi i} = (m_1^{\pi i}, m_2^{\pi i}, \dots, m_T^{\pi i})'$$

$$K_{\pi i} = \begin{pmatrix} 1 & 0 & 0 & \cdots & 0 \\ -\rho^i & 1 & 0 & \cdots & 0 \\ 0 & -\rho^i & 1 & \cdots & 0 \\ \vdots & & & \ddots & \vdots \\ 0 & 0 & \cdots & -\rho^i & 1 \end{pmatrix}, \quad \Gamma_{\pi} = \begin{pmatrix} -\kappa^i & 0 & 0 & \cdots & 0 \\ 0 & -\kappa^i & 0 & \cdots & 0 \\ 0 & 0 & -\kappa^i & \cdots & 0 \\ \vdots & & & \ddots & \vdots \\ 0 & 0 & \cdots & 0 & -\kappa^i \end{pmatrix}, \quad \alpha_{\pi i} = \begin{pmatrix} -\rho^i \pi_0^* \\ 0 \\ 0 \\ \vdots \\ 0 \end{pmatrix}$$

$$\log p(i|\pi^*, \pi, \bullet) \propto -\frac{1}{2}(M^{\pi i} - (\alpha_{\pi i} + (K_{\pi i} + \Gamma_{\pi})\pi^*))' \Omega_i^{-1} (M^{\pi i} - (\alpha_{\pi i} + (K_{\pi i} + \Gamma_{\pi})\pi^*))$$

The sixth source of information comes from the measurement equation that links surveys to π^* . Rewrite the equation in a matrix notation,

$$F^{\pi} = \beta^{\pi} \pi^* + \varepsilon^{z\pi} \quad \varepsilon^{z\pi} \sim N(0, \Omega_{z\pi}), \quad \text{where } \Omega_{z\pi} = \text{diag}(\sigma_{z\pi}^2, \dots, \sigma_{z\pi}^2) \quad (58)$$

where,

$$f_t^{\pi} = Z_t^{\pi} - C_t^{\pi},$$

$$F^{\pi} = (f_1^{\pi}, \dots, f_T^{\pi})'$$

Ignoring any terms not involving π^* , we have

$$\log p(Z^{\pi}|\pi^*, \pi, \bullet) \propto -\frac{1}{2}(F^{\pi} - \beta^{\pi} \pi^*)' \Omega_{z\pi}^{-1} (F^{\pi} - \beta^{\pi} \pi^*)$$

Combining the above six conditional densities we obtain,

$$\log p(\pi^*|Y, \bullet) \propto -\frac{1}{2}(\pi^* - \hat{\pi}^*)' D_{\pi^*}^{-1} (\pi^* - \hat{\pi}^*)$$

where,

$$D_{\pi^*} = (H' \Omega_{\pi^*}^{-1} H + K_{\pi}^{\prime} \Omega_{\pi}^{-1} K_{\pi} + \Omega_{w^*}^{-1} + X'_{w\pi} \Omega_w^{-1} X_{w\pi} + (K'_{\pi i} + \Gamma_{\pi})' \Omega_i^{-1} (K'_{\pi i} + \Gamma_{\pi}) + (\beta^{\pi})^2 \Omega_{zr}^{-1})^{-1}$$

$$\hat{\pi}^* = D_{\pi^*} (H' \Omega_{\pi^*}^{-1} \alpha_{\pi} + K_{\pi}^{\prime} \Omega_{\pi}^{-1} K_{\pi} (\pi - K_{\pi}^{-1} \mu_{\pi}) + \Omega_{w^*}^{-1} (W^* - P^*) + X'_{w\pi} \Omega_w^{-1} M^{w\pi} + (K'_{\pi i} + \Gamma_{\pi})' \Omega_i^{-1} (M^{\pi i} - \alpha_{\pi i}) + \beta^{\pi} \Omega_{zr}^{-1} F^{\pi})$$

The candidate draws are sampled from $N(\hat{\pi}^*, D_{\pi^*})$ using the precision-based algorithm.

Step 5. Derive the conditional distribution $p(w^*|Y, \bullet)$

The information about w^* comes from two sources. Below, I derive an expression for each of these sources.

The first source is the nominal wage measurement equation. Rewrite it in a matrix notation as,

$$K_w W = \mu_w + K_w W^* + \varepsilon^w \quad \varepsilon^w \sim N(0, \Omega_w), \quad \text{where } \Omega_w = \text{diag}(e^{h_1^w}, e^{h_2^w}, \dots, e^{h_T^w}) \quad (59)$$

where,

$$\mu_w = \begin{pmatrix} \rho_1^w (W_0 - W_0^*) + \lambda_1^w (U_1 - U_1^*) + \kappa_1^w (\pi_1 - \pi_1^*) \\ \lambda_2^w (U_2 - U_2^*) + \kappa_2^w (\pi_2 - \pi_2^*) \\ \lambda_3^w (U_3 - U_3^*) + \kappa_3^w (\pi_3 - \pi_3^*) \\ \vdots \\ \lambda_T^w (U_T - U_T^*) + \kappa_T^w (\pi_T - \pi_T^*) \end{pmatrix}, \quad K_w = \begin{pmatrix} 1 & 0 & 0 & \dots & 0 \\ -\rho_2^w & 1 & 0 & \dots & 0 \\ 0 & -\rho_3^w & 1 & \dots & 0 \\ \vdots & & & \ddots & \vdots \\ 0 & 0 & \dots & -\rho_T^w & 1 \end{pmatrix}$$

Since $|K_w| = 1$ for any ρ_w , K_w is invertible. Therefore, the likelihood is

Ignoring any terms not involving w^* ,

$$\log p(W|W^*, \bullet) \propto -\frac{1}{2} \iota_T h^w - \frac{1}{2} (W - (K_w^{-1} \mu_w + W^*))' K_w' \Omega_w^{-1} K_w (W - (K_w^{-1} \mu_w + W^*))$$

The second source is the state equation of W^* , which describes W^* as the sum of P^* and π^* . This equation can be thought of as describing the prior density for W^* . Rewrite it in a matrix form.

$$W^* = P^* + \pi^* + Wedge + \varepsilon^{w^*} \quad \varepsilon^{w^*} \sim N(0, \Omega_{w^*}) \quad (60)$$

$$p(W^*|P^*, \pi^*, \sigma_{w^*}^2) \propto -\frac{1}{2} (W^* - (P^* + \pi^* + Wedge))' \Omega_{w^*}^{-1} (W^* - (P^* + \pi^* + Wedge))$$

Combining the above two conditional densities we obtain,

$$\log p(W^*|Y, \bullet) \propto -\frac{1}{2} (W^* - \hat{W}^*)' D_{W^*}^{-1} (W^* - \hat{W}^*)$$

where,

$$D_{W^*} = (K_w' \Omega_w^{-1} K_w + \Omega_{W^*}^{-1})^{-1}$$

$$\hat{W}^* = D_{W^*} (K_w' \Omega_w^{-1} (K_w W - \mu_w) + \Omega_{w^*}^{-1} (P^* + \pi^*))$$

The candidate draws are sampled from $N(\hat{W}^*, D_{W^*})$ using the precision-based algorithm.

Step 6. Derive the conditional distribution $p(r^*|Y, \bullet)$

The information about r^* comes from four sources. Below, I derive an expression for each of these sources.

The first source is the output gap measurement equation. We rewrite it in a matrix notation as follows,

$$H_{rhog}ogap = \alpha_{ogap} - a^r r^* + \varepsilon^{ogap} \quad \varepsilon^{ogap} \sim N(0, \Omega_{ogap}) \quad (61)$$

where,

$$\alpha_{ogap} = \begin{pmatrix} \rho_1^g(ogap_0) + \rho_2^g(ogap_{-1}) + a^r r_1 + \lambda^g(U_1 - U_1^*) \\ \rho_2^g(ogap_0) + a^r r_2 + \lambda^g(U_2 - U_2^*) \\ a^r r_3 + \lambda^g(U_3 - U_3^*) \\ \vdots \\ a^r r_T + \lambda^g(U_T - U_T^*) \end{pmatrix}$$

Ignoring any terms not involving r^* , we have

$$\log p(ogap|r^*, \bullet) \propto -\frac{1}{2}(ogap - H_{rhog}^{-1}(\alpha_{ogap} - a^r r^*))' H_{rhog}' \Omega_{ogap}^{-1} H_{rhog} (ogap - H_{rhog}^{-1}(\alpha_{ogap} - a^r r^*))$$

The second source is the state equation linking r^* to g^* . We rewrite it in a matrix notation as follows,

$$r^* = \zeta \Delta gdp^* + H^{-1} \varepsilon^d \quad \varepsilon^d \sim N(0, \Omega_d), \quad \text{where } \Omega_d = \text{diag}(\omega_d^2, \sigma_d^2, \dots, \sigma_d^2) \quad (62)$$

Ignoring any terms not involving r^* , the prior density for r^* is given by

$$\log p(r^*|gdp^*, \sigma_d^2, \bullet) \propto -\frac{1}{2}(r^* - \zeta \Delta gdp^*)' H' \Omega_d^{-1} H (r^* - \zeta \Delta gdp^*)$$

The third source is the Taylor-type rule equation. We rewrite it in a matrix notation as follows,

$$M^{ri} = \alpha_{ri} + K_{\pi i} r^* + \varepsilon^i \quad \varepsilon^i \sim N(0, \Omega_i), \quad \text{where } \Omega_i = \text{diag}(e^{h_1^i}, e^{h_2^i}, \dots, e^{h_T^i}) \quad (63)$$

where,

$$m_t^{ri} = i_t - \rho^i i_{t-1} - \pi_t^* + \rho^i \pi_{t-1}^* - \lambda^i (U_t - U_t^*) - \kappa^i (\pi_t - \pi_t^*),$$

$$M^{ri} = (m_1^{ri}, m_2^{ri}, \dots, m_T^{ri})'$$

$$\alpha_{ri} = \begin{pmatrix} -\rho^i r_0^* \\ 0 \\ 0 \\ \vdots \\ 0 \end{pmatrix}, \quad K_{\pi i} = \begin{pmatrix} 1 & 0 & 0 & \cdots & 0 \\ -\rho^i & 1 & 0 & \cdots & 0 \\ 0 & -\rho^i & 1 & \cdots & 0 \\ \vdots & & & \ddots & \vdots \\ 0 & 0 & \cdots & -\rho^i & 1 \end{pmatrix}$$

Ignoring any terms not involving r^* , we have

$$\log p(i|r^*, \bullet) \propto -\frac{1}{2} \iota_T h^i - \frac{1}{2} (M^{ri} - (\alpha_{ri} + K_{\pi_i} r^*))' \Omega_i^{-1} (M^{ri} - (\alpha_{ri} + K_{\pi_i} r^*))$$

The fourth source of information comes from the measurement equation that links surveys to r^* . Rewrite the equation in a matrix notation,

$$F^r = \beta^r r^* + \varepsilon^{zr} \quad \varepsilon^{zr} \sim N(0, \Omega_{zr}), \quad \text{where } \Omega_{zr} = \text{diag}(\sigma_{zr}^2, \dots, \sigma_{zr}^2) \quad (64)$$

where,

$$f_t^r = Z_t^r - C_t^r,$$

$$F^r = (f_1^r, \dots, f_T^r)'$$

Ignoring any terms not involving r^* , we have

$$\log p(Z^r|r^*, \bullet) \propto -\frac{1}{2} (F^r - \beta^r r^*)' \Omega_{zr}^{-1} (F^r - \beta^r r^*)$$

Combining the above four conditional densities we obtain,

$$\log p(r^*|Y, \bullet) \propto -\frac{1}{2} (r^* - \hat{r}^*)' D_{r^*}^{-1} (r^* - \hat{r}^*)$$

where,

$$D_{r^*} = ((-a^r)^2 \Omega_{ogap}^{-1} + H' \Omega_d^{-1} H + K_{\pi_i}' \Omega_i^{-1} K_{\pi_i} + (\beta^r)' (2) \Omega_{zr}^{-1})^{-1}$$

$$\hat{r}^* = D_{r^*} (-a^r \Omega_{ogap}^{-1} (H_{rhogogap} - \alpha_{ogap}) + H' \Omega_d^{-1} H \zeta \Delta g d p^* + K_{\pi_i}' \Omega_i^{-1} (M^{ri} - \alpha_{ri}) + \beta^r \Omega_{zr}^{-1} F^r)$$

The candidate draws are sampled from $N(\hat{r}^*, D_{r^*})$ using the precision-based algorithm.

Step 7. Derive the conditional distribution $p(\lambda^p|Y, \bullet)$

The information about λ^p comes from two sources. Below, I derive an expression for each of these two sources.

The first source is the productivity measurement equation. Rewrite it in a matrix notation,

$$B = X_u \lambda^p + \varepsilon^p \quad \varepsilon^p \sim N(0, \Omega_p) \quad (65)$$

where,

$$B = (\tilde{p}_1 - \rho^p \tilde{p}_0, \dots, \tilde{p}_T - \rho^p \tilde{p}_{T-1})$$

$$\tilde{p}_t = p_t - p_t^*$$

$$\tilde{u}_t = U_t - U_t^*$$

$$X_u = \text{diag}(\tilde{u}_1, \dots, \tilde{u}_T)$$

Ignoring any terms not involving λ^p , the likelihood is

$$\log p(p|\lambda^p, \bullet) \propto -\frac{1}{2}(B - X_u \lambda^p)' \Omega_p^{-1} (B - X_u \lambda^p)$$

The second source of information comes from the state equation for λ^p . We rewrite it in a matrix notation as follows,

$$H \lambda^p = \varepsilon^{\lambda^p} \quad \varepsilon^{\lambda^p} \sim N(0, \Omega_{\lambda^p}), \quad \text{where } \Omega_{\lambda^p} = \text{diag}(\omega_{\lambda^p}^2, \sigma_{\lambda^p}^2, \dots, \sigma_{\lambda^p}^2) \quad (66)$$

Ignoring any terms not involving λ^p , the prior density for λ^p is given by

$$\log p(\lambda^p | \sigma_{\lambda^p}^2, \Omega_{\lambda^p}) \propto -\frac{1}{2}(\lambda^p)' H' \Omega_{\lambda^p}^{-1} H (\lambda^p)$$

Combining the above two conditional densities we obtain,

$$\log p(\lambda^p | Y, \bullet) \propto -\frac{1}{2}(\lambda^p - \hat{\lambda}^p)' D_{\lambda^p}^{-1} (\lambda^p - \hat{\lambda}^p)$$

where,

$$D_{\lambda^p} = (H' \Omega_{\lambda^p}^{-1} H + X_u' \Omega_p^{-1} X_u)^{-1}$$

$$\hat{\lambda}^p = D_{\lambda^p} (X_u' \Omega_p^{-1} B)$$

The candidate draws are sampled from $N(\hat{\lambda}^p, D_{\lambda^p})$ using the precision-based algorithm.

Step 8. Derive the conditional distribution $p(\rho^\pi | Y, \bullet)$

The information about ρ^π comes from two sources. Below, I derive an expression for each of these two sources.

First, I define some notation,

$$\begin{aligned} \tilde{\pi}_t &= \pi_t - \pi_t^* \\ \tilde{u}_t &= U_t - U_t^* \\ \tilde{\Pi} &= (\tilde{\pi}_1, \dots, \tilde{\pi}_T)' \\ \tilde{u} &= (\tilde{u}_1, \dots, \tilde{u}_T)' \end{aligned}$$

The first source is the price inflation measurement equation. Rewrite it in a matrix notation,

$$\tilde{\Pi} + \Lambda \tilde{u} = X_\pi \rho^\pi + \varepsilon^\pi \quad \varepsilon^\pi \sim N(0, \Omega_\pi) \quad (67)$$

where,

$$\begin{aligned} X_\pi &= \text{diag}(\tilde{\pi}_0, \dots, \tilde{\pi}_{T-1}) \\ \Lambda &= \text{diag}(-\lambda_1^\pi, \dots, -\lambda_T^\pi) \end{aligned}$$

Ignoring any terms not involving ρ^π , the likelihood is

$$\log p(\pi|\rho^\pi, \bullet) \propto -\frac{1}{2}(\tilde{\Pi} - (X_\pi \rho^\pi - \Lambda \tilde{u}))' \Omega_\pi^{-1} (\tilde{\Pi} - (X_\pi \rho^\pi - \Lambda \tilde{u}))$$

The second source comes from the state equation for ρ^π . We rewrite it in a matrix notation as follows,

$$H \rho^\pi = \varepsilon^{\rho^\pi} \quad \varepsilon^{\rho^\pi} \sim N(0, \Omega_{\rho^\pi}), \quad \text{where } \Omega_{\rho^\pi} = \text{diag}(\omega_{\rho^\pi}^2, \sigma_{\rho^\pi}^2, \dots, \sigma_{\rho^\pi}^2) \quad (68)$$

$$0 < \rho_t^\pi < 1 \text{ for } t=1, \dots, T$$

Ignoring any terms not involving ρ^π , the prior density for ρ^π is given by

$$\log p(\rho^\pi | \sigma_{\rho^\pi}^2, \Omega_{\rho^\pi}) \propto -\frac{1}{2}(\rho^\pi)' H' \Omega_{\rho^\pi}^{-1} H (\rho^\pi) + g_{\rho^\pi}(\rho^\pi, \sigma_{\rho^\pi}^2)$$

where,

$$g_{\rho^\pi}(\rho^\pi, \sigma_{\rho^\pi}^2) = -\sum_{t=2}^T \log \left(\Phi \left(\frac{1 - \rho_{t-1}^\pi}{\sigma_{\rho^\pi}} \right) - \Phi \left(\frac{0 - \rho_{t-1}^\pi}{\sigma_{\rho^\pi}} \right) \right)$$

Combining the above two conditional densities we obtain,

$$\log p(\rho^\pi | Y, \bullet) \propto -\frac{1}{2}(\rho^\pi - \hat{\rho}^\pi)' D_{\rho^\pi}^{-1} (\rho^\pi - \hat{\rho}^\pi) + g_{\rho^\pi}(\rho^\pi, \sigma_{\rho^\pi}^2)$$

where,

$$D_{\rho^\pi} = (H' \Omega_{\rho^\pi}^{-1} H + X_\pi' \Omega_\pi^{-1} X_\pi)^{-1}$$

$$\hat{\rho}^\pi = D_{\rho^\pi} (X_\pi' \Omega_\pi^{-1} (\tilde{\Pi} + \Lambda \tilde{u}))$$

The addition of the term $g_{\rho^\pi}(\rho^\pi, \sigma_{\rho^\pi}^2)$ leads to a non-standard density. Accordingly, I sample ρ^π using an independence-chain Metropolis-Hastings (MH) procedure. This involves first generating candidate draws from $N(\hat{\rho}^\pi, D_{\rho^\pi})$ using the precision-based algorithm that are then accepted or rejected based on the accept-reject Metropolis-Hastings (ARMH) algorithm (discussed in Chan and Strachan, 2012).

Step 9. Derive the conditional distribution $p(\lambda^\pi | Y, \bullet)$

The information about λ^π comes from two sources. Below, I derive an expression for each of these two sources.

First, I define some notation,

$$\tilde{\pi}_t = \pi_t - \pi_t^*$$

$$\tilde{u}_t = U_t - U_t^*$$

$$NW = (\tilde{\pi}_1 - \rho_1^\pi \tilde{\pi}_0, \dots, \tilde{\pi}_T - \rho_T^\pi \tilde{\pi}_{T-1})'$$

The first source is the price inflation measurement equation. Rewrite it in a matrix notation,

$$NW = X_u \lambda^\pi + \varepsilon^\pi \quad \varepsilon^\pi \sim N(0, \Omega_\pi) \quad (69)$$

where,

$$X_u = \text{diag}(\tilde{u}_1, \dots, \tilde{u}_T)$$

Ignoring any terms not involving λ^π , the likelihood is

$$\log p(\pi | \lambda^\pi, \bullet) \propto -\frac{1}{2}(NW - X_u \lambda^\pi)' \Omega_\pi^{-1} (NW - X_u \lambda^\pi)$$

The second source comes from the state equation for λ^π . We rewrite it in a matrix notation as follows,

$$H \lambda^\pi = \varepsilon^{\lambda^\pi} \quad \varepsilon^{\lambda^\pi} \sim N(0, \Omega_{\lambda^\pi}), \quad \text{where } \Omega_{\lambda^\pi} = \text{diag}(\omega_{\lambda^\pi}^2, \sigma_{\lambda^\pi}^2, \dots, \sigma_{\lambda^\pi}^2) \quad (70)$$

$$-1 < \lambda_t^\pi < 0 \text{ for } t=1, \dots, T$$

Ignoring any terms not involving λ^π , the prior density for λ^π is given by

$$\log p(\lambda^\pi | \sigma_{\lambda^\pi}^2, \Omega_{\lambda^\pi}) \propto -\frac{1}{2}(\lambda^\pi)' H' \Omega_{\lambda^\pi}^{-1} H (\lambda^\pi) + g_{\lambda^\pi}(\lambda^\pi, \sigma_{\lambda^\pi}^2)$$

where,

$$g_{\lambda^\pi}(\lambda^\pi, \sigma_{\lambda^\pi}^2) = -\sum_{t=2}^T \log \left(\Phi \left(\frac{0 - \lambda_{t-1}^\pi}{\sigma_{\lambda^\pi}} \right) - \Phi \left(\frac{-1 - \lambda_{t-1}^\pi}{\sigma_{\lambda^\pi}} \right) \right)$$

Combining the above two conditional densities we obtain,

$$\log p(\lambda^\pi | Y, \bullet) \propto -\frac{1}{2}(\lambda^\pi - \hat{\lambda}^\pi)' D_{\lambda^\pi}^{-1} (\lambda^\pi - \hat{\lambda}^\pi) + g_{\lambda^\pi}(\lambda^\pi, \sigma_{\lambda^\pi}^2)$$

where,

$$D_{\lambda^\pi} = (H' \Omega_{\lambda^\pi}^{-1} H + X_u' \Omega_\pi^{-1} X_u)^{-1}$$

$$\hat{\lambda}^\pi = D_{\lambda^\pi} (X_u' \Omega_\pi^{-1} NW)$$

The addition of the term $g_{\lambda^\pi}(\lambda^\pi, \sigma_{\lambda^\pi}^2)$ leads to a non-standard density. Accordingly, I sample λ^π using an independence-chain Metropolis-Hastings (MH) procedure. This involves first generating candidate draws from $N(\hat{\lambda}^\pi, D_{\lambda^\pi})$ using the precision-based algorithm that are then accepted or rejected based on the accept-reject Metropolis-Hastings (ARMH) algorithm (discussed in Chan and Strachan, 2012).

Step 10. Derive the conditional distribution $p(\rho^w|Y, \bullet)$

The information about ρ^w comes from two sources. Below, I derive an expression for each of these two sources.

First, I define some notation,

$$\begin{aligned}\tilde{w}_t &= w_t - w_t^* \\ \tilde{u}_t &= U_t - U_t^* \\ \tilde{w} &= (\tilde{w}_1, \dots, \tilde{w}_T)' \\ \tilde{u} &= (\tilde{u}_1, \dots, \tilde{u}_T)' \\ \tilde{\pi}_t &= \pi_t - \pi_t^* \\ \tilde{\pi} &= (\tilde{\pi}_1, \dots, \tilde{\pi}_T)'\end{aligned}$$

The first source is the wage inflation measurement equation. Rewrite it in a matrix notation,

$$\tilde{w} + \Lambda^w \tilde{u} + \Lambda^{w\pi} \tilde{\pi} = X_w \rho^w + \varepsilon^{\rho w} \quad \varepsilon^{\rho w} \sim N(0, \Omega_w) \quad (71)$$

where,

$$\begin{aligned}X_w &= \text{diag}(\tilde{w}_0, \dots, \tilde{w}_{T-1}) \\ \Lambda^w &= \text{diag}(-\lambda_1^w, \dots, -\lambda_T^w) \\ \Lambda^{w\pi} &= \text{diag}(-\kappa_1^w, \dots, -\kappa_T^w)\end{aligned}$$

Ignoring any terms not involving ρ^w , the likelihood is

$$\log p(w|\rho^w, \bullet) \propto -\frac{1}{2}(\tilde{w} - (X_w \rho^w - \Lambda^w \tilde{u} - \Lambda^{w\pi} \tilde{\pi}))' \Omega_w^{-1} (\tilde{w} - (X_w \rho^w - \Lambda^w \tilde{u} - \Lambda^{w\pi} \tilde{\pi}))$$

The second source comes from the state equation for ρ^w . We rewrite it in a matrix notation as follows,

$$H \rho^w = \varepsilon^{\rho w} \quad \varepsilon^{\rho w} \sim N(0, \Omega_{\rho w}), \quad \text{where } \Omega_{\rho w} = \text{diag}(\omega_{\rho w}^2, \sigma_{\rho w}^2, \dots, \sigma_{\rho w}^2) \quad (72)$$

$$0 < \rho_t^w < 1 \text{ for } t=1, \dots, T$$

Ignoring any terms not involving ρ^w , the prior density for ρ^w is given by

$$\log p(\rho^w | \sigma_{\rho w}^2, \Omega_{\rho w}) \propto -\frac{1}{2}(\rho^w)' H' \Omega_{\rho w}^{-1} H (\rho^w) + g_{\rho w}(\rho^w, \sigma_{\rho w}^2)$$

where,

$$g_{\rho^w}(\rho^w, \sigma_{\rho^w}^2) = - \sum_{t=2}^T \log \left(\Phi \left(\frac{1 - \rho_{t-1}^w}{\sigma_{\rho^w}} \right) - \Phi \left(\frac{0 - \rho_{t-1}^w}{\sigma_{\rho^w}} \right) \right)$$

Combining the above two conditional densities we obtain,

$$\log p(\rho^w | Y, \bullet) \propto -\frac{1}{2}(\rho^w - \hat{\rho}^w)' D_{\rho^w}^{-1}(\rho^w - \hat{\rho}^w) + g_{\rho^w}(\rho^w, \sigma_{\rho^w}^2)$$

where,

$$D_{\rho^w} = (H' \Omega_{\rho^w}^{-1} H + X_w' \Omega_w^{-1} X_w)^{-1}$$

$$\hat{\rho}^w = D_{\rho^w} (X_w' \Omega_w^{-1} (\tilde{w} + \Lambda^w \tilde{u} + \Lambda^{w\pi} \tilde{\pi}))$$

The addition of the term $g_{\rho^\pi}(\rho^\pi, \sigma_{\rho^\pi}^2)$ leads to a non-standard density. Accordingly, I sample ρ^π using an independence-chain Metropolis-Hastings (MH) procedure. This involves first generating candidate draws from $N(\hat{\rho}^\pi, D_{\rho^\pi})$ using the precision-based algorithm that are then accepted or rejected based on the accept-reject Metropolis-Hastings (ARMH) algorithm (discussed in Chan and Strachan, 2012).

Step 11. Derive the conditional distribution $p(\lambda^w | Y, \bullet)$

The information about λ^w comes from two sources. Below, I derive an expression for each of these two sources.

First, I define some notation,

$$\begin{aligned} \tilde{w}_t &= w_t - w_t^* \\ \tilde{u}_t &= U_t - U_t^* \\ \tilde{\pi}_t &= \pi_t - \pi_t^* \\ B^w &= (\tilde{w}_1 - \rho_1^w \tilde{w}_0 - \kappa_1^w \tilde{\pi}_1, \dots, \tilde{w}_T - \rho_T^w \tilde{w}_{T-1} - \kappa_{T-1}^w \tilde{\pi}_T)' \end{aligned}$$

The first source is the wage inflation measurement equation. Rewrite it in a matrix notation,

$$B^w = X_u \lambda^w + \varepsilon^w \quad \varepsilon^w \sim N(0, \Omega_w) \quad (73)$$

where,

$$X_u = \text{diag}(\tilde{u}_1, \dots, \tilde{u}_T)$$

Ignoring any terms not involving λ^w , the likelihood is

$$\log p(w | \lambda^w, \bullet) \propto -\frac{1}{2} (B^w - X_u \lambda^w)' \Omega_w^{-1} (B^w - X_u \lambda^w)$$

The second source comes from the state equation for λ^w . We rewrite it in a matrix notation as

follows,

$$H\lambda^w = \varepsilon^{\lambda w} \quad \varepsilon^{\lambda w} \sim N(0, \Omega_{\lambda w}), \quad \text{where } \Omega_{\lambda w} = \text{diag}(\omega_{\lambda w}^2, \sigma_{\lambda w}^2, \dots, \sigma_{\lambda w}^2) \quad (74)$$

$$-1 < \lambda_t^w < 0 \text{ for } t=1, \dots, T$$

Ignoring any terms not involving λ^w , the prior density for λ^w is given by

$$\log p(\lambda^w | \sigma_{\lambda w}^2, \Omega_{\lambda w}) \propto -\frac{1}{2}(\lambda^w)' H' \Omega_{\lambda w}^{-1} H(\lambda^w) + g_{\lambda w}(\lambda^w, \sigma_{\lambda w}^2)$$

where,

$$g_{\lambda w}(\lambda^w, \sigma_{\lambda w}^2) = -\sum_{t=2}^T \log \left(\Phi \left(\frac{0 - \lambda_{t-1}^w}{\sigma_{\lambda w}} \right) - \Phi \left(\frac{-1 - \lambda_{t-1}^w}{\sigma_{\lambda w}} \right) \right)$$

Combining the above two conditional densities we obtain,

$$\log p(\lambda^w | Y, \bullet) \propto -\frac{1}{2}(\lambda^w - \hat{\lambda}^w)' D_{\lambda^w}^{-1} (\lambda^w - \hat{\lambda}^w) + g_{\lambda w}(\lambda^w, \sigma_{\lambda w}^2)$$

where,

$$D_{\lambda^w} = (H' \Omega_{\lambda w}^{-1} H + X_u' \Omega_w^{-1} X_u)^{-1}$$

$$\hat{\lambda}^w = D_{\lambda^w} (X_u' \Omega_w^{-1} B^w)$$

The addition of the term $g_{\lambda w}(\lambda^w, \sigma_{\lambda w}^2)$ leads to a non-standard density. Accordingly, I sample λ^w using an independence-chain Metropolis-Hastings (MH) procedure. This involves first generating candidate draws from $N(\hat{\lambda}^w, D_{\lambda^w})$ using the precision-based algorithm that are then accepted or rejected based on the accept-reject Metropolis-Hastings (ARMH) algorithm (discussed in Chan and Strachan, 2012).

Step 12. Derive the conditional distribution $p(\kappa^w | Y, \bullet)$

The information about κ^w comes from two sources. Below, I derive an expression for each of these two sources.

First, I define some notation,

$$\begin{aligned} \tilde{w}_t &= w_t - w_t^* \\ \tilde{u}_t &= U_t - U_t^* \\ \tilde{\pi}_t &= \pi_t - \pi_t^* \\ B^{\kappa w} &= (\tilde{w}_1 - \rho_1^w \tilde{w}_0 - \lambda_1^w \tilde{u}_1, \dots, \tilde{w}_T - \rho_T^w \tilde{w}_{T-1} - \lambda_{T-1}^w \tilde{u}_T)' \end{aligned}$$

The first source is the wage inflation measurement equation. Rewrite it in a matrix notation,

$$B^{\kappa w} = X_{\pi} \kappa^w + \varepsilon^w \quad \varepsilon^w \sim N(0, \Omega_w) \quad (75)$$

where,

$$X_\pi = \text{diag}(\tilde{\pi}_1, \dots, \tilde{\pi}_T)$$

Ignoring any terms not involving κ^w , the likelihood is

$$\log p(w|\kappa^w, \bullet) \propto -\frac{1}{2}(B^{\kappa w} - X_\pi \kappa^w)' \Omega_w^{-1} (B^{\kappa w} - X_\pi \kappa^w)$$

The second source comes from the state equation for κ^w . We rewrite it in a matrix notation as follows,

$$H\kappa^w = \varepsilon^{\kappa w} \quad \varepsilon^{\kappa w} \sim N(0, \Omega_{\kappa w}), \quad \text{where } \Omega_{\kappa w} = \text{diag}(\omega_{\kappa w}^2, \sigma_{\kappa w}^2, \dots, \sigma_{\kappa w}^2) \quad (76)$$

Ignoring any terms not involving κ^w , the prior density for κ^w is given by

$$\log p(\kappa^w | \sigma_{\kappa w}^2, \Omega_{\kappa w}) \propto -\frac{1}{2}(\kappa^w)' H' \Omega_{\kappa w}^{-1} H (\kappa^w)$$

Combining the above two conditional densities we obtain,

$$\log p(\kappa^w | Y, \bullet) \propto -\frac{1}{2}(\kappa^w - \hat{\kappa}^w)' D_{\kappa^w}^{-1} (\kappa^w - \hat{\kappa}^w)$$

where,

$$D_{\kappa^w} = (H' \Omega_{\kappa w}^{-1} H + X_\pi' \Omega_w^{-1} X_\pi)^{-1}$$

$$\hat{\kappa}^w = D_{\kappa^w} (X_\pi' \Omega_w^{-1} B^{\kappa w})$$

The candidate draws are sampled from $N(\hat{\kappa}^w, D_{\kappa^w})$ using the precision-based algorithm.

Step 13. Derive the conditional distribution $p(h^u, h^o, h^p, h^\pi, h^w, h^i | Y, \bullet)$

Given parameters and other latent states, the stochastic volatility, $h^u, h^o, h^p, h^\pi, h^w, h^i$ are conditionally independent and so can be drawn separately. Following, Chan, Koop, and Potter (2013; 2016), I draw $h^u, h^o, h^p, h^\pi, h^w, h^i$ using the accept-reject independence-chain Metropolis Hastings (ARMH) algorithm of Chan and Strachan (2012; page 32-34).

Step 14. Derive the conditional distribution $p(C^u, C^g, C^\pi, C^r, \text{Wedge} | Y, \bullet)$

Given parameters and other latent states, C^u, C^g, C^π, C^r are conditionally independent and so can be drawn separately.

Beginning with C^u , the information about it comes from two sources. Below, I derive an expression for each of these two sources.

The first source is the measurement equation linking survey to U^* . Rewrite it in a matrix notation,

$$N^{zu} = C^u + \varepsilon^{zu} \quad \varepsilon^{zu} \sim N(0, \Omega_{zu}) \quad (77)$$

where,

$$\begin{aligned} n_t^{zu} &= Z_t^u - \beta^u U^* \\ N^{zu} &= (n_1^{zu}, n_2^{zu}, \dots, n_T^{zu})' \\ \Omega_{zu} &= \text{diag}(\sigma_{zu}^2, \dots, \sigma_{zu}^2) \end{aligned}$$

Ignoring any terms not involving C^u , the likelihood is

$$\log p(Z^u | C^u, \bullet) \propto -\frac{1}{2} (N^{zu} - C^u)' \Omega_{zu}^{-1} (N^{zu} - C^u)$$

The second source comes from the state equation for C^u . We rewrite it in a matrix notation as follows,

$$HC^u = \alpha_{cu} + \varepsilon^{cu} \quad \varepsilon^{cu} \sim N(0, \Omega_{cu}), \quad \text{where } \Omega_{cu} = \text{diag}(\omega_{cu}^2, \sigma_{cu}^2, \dots, \sigma_{cu}^2) \quad (78)$$

where,

$$\alpha_{cu} = \begin{pmatrix} C_0^u \\ 0 \\ 0 \\ \vdots \\ 0 \end{pmatrix}$$

Ignoring any terms not involving C^u , the prior density for C^u is given by

$$\log p(C^u | \sigma_{cu}^2, \Omega_{cu}) \propto -\frac{1}{2} (C^u - H^{-1} \alpha_{cu})' H' \Omega_{cu}^{-1} H (C^u - H^{-1} \alpha_{cu})$$

Combining the above two conditional densities we obtain,

$$\log p(C^u | Y, \bullet) \propto -\frac{1}{2} (C^u - \hat{C}^u)' D_{C^u}^{-1} (C^u - \hat{C}^u)$$

where,

$$\begin{aligned} D_{C^u} &= (H' \Omega_{cu}^{-1} H + \Omega_{zu}^{-1})^{-1} \\ \hat{C}^u &= D_{C^u} (H' \Omega_{cu}^{-1} \alpha_{cu} + \Omega_{zu}^{-1} N^{zu}) \end{aligned}$$

The candidate draws are sampled from $N(\hat{C}^u, D_{C^u})$ using the precision-based algorithm.

Following similar logic,

$$N(\hat{C}^r, D_{C^r})$$

$$D_{C^r} = (H' \Omega_{cr}^{-1} H + \Omega_{zr}^{-1})^{-1}$$

$$\hat{C}^r = D_{C^r} (H' \Omega_{cr}^{-1} \alpha_{cr} + \Omega_{zr}^{-1} N^{zr})$$

where,

$$n_t^{zr} = Z_t^r - \beta^r r^*$$

$$N^{zr} = (n_1^{zr}, n_2^{zr}, \dots, n_T^{zr})'$$

$$\Omega_{zr} = \text{diag}(\sigma_{zr}^2, \dots, \sigma_{zr}^2)$$

$$N(\hat{C}^\pi, D_{C^\pi})$$

$$D_{C^\pi} = (H' \Omega_{c\pi}^{-1} H + \Omega_{z\pi}^{-1})^{-1}$$

$$\hat{C}^\pi = D_{C^\pi} (H' \Omega_{c\pi}^{-1} \alpha_{c\pi} + \Omega_{z\pi}^{-1} N^{z\pi})$$

where,

$$n_t^{z\pi} = Z_t^\pi - \beta^\pi \pi^*$$

$$N^{z\pi} = (n_1^{z\pi}, n_2^{z\pi}, \dots, n_T^{z\pi})'$$

$$\Omega_{z\pi} = \text{diag}(\sigma_{z\pi}^2, \dots, \sigma_{z\pi}^2)$$

$$N(\hat{C}^g, D_{C^g})$$

$$D_{C^g} = (H' \Omega_{cg}^{-1} H + \Omega_{zg}^{-1})^{-1}$$

$$\hat{C}^g = D_{C^g} (H' \Omega_{cg}^{-1} \alpha_{cg} + \Omega_{zg}^{-1} N^{zg})$$

where,

$$n_t^{zg} = Z_t^g + \beta^g \alpha_g - \beta^g g dp^*$$

$$N^{zg} = (n_1^{zg}, n_2^{zg}, \dots, n_T^{zg})'$$

$$\Omega_{zg} = \text{diag}(\sigma_{zg}^2, \dots, \sigma_{zg}^2)$$

$$\alpha_g = (g dp_0^*, 0, 0, \dots, 0)'$$

$$N(\hat{Wedge}, D_{Wedge})$$

$$D_{Wedge} = (H' \Omega_{wlr}^{-1} H + \Omega_{w*}^{-1})^{-1}$$

$$\hat{Wedge} = D_{Wedge} (H' \Omega_{wlr}^{-1} \alpha_{wedge} + \Omega_{w*}^{-1} N^{wedge})$$

where,

$$\begin{aligned}
n_t^{wedge} &= W_t^* - P_t^* - \pi_{*t} \\
N^{wedge} &= (n_1^{wedge}, n_2^{wedge}, \dots, n_T^{wedge})' \\
\Omega_{w*} &= \text{diag}(\sigma_{w*}^2, \dots, \sigma_{w*}^2) \\
\Omega_{wlr} &= \text{diag}(\omega_{wlr}^2, \sigma_{wlr}^2, \dots, \sigma_{wlr}^2) \\
\alpha_{wedge} &= (Wedge_0, 0, 0, \dots, 0)'
\end{aligned}$$

Step 15. Derive the conditional distribution $p(D|Y, \bullet)$

Given the posterior draws of r^* , ζ , and g^* , the posterior draw for D is constructed as,

$$D = r^* - \zeta g^* \tag{79}$$

Step 16. Derive the conditional distribution $p(\theta|Y, \bullet)$

There are 41 parameters in the vector θ . These parameters are drawn in 39 separate blocks using standard regression procedures. Following similar notation to Chan, Koop, and Potter (2016), I denote θ_{-x} to refer all parameters in θ except the parameter x .

Substep 16.1 Derive the conditional distribution $p(\rho^u|Y, \bullet)$

Given the stationary constraints, $\rho_1^u + \rho_2^u < 1$, $\rho_2^u - \rho_1^u < 1$, and $|\rho_2^u| < 1$

$\rho^u = (\rho_1^u, \rho_2^u)'$ is a bivariate truncated normal. To obtain draws from this truncated normal distribution, ARMH sampling algorithm is applied to the candidate draws from the proposal density, $N(\hat{\rho}^u, D_{\rho u})$.

$$\begin{aligned}
D_{\rho u} &= (V_{\rho u}^{-1} + X_u' \Omega_u^{-1} X_u)^{-1} \\
\hat{\rho}^u &= D_{\rho u} (V_{\rho u}^{-1} \rho_0^u + X_u' \Omega_{wlr}^{-1} (\tilde{u} - \phi^u \text{ogap}))
\end{aligned}$$

where,

$V_{\rho u}^{-1}$ is the prior variance and ρ_0^u is the prior mean,

$$X_u = \begin{pmatrix} \tilde{u}_0 & \tilde{u}_{-1} \\ \tilde{u}_1 & \tilde{u}_0 \\ \vdots & \\ \tilde{u}_{T-1} & \tilde{u}_{T-2} \end{pmatrix}$$

Substep 16.2 Derive the conditional distribution $p(\sigma_{hu}^2|Y, \bullet)$

$p(\sigma_{hu}^2|Y, \bullet)$ is a standard inverse-Gamma density,

Candidate draws are sampled from

$$p(\sigma_{hu}^2|Y, \bullet) \sim IG(\nu_{hu0} + \frac{T-1}{2}, S_{hu0} + \frac{1}{2} \sum_{t=2}^T (h_t^u - h_{t-1}^u)^2)$$

Substep 16.3 Derive the conditional distribution $p(\phi^u|Y, \bullet)$

Given the constraint $\phi^u < 0$, the conditional distribution $p(\phi^u|Y, \bullet)$ is a truncated normal density. The candidate draws are sampled from the proposal distribution $N(\hat{\phi}^u, D_{\phi^u})$ using the precision-based algorithm, and a simple accept-reject step is applied to the candidate draws.

Rewrite the unemployment rate (gap) measurement equation in matrix notation as

$$Y^\phi = \phi^u \text{ogap} + \varepsilon^u \quad \varepsilon^u \sim N(0, \Omega_u) \quad (80)$$

where,

$$y_t^\phi = \tilde{u}_t - \rho_1^u \tilde{u}_{t-1} - \rho_2^u \tilde{u}_{t-2}$$

$$Y^\phi = (y_1^\phi, \dots, y_T^\phi)'$$

$$D_{\phi^u} = (V_{\phi^u}^{-1} + \text{ogap}' \Omega_u^{-1} \text{ogap})^{-1}$$

$$\hat{\phi}^u = D_{\phi^u} (V_{\phi^u}^{-1} \phi_0^u + \text{ogap}' \Omega_u^{-1} Y^\phi)$$

where,

$V_{\phi^u}^{-1}$ is the prior variance and ϕ_0^u is the prior mean,

Substep 16.4 Derive the conditional distribution $p(\sigma_{u*}^2|Y, \bullet)$

$p(\sigma_{u*}^2|Y, \bullet)$ is a non-standard density because U^* is a bounded random walk,

$$\log p(\sigma_{u*}^2|Y, \bullet) \propto -(\nu_{u*0} + 1) \log \sigma_{u*}^2 - \frac{S_{u*0}}{\sigma_{u*}^2} - \frac{T-1}{2} \log \sigma_{u*}^2 - \frac{1}{2\sigma_{u*}^2} \sum_{t=2}^T (U_t^* - U_{t-1}^*)^2 + g_{u*}(U^*, \sigma_{u*}^2)$$

The candidate draws from $p(\sigma_{u*}^2|Y, \bullet)$ are obtained via the MH step with the proposal density

$$IG(\nu_{u*0} + \frac{T-1}{2}, S_{u*0} + \frac{1}{2} \sum_{t=2}^T (U_t^* - U_{t-1}^*)^2)$$

Substep 16.5 Derive the conditional distribution $p(\beta^u|Y, \bullet)$

Candidate draws are sampled from $N(\hat{\beta}^u, D_{\beta u})$ using the precision-based algorithm.

where,

$$D_{\beta u} = (V_{\beta u}^{-1} + U^{*'}\Omega_{zu}^{-1}U^*)^{-1}$$

$$\hat{\beta}^u = D_{\beta u}(V_{\beta u}^{-1}\beta_0^u + U^{*'}\Omega_{zu}^{-1}J^{zu})$$

$$j_t^{zu} = Z_t^u - C_t^u$$

$$J^{zu} = (j_1^{zu}, \dots, j_T^{zu})'$$

$V_{\beta u}^{-1}$ is the prior variance and β_0^u is the prior mean for β^u

Substep 16.6 Derive the conditional distribution $p(\sigma_{zu}^2|Y, \bullet)$

$p(\sigma_{zu}^2|Y, \bullet)$ is a standard inverse-Gamma density,

Candidate draws are sampled from

$$p(\sigma_{zu}^2|Y, \bullet) \sim IG(\nu_{zu0} + \frac{T}{2}, S_{zu0} + \frac{1}{2} \sum_{t=1}^T (Z_t^u - C_t^u - \beta^u U^*)^2)$$

Substep 16.7 Derive the conditional distribution $p(\sigma_{cu}^2|Y, \bullet)$

$p(\sigma_{cu}^2|Y, \bullet)$ is a standard inverse-Gamma density,

Candidate draws are sampled from

$$p(\sigma_{cu}^2|Y, \bullet) \sim IG(\nu_{cu0} + \frac{T-1}{2}, S_{cu0} + \frac{1}{2} \sum_{t=2}^T (C_t^u - C_{t-1}^u)^2)$$

Substep 16.8 Derive the conditional distribution $p(\sigma_{gdp^*}^2|Y, \bullet)$

$p(\sigma_{gdp^*}^2|Y, \bullet)$ is a standard inverse-Gamma density,

Candidate draws are sampled from

$$p(\sigma_{gdp^*}^2|Y, \bullet) \sim IG(\nu_{gdp^*0} + \frac{T-1}{2}, S_{gdp^*0} + (gdp^* - \alpha_{gdp^*})' * H_2 H_2 * (gdp^* - \alpha_{gdp^*})/2)$$

where (although they are defined above but for convenience I redefine them),

$$\alpha_{gdp^*} = \begin{pmatrix} gdp_0^* + \Delta gdp_0^* \\ -gdp_0^* \\ 0 \\ \vdots \\ 0 \end{pmatrix}, \quad H_2 = \begin{pmatrix} 1 & 0 & 0 & 0 & \cdots & 0 \\ -2 & 1 & 0 & 0 & \cdots & 0 \\ 1 & -2 & 1 & 0 & \cdots & 0 \\ 0 & 1 & -2 & 1 & \cdots & 0 \\ \vdots & & & & \ddots & \vdots \\ 0 & \cdots & 0 & 1 & -2 & 1 \end{pmatrix}$$

H_2 is a band matrix with unit determinant and hence is invertible.

Substep 16.9 Derive the conditional distribution $p(\rho^g|Y, \bullet)$

Given the stationary constraints, $\rho_1^g + \rho_2^g < 1$, $\rho_2^g - \rho_1^g < 1$, and $|\rho_2^g| < 1$

$\rho^g = (\rho_1^g, \rho_2^g)'$ is a bivariate truncated normal. To obtain draws from this truncated normal distribution, ARMH sampling algorithm is applied to the candidate draws from the proposal density, $N(\hat{\rho}^g, D_{\rho g})$.

$$D_{\rho g} = (V_{\rho g}^{-1} + X'_{\rho g} \Omega_{ogap}^{-1} X_{\rho g})^{-1}$$

$$\hat{\rho}^g = D_{\rho g} (V_{\rho g}^{-1} \rho_0^g + X'_{\rho g} \Omega_{ogap}^{-1} Y_{ogap})$$

where,

$V_{\rho g}^{-1}$ is the prior variance and ρ_0^g is the prior mean,

$$X_{\rho g} = \begin{pmatrix} 0 & 0 \\ ogap_1 & 0 \\ ogap_2 & ogap_1 \\ \vdots & \\ ogap_{T-1} & ogap_{T-2} \end{pmatrix}$$

$$y_t^{ogap} = ogap_t - a^r(r_t - r_{t-1}) - \lambda^g \tilde{u}_t$$

$$Y_{ogap} = (y_1^{ogap}, \dots, y_T^{ogap})'$$

Substep 16.10 Derive the conditional distribution $p(a^r|Y, \bullet)$

Candidate draws are sampled from $N(\hat{a}^r, D_{ar})$ using the precision-based algorithm.

where,

$$D_{ar} = (V_{ar}^{-1} + X'_{ar} \Omega_{ogap}^{-1} X_{ar})^{-1}$$

$$\hat{a}^r = D_{ar} (V_{ar}^{-1} a_0^r + X'_{ar} \Omega_{ogap}^{-1} J^{ar})$$

$$j_t^{ar} = ogap_t - \rho_1^g ogap_{t-1} - \rho_2^g ogap_{t-2} - \lambda^g \tilde{u}_t$$

$$J^{ar} = (j_1^{ar}, \dots, j_T^{ar})'$$

$$X_{ar} = (\tilde{r}_1, \dots, \tilde{r}_T)'$$

$$\tilde{r}_t = r_t - r_t^*$$

V_{ar}^{-1} is the prior variance and a_0^r is the prior mean for a^r

Substep 16.11 Derive the conditional distribution $p(\lambda^g|Y, \bullet)$

Given the constraint $\lambda^g < 0$, the conditional distribution $p(\lambda^g|Y, \bullet)$ is a truncated normal density. The candidate draws are sampled from the proposal distribution $N(\hat{\lambda}^g, D_{\lambda^g})$ using the precision-based algorithm, and a simple accept-reject step is applied to the candidate draws.

where,

$$D_{\lambda^g} = (V_{\lambda^g}^{-1} + X_u' \Omega_{ogap}^{-1} X_u)^{-1}$$

$$\hat{\lambda}^g = D_{\lambda^g} (V_{\lambda^g}^{-1} \lambda_0^g + X_u' \Omega_{ogap}^{-1} B^g)$$

$$b_t^g = ogap_t - \rho_1^g ogap_{t-1} - \rho_2^g ogap_{t-2} - a^r \tilde{r}_t$$

$$B^g = (b_1^g, \dots, b_T^g)'$$

$$X_u = diag(\tilde{u}_1, \dots, \tilde{u}_T)'$$

$$\tilde{r}_t = r_t - r_t^*$$

$V_{\lambda^g}^{-1}$ is the prior variance and λ_0^g is the prior mean for λ^g

Substep 16.12 Derive the conditional distribution $p(\sigma_{ho}^2|Y, \bullet)$

$p(\sigma_{ho}^2|Y, \bullet)$ is a standard inverse-Gamma density,

Candidate draws are sampled from

$$p(\sigma_{ho}^2|Y, \bullet) \sim IG(\nu_{ho0} + \frac{T-1}{2}, S_{ho0} + \frac{1}{2} \sum_{t=2}^T (h_t^o - h_{t-1}^o)^2)$$

Substep 16.13 Derive the conditional distribution $p(\sigma_{zg}^2|Y, \bullet)$

$p(\sigma_{zg}^2|Y, \bullet)$ is a standard inverse-Gamma density,

Candidate draws are sampled from

$$p(\sigma_{zg}^2|Y, \bullet) \sim IG(\nu_{zg0} + \frac{T}{2}, S_{zg0} + \frac{1}{2} \sum_{t=1}^T (Z_t^g - C_t^g - \beta^g gdp_{t-1}^* + \beta^g gdp_t^*)^2)$$

Substep 16.14 Derive the conditional distribution $p(\sigma_{cg}^2|Y, \bullet)$

$p(\sigma_{cg}^2|Y, \bullet)$ is a standard inverse-Gamma density,

Candidate draws are sampled from

$$p(\sigma_{cg}^2|Y, \bullet) \sim IG(\nu_{cg0} + \frac{T-1}{2}, S_{cg0} + \frac{1}{2} \sum_{t=2}^T (C_t^g - C_{t-1}^g)^2)$$

Substep 16.15 Derive the conditional distribution $p(\beta^g|Y, \bullet)$

Candidate draws are sampled from $N(\hat{\beta}^g, D_{\beta g})$ using the precision-based algorithm.

where,

$$D_{\beta g} = (V_{\beta g}^{-1} + (Hgd p^* - \alpha_g)' \Omega_{zg}^{-1} (Hgd p^* - \alpha_g))^{-1}$$

$$\hat{\beta}^g = D_{\beta g} (V_{\beta g}^{-1} \beta_0^g + (Hgd p^* - \alpha_g) \Omega_{zg}^{-1} J^{zg})$$

$$j_t^{zg} = Z_t^g - C_t^g$$

$$J^{zg} = (j_1^{zg}, \dots, j_T^{zg})'$$

$$\alpha_g = (gd p_0^*, 0, 0, \dots, 0)'$$

$V_{\beta g}^{-1}$ is the prior variance and β_0^g is the prior mean for β^g

Substep 16.16 Derive the conditional distribution $p(\rho^p | Y, \bullet)$

Given the stationary constraint, $|\rho^p| < 1$

ρ^p is a truncated normal. To obtain draws from this truncated normal distribution, AR sampling step is applied to the candidate draws from the proposal density, $N(\hat{\rho}^p, D_{\rho p})$.

$$D_{\rho p} = (V_{\rho p}^{-1} + X'_{prod} \Omega_P^{-1} X_{prod})^{-1}$$

$$\hat{\rho}^p = D_{\rho p} (V_{\rho p}^{-1} \rho_0^p + X'_{prod} \Omega_P^{-1} Y^{prod})$$

where,

$V_{\rho p}^{-1}$ is the prior variance and ρ_0^p is the prior mean,

$$\tilde{p}_t = P_t - P_t^*$$

$$X_{prod} = (\tilde{p}_0, \dots, \tilde{p}_{T-1})'$$

$$y_t^{prod} = \tilde{p}_t - \lambda_t^p \tilde{u}_t$$

$$Y^{prod} = (y_1^{prod}, \dots, y_T^{prod})'$$

Substep 16.17 Derive the conditional distribution $p(\sigma_{hp}^2 | Y, \bullet)$

$p(\sigma_{hp}^2 | Y, \bullet)$ is a standard inverse-Gamma density,

Candidate draws are sampled from

$$p(\sigma_{hp}^2|Y, \bullet) \sim IG(\nu_{hp0} + \frac{T-1}{2}, S_{hp0} + \frac{1}{2} \sum_{t=2}^T (h_t^p - h_{t-1}^p)^2)$$

Substep 16.18 Derive the conditional distribution $p(\sigma_{p^*}^2|Y, \bullet)$

$p(\sigma_{p^*}^2|Y, \bullet)$ is a standard inverse-Gamma density,

Candidate draws are sampled from

$$p(\sigma_{p^*}^2|Y, \bullet) \sim IG(\nu_{p^*0} + \frac{T-1}{2}, S_{p^*0} + \frac{1}{2} \sum_{t=2}^T (P_t^* - P_{t-1}^*)^2)$$

Substep 16.19 Derive the conditional distribution $p(\sigma_{\lambda^\pi}^2|Y, \bullet)$

$p(\sigma_{\lambda^\pi}^2|Y, \bullet)$ is a non-standard density because of the constraints on λ^π ,

$$\log p(\sigma_{\lambda^\pi}^2|Y, \bullet) \propto -(\nu_{\lambda^\pi0} + 1) \log \sigma_{\lambda^\pi}^2 - \frac{S_{\lambda^\pi0}}{\sigma_{\lambda^\pi}^2} - \frac{T-1}{2} \log \sigma_{\lambda^\pi}^2 - \frac{1}{2\sigma_{\lambda^\pi}^2} \sum_{t=2}^T (\lambda_t^\pi - \lambda_{t-1}^\pi)^2 + g_{\lambda^\pi}(\lambda^\pi, \sigma_{\lambda^\pi}^2)$$

The candidate draws from $p(\sigma_{\lambda^\pi}^2|Y, \bullet)$ are obtained via the MH step with the proposal density

$$IG(\nu_{\lambda^\pi0} + \frac{T-1}{2}, S_{\lambda^\pi0} + \frac{1}{2} \sum_{t=2}^T (\lambda_t^\pi - \lambda_{t-1}^\pi)^2)$$

Substep 16.20 Derive the conditional distribution $p(\sigma_{\rho^\pi}^2|Y, \bullet)$

$p(\sigma_{\rho^\pi}^2|Y, \bullet)$ is a non-standard density because of the constraints on ρ^π ,

$$\log p(\sigma_{\rho^\pi}^2|Y, \bullet) \propto -(\nu_{\rho^\pi0} + 1) \log \sigma_{\rho^\pi}^2 - \frac{S_{\rho^\pi0}}{\sigma_{\rho^\pi}^2} - \frac{T-1}{2} \log \sigma_{\rho^\pi}^2 - \frac{1}{2\sigma_{\rho^\pi}^2} \sum_{t=2}^T (\rho_t^\pi - \rho_{t-1}^\pi)^2 + g_{\rho^\pi}(\rho^\pi, \sigma_{\rho^\pi}^2)$$

The candidate draws from $p(\sigma_{\rho^\pi}^2|Y, \bullet)$ are obtained via the MH step with the proposal density

$$IG(\nu_{\rho^\pi0} + \frac{T-1}{2}, S_{\rho^\pi0} + \frac{1}{2} \sum_{t=2}^T (\rho_t^\pi - \rho_{t-1}^\pi)^2)$$

Substep 16.21 Derive the conditional distribution $p(\sigma_{h^\pi}^2|Y, \bullet)$

$p(\sigma_{h^\pi}^2|Y, \bullet)$ is a standard inverse-Gamma density,

Candidate draws are sampled from

$$p(\sigma_{h^\pi}^2|Y, \bullet) \sim IG(\nu_{h^\pi0} + \frac{T-1}{2}, S_{h^\pi0} + \frac{1}{2} \sum_{t=2}^T (h_t^\pi - h_{t-1}^\pi)^2)$$

Substep 16.22 Derive the conditional distribution $p(\sigma_{\pi^*}^2|Y, \bullet)$

$p(\sigma_{\pi^*}^2|Y, \bullet)$ is a standard inverse-Gamma density,

Candidate draws are sampled from

$$p(\sigma_{\pi^*}^2|Y, \bullet) \sim IG(\nu_{\pi^*0} + \frac{T-1}{2}, S_{\pi^*0} + \frac{1}{2} \sum_{t=2}^T (\pi_t^* - \pi_{t-1}^*)^2)$$

Substep 16.23 Derive the conditional distribution $p(\sigma_{z^\pi}^2|Y, \bullet)$

$p(\sigma_{z^\pi}^2|Y, \bullet)$ is a standard inverse-Gamma density,

Candidate draws are sampled from

$$p(\sigma_{z^\pi}^2|Y, \bullet) \sim IG(\nu_{z^\pi0} + \frac{T}{2}, S_{z^\pi0} + \frac{1}{2} \sum_{t=1}^T (Z_t^\pi - C_t^\pi - \beta^\pi \pi^*)^2)$$

Substep 16.24 Derive the conditional distribution $p(\sigma_{c^\pi}^2|Y, \bullet)$

$p(\sigma_{c^\pi}^2|Y, \bullet)$ is a standard inverse-Gamma density,

Candidate draws are sampled from

$$p(\sigma_{c^\pi}^2|Y, \bullet) \sim IG(\nu_{c^\pi0} + \frac{T-1}{2}, S_{c^\pi0} + \frac{1}{2} \sum_{t=2}^T (C_t^\pi - C_{t-1}^\pi)^2)$$

Substep 16.25 Derive the conditional distribution $p(\beta^\pi|Y, \bullet)$

Candidate draws are sampled from $N(\hat{\beta}^\pi, D_{\beta^\pi})$ using the precision-based algorithm.

where,

$$D_{\beta^\pi} = (V_{\beta^\pi}^{-1} + \pi^{*\prime} \Omega_{z^\pi}^{-1} \pi^*)^{-1}$$

$$\hat{\beta}^\pi = D_{\beta^\pi} (V_{\beta^\pi}^{-1} \beta_0^\pi + \pi^{*\prime} \Omega_{z^\pi}^{-1} J^{z^\pi})$$

$$j_t^{z^\pi} = Z_t^\pi - C_t^\pi$$

$$J^{z^\pi} = (j_1^{z^\pi}, \dots, j_T^{z^\pi})'$$

$V_{\beta^\pi}^{-1}$ is the prior variance and β_0^π is the prior mean for β^π

Substep 16.26 Derive the conditional distribution $p(\sigma_{w^*}^2|Y, \bullet)$

$p(\sigma_{w^*}^2|Y, \bullet)$ is a standard inverse-Gamma density,

Candidate draws are sampled from

$$p(\sigma_{w*}^2|Y, \bullet) \sim IG(\nu_{w*0} + \frac{T-1}{2}, S_{w*0} + \frac{1}{2} \sum_{t=2}^T (w_t^* - \pi_t^* - P_t^*)^2)$$

Substep 16.27 Derive the conditional distribution $p(\sigma_{hw}^2|Y, \bullet)$

$p(\sigma_{hw}^2|Y, \bullet)$ is a standard inverse-Gamma density,

Candidate draws are sampled from

$$p(\sigma_{hw}^2|Y, \bullet) \sim IG(\nu_{hw0} + \frac{T-1}{2}, S_{hw0} + \frac{1}{2} \sum_{t=2}^T (h_t^w - h_{t-1}^w)^2)$$

Substep 16.28 Derive the conditional distribution $p(\sigma_{\rho w}^2|Y, \bullet)$

$p(\sigma_{\rho w}^2|Y, \bullet)$ is a non-standard density because of the constraints on ρ^w ,

$$\log p(\sigma_{\rho w}^2|Y, \bullet) \propto -(\nu_{\rho w0}+1)\log \sigma_{\rho w}^2 - \frac{S_{\rho w0}}{\sigma_{\rho w}^2} - \frac{T-1}{2}\log \sigma_{\rho w}^2 - \frac{1}{2\sigma_{\rho w}^2} \sum_{t=2}^T (\rho_t^w - \rho_{t-1}^w)^2 + g_{\rho w}(\rho^w, \sigma_{\rho w}^2)$$

The candidate draws from $p(\sigma_{\rho w}^2|Y, \bullet)$ are obtained via the MH step with the proposal density

$$IG(\nu_{\rho w0} + \frac{T-1}{2}, S_{\rho w0} + \frac{1}{2} \sum_{t=2}^T (\rho_t^w - \rho_{t-1}^w)^2)$$

Substep 16.29 Derive the conditional distribution $p(\sigma_{\lambda w}^2|Y, \bullet)$

$p(\sigma_{\lambda w}^2|Y, \bullet)$ is a non-standard density because of the constraints on λ^w ,

$$\log p(\sigma_{\lambda w}^2|Y, \bullet) \propto -(\nu_{\lambda w0}+1)\log \sigma_{\lambda w}^2 - \frac{S_{\lambda w0}}{\sigma_{\lambda w}^2} - \frac{T-1}{2}\log \sigma_{\lambda w}^2 - \frac{1}{2\sigma_{\lambda w}^2} \sum_{t=2}^T (\lambda_t^w - \lambda_{t-1}^w)^2 + g_{\lambda w}(\lambda^w, \sigma_{\lambda w}^2)$$

The candidate draws from $p(\sigma_{\lambda w}^2|Y, \bullet)$ are obtained via the MH step with the proposal density

$$IG(\nu_{\lambda w0} + \frac{T-1}{2}, S_{\lambda w0} + \frac{1}{2} \sum_{t=2}^T (\lambda_t^w - \lambda_{t-1}^w)^2)$$

Substep 16.30 Derive the conditional distribution $p(\sigma_{\kappa w}^2|Y, \bullet)$

The candidate draws are obtained from

$$IG(\nu_{\kappa w0} + \frac{T-1}{2}, S_{\kappa w0} + \frac{1}{2} \sum_{t=2}^T (\kappa_t^w - \kappa_{t-1}^w)^2)$$

Substep 16.31 Derive the conditional distribution $p(\rho^i|Y, \bullet)$

Given the constraint $|\rho^i| < 1$, the conditional distribution $p(\rho^i|Y, \bullet)$ is a truncated normal density. The candidate draws are sampled from the proposal distribution $N(\hat{\rho}^i, D_{\rho^i})$ using the precision-based algorithm, and a simple accept-reject step is applied to the candidate draws.

where,

$$D_{\rho^i} = (V_{\rho^i}^{-1} + X'_{\rho^i} \Omega_i^{-1} X_{\rho^i})^{-1}$$

$$\hat{\rho}^i = D_{\rho^i} (V_{\rho^i}^{-1} \rho_0^i + X'_{\rho^i} \Omega_i^{-1} M^{\rho^i})$$

$$m_t^{\rho^i} = i_t - \pi_t^* - r_t^* - \lambda^i \tilde{u}_t - \kappa^i \tilde{\pi}_t$$

$$M^{\rho^i} = (m_1^{\rho^i}, \dots, m_T^{\rho^i})'$$

$$X_{\rho^i} = (i_0 - \pi_0^* - r_0^*, \dots, i_{T-1} - \pi_{T-1}^* - r_{T-1}^*)'$$

$V_{\rho^i}^{-1}$ is the prior variance and ρ_0^i is the prior mean for ρ^i

Substep 16.32 Derive the conditional distribution $p(\lambda^i|Y, \bullet)$

The candidate draws are sampled from the proposal distribution $N(\hat{\lambda}^i, D_{\lambda^i})$ using the precision-based algorithm.

where,

$$D_{\lambda^i} = (V_{\lambda^i}^{-1} + X'_{\lambda^i} \Omega_i^{-1} X_{\lambda^i})^{-1}$$

$$\hat{\lambda}^i = D_{\lambda^i} (V_{\lambda^i}^{-1} \lambda_0^i + X'_{\lambda^i} \Omega_i^{-1} M^{\lambda^i})$$

$$m_t^{\lambda^i} = i_t - \pi_t^* - r_t^* - \rho^i (i_{t-1} - \pi_{t-1}^* - r_{t-1}^*) - \kappa^i \tilde{\pi}_t$$

$$M^{\lambda^i} = (m_1^{\lambda^i}, \dots, m_T^{\lambda^i})'$$

$$X_{\lambda^i} = (\tilde{u}_1, \dots, \tilde{u}_T)'$$

$V_{\lambda^i}^{-1}$ is the prior variance and λ_0^i is the prior mean for λ^i

Substep 16.33 Derive the conditional distribution $p(\kappa^i|Y, \bullet)$

The candidate draws are sampled from the proposal distribution $N(\hat{\kappa}^i, D_{\kappa^i})$ using the precision-based algorithm.

where,

$$D_{\kappa i} = (V_{\kappa i}^{-1} + X'_{\kappa i} \Omega_i^{-1} X_{\kappa i})^{-1}$$

$$\hat{\kappa}^i = D_{\kappa i} (V_{\kappa i}^{-1} \kappa_0^i + X'_{\kappa i} \Omega_i^{-1} M^{\kappa i})$$

$$m_t^{\kappa i} = i_t - \pi_t^* - r_t^* - \rho^i (i_{t-1} - \pi_{t-1}^* - r_{t-1}^*) - \lambda^i \tilde{u}_t$$

$$M^{\kappa i} = (m_1^{\kappa i}, \dots, m_T^{\kappa i})'$$

$$X_{\kappa i} = (\tilde{\pi}_1, \dots, \tilde{\pi}_T)'$$

$V_{\kappa i}^{-1}$ is the prior variance and κ_0^i is the prior mean for κ^i

Substep 16.34 Derive the conditional distribution $p(\sigma_{hi}^2 | Y, \bullet)$

$p(\sigma_{hi}^2 | Y, \bullet)$ is a standard inverse-Gamma density,

Candidate draws are sampled from

$$p(\sigma_{hi}^2 | Y, \bullet) \sim IG(\nu_{hi0} + \frac{T-1}{2}, S_{hi0} + \frac{1}{2} \sum_{t=2}^T (h_t^i - h_{t-1}^i)^2)$$

Substep 16.35 Derive the conditional distribution $p(\sigma_{zr}^2 | Y, \bullet)$

$p(\sigma_{zr}^2 | Y, \bullet)$ is a standard inverse-Gamma density,

Candidate draws are sampled from

$$p(\sigma_{zr}^2 | Y, \bullet) \sim IG(\nu_{zr0} + \frac{T}{2}, S_{zr0} + \frac{1}{2} \sum_{t=1}^T (Z_t^r - C_t^r - \beta^r r_t^*)^2)$$

Substep 16.36 Derive the conditional distribution $p(\sigma_{cr}^2 | Y, \bullet)$

$p(\sigma_{cr}^2 | Y, \bullet)$ is a standard inverse-Gamma density,

Candidate draws are sampled from

$$p(\sigma_{cr}^2 | Y, \bullet) \sim IG(\nu_{cr0} + \frac{T-1}{2}, S_{cr0} + \frac{1}{2} \sum_{t=2}^T (C_t^r - C_{t-1}^r)^2)$$

Substep 16.37 Derive the conditional distribution $p(\beta^r | Y, \bullet)$

Candidate draws are sampled from $N(\hat{\beta}^r, D_{\beta r})$ using the precision-based algorithm.

where,

$$D_{\beta r} = (V_{\beta r}^{-1} + r^{*'} \Omega_{zr}^{-1} r^*)^{-1}$$

$$\hat{\beta}^r = D_{\beta^r}(V_{\beta^r}^{-1}\beta_0^r + r^{*'}\Omega_{z^r}^{-1}J^{zr})$$

$$j_t^{zr} = Z_t^r - C_t^r$$

$$J^{zr} = (j_1^{zr}, \dots, j_T^{zr})'$$

$V_{\beta^r}^{-1}$ is the prior variance and β_0^r is the prior mean for β^r

Substep 16.38 Derive the conditional distribution $p(\sigma_d^2|Y, \bullet)$

$p(\sigma_d^2|Y, \bullet)$ is a standard inverse-Gamma density,

Candidate draws are sampled from

$$p(\sigma_d^2|Y, \bullet) \sim IG(\nu_{d0} + \frac{T-1}{2}, S_{d0} + \frac{1}{2} \sum_{t=2}^T (D_t - D_{t-1})^2)$$

Substep 16.39 Derive the conditional distribution $p(\sigma_{wlr}^2|Y, \bullet)$

$p(\sigma_{wlr}^2|Y, \bullet)$ is a standard inverse-Gamma density,

Candidate draws are sampled from

$$p(\sigma_{wlr}^2|Y, \bullet) \sim IG(\nu_{wlr0} + \frac{T-1}{2}, S_{wlr0} + \frac{1}{2} \sum_{t=2}^T (Wedge_t - Wedge_{t-1})^2)$$

A5.d Marginal likelihood computation

Bayesian model comparison is based on the marginal likelihood (marginal data density) metric. In computing marginal likelihood for various models, I use the approach proposed by CCK, which decomposes the marginal density of the data (e.g., inflation) into the product of predictive likelihoods. This approach allows us to separately compute marginal data density for each variable of interest: inflation, nominal wages, interest rate, real GDP, the unemployment rate, and labor productivity. The variable-specific marginal densities prove quite useful because they allow for deeper insights about the source of the deficiencies, which in turn helps differentiate models at a more disaggregated level.

Specifically, the marginal data density of the variables of interest is computed as follows,

$$p(y^j | X_i^j, M_i) = \prod_{t=3}^T p(y_t^j | y_{1:t-1}^j, X_{1:t,i}^j, M_i) \quad (81)$$

where, $j =$ PCE inflation (π), unemployment rate (ur), real GDP (gdp), labor productivity ($prod$), nominal wage inflation ($wage$), nominal short-term interest rate (int); $p(y_t^j | y_{1:t-1}^j, X_{1:t,i}^j, M_i)$ is the predictive likelihood for variable j , and X_i^j is a set of covariates that influences variable j in model M_i . For example, in the case of the short-term interest rate, the covariates in the Base model include ur , π , gdp , and survey data, whereas in the Base-NoSurv model, the covariates will not include the survey data.

To compute the overall marginal data density of $Y = (y^\pi, y^{ur}, y^{gdp}, y^{prod}, y^{wage}, y^{int})'$ for model M_i ,

$$\begin{aligned} p(Y | X_i, M_i) &= p(y^\pi | X_i^\pi, M_i) \times p(y^{ur} | X_i^{ur}, M_i) \times p(y^{gdp} | X_i^{gdp}, M_i) \dots \\ &\times p(y^{prod} | X_i^{prod}, M_i) \times p(y^{wage} | X_i^{wage}, M_i) \times p(y^{int} | X_i^{int}, M_i) \end{aligned} \quad (82)$$

A6. Posterior Parameter Estimates: Base Model

Table 2: Parameter Estimates Based on Estimation Sample, 1959Q4-2023Q3

Parameter	Parameter description	Posterior estimates		
		Base		
		Mean	5%	95%
a^r	Coefficient on interest-rate gap	-0.053	-0.102	-0.007
$\rho_1^g + \rho_2^g$	Persistence in output gap	0.725	0.668	0.783
ρ_1^u	Lag 1 coefficient on UR gap	1.274	1.230	1.320
ρ_2^u	Lag 2 coefficient on UR gap	-0.492	-0.528	-0.456
$\rho_1^u + \rho_2^u$	Persistence in UR gap	0.783	0.742	0.825
ρ^p	Persistence in productivity gap	-0.012	-0.126	0.100
$m = \frac{\zeta}{4}$	Relationship between r^* and g^*	0.652	0.571	0.737
ρ^i	Persistence in interest-rate gap	0.882	0.844	0.921
λ^i	Interest rate sensitivity to UR gap	-0.254	-0.302	-0.205
κ^i	Interest rate sensitivity to inflation	0.058	0.013	0.102
λ^g	Output gap response to UR gap	-0.464	-0.593	-0.339
ϕ^u	UR gap response to Output gap	-0.102	-0.121	-0.082
$\frac{(1-\rho_1^u-\rho_2^u)}{\phi_u}$	Implied Okun's Law	-2.145	-2.403	-1.908
β^g	Link between g^* and survey	0.876	0.720	1.033
β^u	Link between u^* and survey	0.948	0.881	1.020
β^r	Link between r^* and survey	1.024	0.921	1.129
β^π	Link between π^* and survey	0.995	0.914	1.074
$\sigma_{\pi^*}^2$	Variance of the shocks to π^*	0.117 ²	0.098 ²	0.136 ²
$\sigma_{p^*}^2$	Variance of the shocks to p^*	0.147 ²	0.113 ²	0.186 ²
$\sigma_{u^*}^2$	Variance of the shocks to u^*	0.091 ²	0.077 ²	0.104 ²
$\sigma_{gdp^*}^2$	Variance of the shocks to gdp^*	0.023 ²	0.018 ²	0.029 ²
σ_d^2	Variance of the shocks to d	0.096 ²	0.079 ²	0.113 ²
$\sigma_{w^*}^2$	Variance of the shocks to w^*	0.032 ²	0.024 ²	0.041 ²
σ_{ho}^2	Var. of the Volatility – Output gap eq.	0.594 ²	0.502 ²	0.693 ²
σ_{hu}^2	Var. of the Volatility – UR gap eq.	0.836 ²	0.669 ²	1.022 ²
σ_{hp}^2	Var. of the Volatility – Productivity eq.	0.280 ²	0.223 ²	0.345 ²
σ_h^2	Var. of the Volatility – Price Inf. eq.	0.306 ²	0.242 ²	0.377 ²
σ_{hw}^2	Var. of the Volatility – Wage Inf. eq.	0.426 ²	0.331 ²	0.531 ²
σ_{hi}^2	Var. of the Volatility – Interest rate eq.	0.390 ²	0.306 ²	0.481 ²
$\sigma_{\lambda^\pi}^2$	Var. of the shocks to TVP λ^π	0.041 ²	0.032 ²	0.053 ²
$\sigma_{\lambda^w}^2$	Var. of the shocks to TVP λ^w	0.041 ²	0.032 ²	0.053 ²
$\sigma_{\lambda^p}^2$	Var. of the shocks to TVP λ^p	0.045 ²	0.034 ²	0.059 ²
$\sigma_{\kappa^w}^2$	Var. of the shocks to TVP κ^w , PT	0.042 ²	0.033 ²	0.053 ²
$\sigma_{\rho^w}^2$	Var. of the shocks to TVP ρ^w	0.041 ²	0.032 ²	0.052 ²
$\sigma_{\rho^\pi}^2$	Var. of the shocks to TVP ρ^π	0.050 ²	0.037 ²	0.064 ²

A7. Prior Sensitivity Analysis

In the paper, I noted that the prior settings (in the baseline model) are similar to those used in CKP, CCK, and Gonzalez-Astudillo and Laforte (2020). As discussed in CCK, UC models with several unobserved variables, such as the one developed in this paper, require informative priors. That said, the priors I use for most variables are only slightly informative. The use of inequality restrictions on some parameters such as the Phillips curve, persistence, bounds on u-star could be viewed as additional sources of information that eliminate the need for tight priors, something also noted by CKP. The parameters for which there is a strong agreement in the empirical literature on their values, such as the Taylor-rule equation parameters, I use relatively tight priors, such that prior distributions are centered on prior means with small variance. So besides the prior on the Taylor-rule equation parameters, all other prior settings are taken from related papers.

Here, I examine the sensitivity of loosening the priors on the variances of the shocks to the pi-star, p-star, u-star, and r-star (i.e., for the process D). Specifically, I double the prior mean of the variances from 0.01 to 0.03. Table reports the posterior estimates. The top panel reports the posterior estimates from the baseline prior setting to facilitate easy comparison, and Panel (B) reports the posterior estimates of re-running the Base and Base-NoSV-NoTVP-NoSurvey models with these new prior values. It is worth noting that these new prior values are too loose to estimate Base-NoSurvey feasibly. In the case of the Base model, the results indicate that for pi-star, u-star, and r-star, the posterior mean estimates' differences between the two panels are small, and interestingly, the posterior mean estimates from the run with looser priors are pushed toward values that are closer to the prior mean estimates used in the main paper, lending credibility to the default prior settings for these parameters. For p-star, the difference between the posterior and prior is small in both runs, suggesting the strong influence of the prior in shaping the posterior. As a result, the difference between the posteriors across the two panels for p-star is non-trivial.

In the case of Base-NoSV-NoTVP-NoSurvey model, with the exception of pi-star, the differences between the two panels are larger than the Base model. In particular, for u-star and r-star, the differences are quite sizable. Unlike in the case of Base, the posterior estimates of p-star are less similar than corresponding priors.

Given the smaller differences in the posterior estimates of pi-star, r-star, and u-star across the two runs of the Base model, the estimates of the stars are similar across the two runs, as shown in Figure 2. In contrast, the sizable differences in some of the stars across the two runs of the Base-NoSV-NoTVP-NoSurvey model translate into bigger differences in the estimates of the stars, especially u-star and r-star, as seen in Figure 3.

Table 3: Parameter Estimates

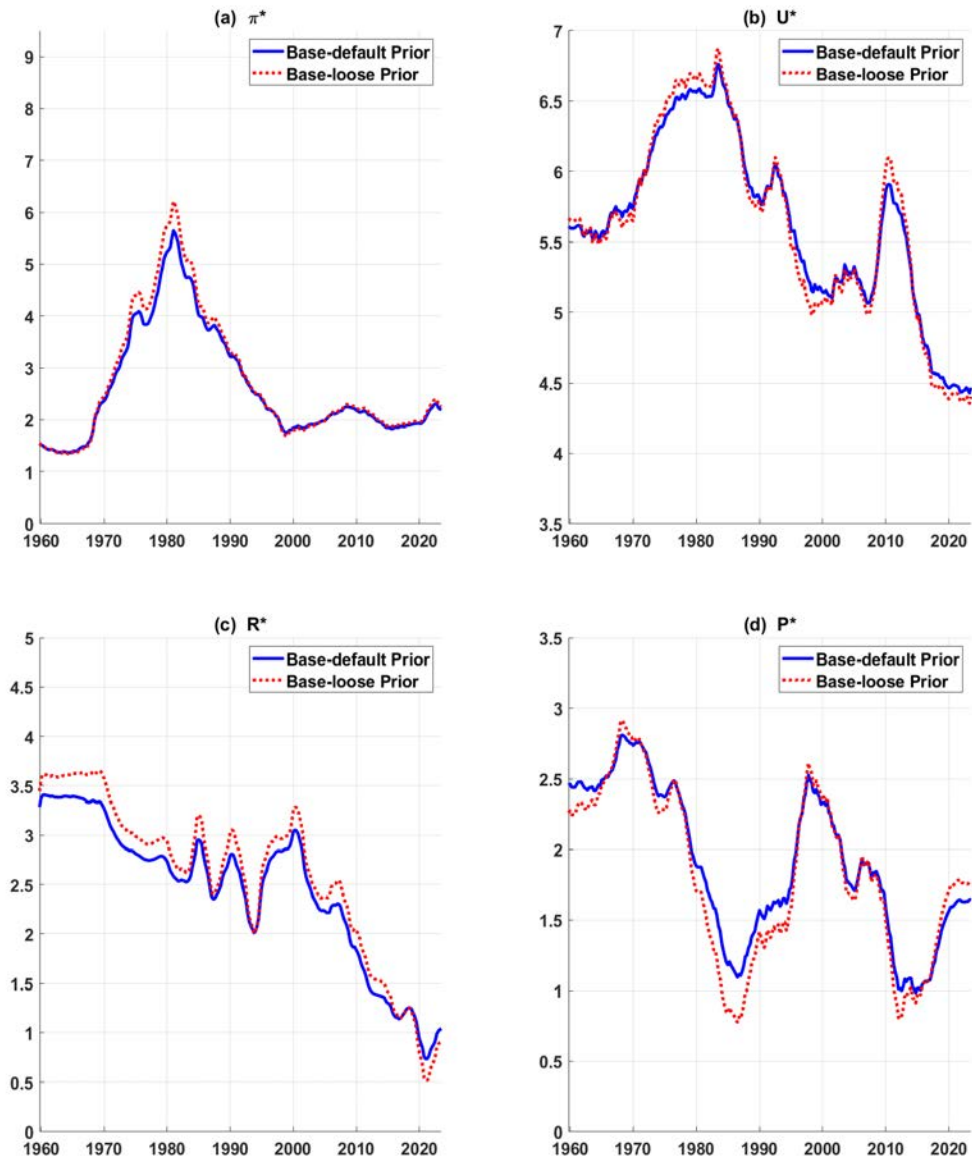
Panel A: Default prior setting, where prior $E(\sigma_{\pi^*}^2) = E(\sigma_{u^*}^2) = E(\sigma_d^2) = 0.1^2$ and $E(\sigma_{p^*}^2) = 0.14^2$

Parameter	Parameter description	Posterior estimates					
		Base			Base-NoSV-NoTVP-NoSurvey		
		Mean	5%	95%	Mean	5%	95%
$\sigma_{\pi^*}^2$	Variance of the shocks to π^*	0.117 ²	0.098 ²	0.136 ²	0.221 ²	0.147 ²	0.288 ²
$\sigma_{p^*}^2$	Variance of the shocks to p^*	0.147 ²	0.113 ²	0.186 ²	0.157 ²	0.119 ²	0.200 ²
$\sigma_{u^*}^2$	Variance of the shocks to u^*	0.091 ²	0.077 ²	0.104 ²	0.130 ²	0.087 ²	0.179 ²
σ_d^2	Variance of the shocks to d	0.096 ²	0.079 ²	0.113 ²	0.101 ²	0.076 ²	0.130 ²

Panel B: Prior sensitivity, where prior $E(\sigma_{\pi^*}^2) = E(\sigma_{u^*}^2) = E(\sigma_d^2) = E(\sigma_{p^*}^2) = 0.173^2$

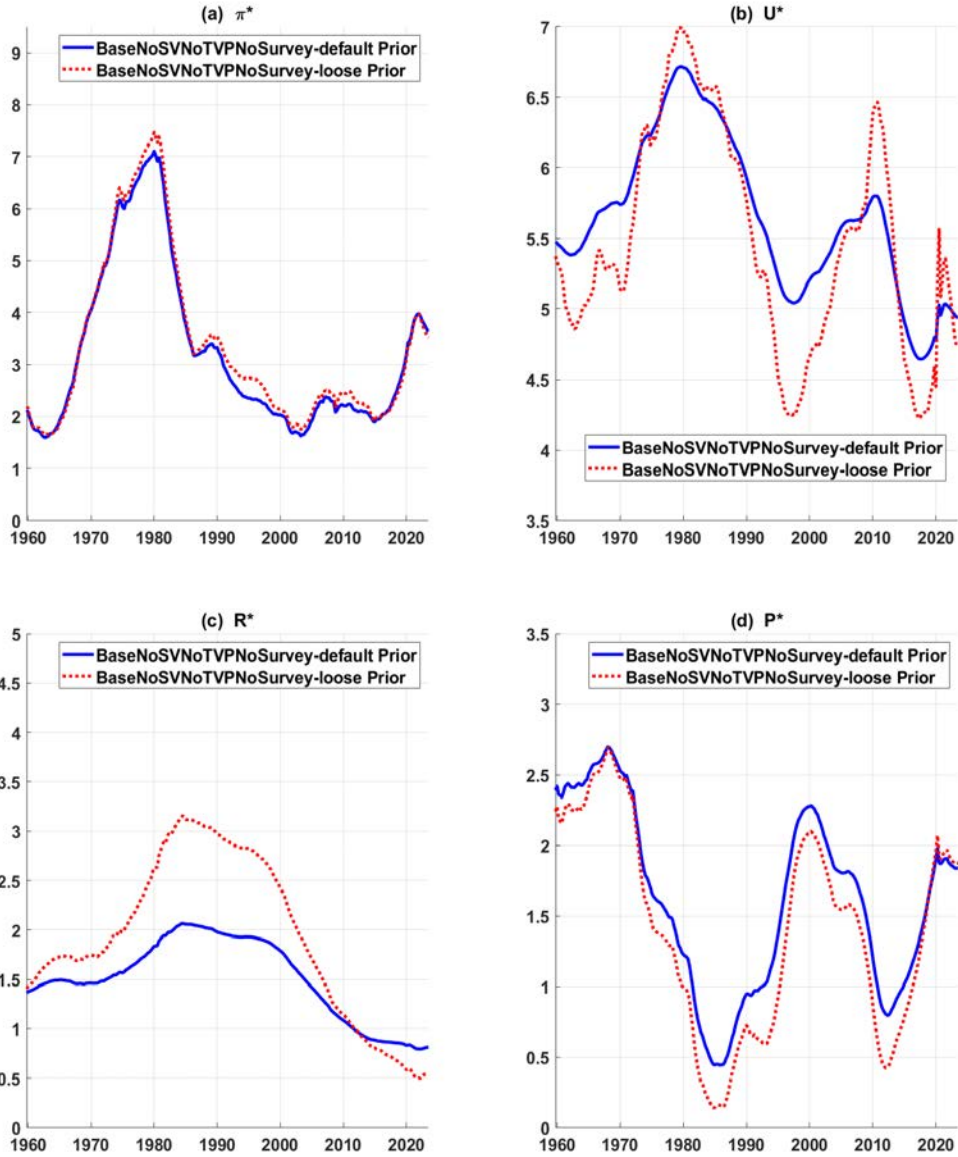
Parameter	Parameter description	Posterior estimates					
		Base			Base-NoSV-NoTVP-NoSurvey		
		Mean	5%	95%	Mean	5%	95%
$\sigma_{\pi^*}^2$	Variance of the shocks to π^*	0.139 ²	0.121 ²	0.157 ²	0.246 ²	0.191 ²	0.300 ²
$\sigma_{p^*}^2$	Variance of the shocks to p^*	0.175 ²	0.135 ²	0.218 ²	0.186 ²	0.139 ²	0.239 ²
$\sigma_{u^*}^2$	Variance of the shocks to u^*	0.113 ²	0.100 ²	0.125 ²	0.299 ²	0.170 ²	0.407 ²
σ_d^2	Variance of the shocks to d	0.124 ²	0.107 ²	0.141 ²	0.169 ²	0.131 ²	0.212 ²

Figure 2: Prior Sensitivity: Base model (default prior) vs. Base model (loose prior)



Note: plots in solid blue are estimates from the Base model with default priors and plots in dotted red are estimates from the Base model with looser priors for the variances of shocks to equations defining stars.

Figure 3: Prior Sensitivity: Base-NoSV-NoTVP-NoSurvey model, default prior vs. loose prior



Note: plots in solid blue are estimates from the Base-NoSV-NoTVP-NoSurvey model with default priors and plots in dotted red are estimates from the Base-NoSV-NoTVP-NoSurvey model with looser priors for the variances of shocks to equations defining stars.

A8. MCMC Convergence Diagnostics

This section documents the diagnostic properties of the Base model’s MCMC algorithm. Following Primiceri (2005), Koop, Leon-Gonzalez, and Strachan (2010), and Korobilis (2017), for the time-invariant parameters (including those governing the time-variation in selected parameters), I report the autocorrelation functions of the posterior draws (10th and 50th order sample autocorrelation), inefficiency factors (IFs), and convergence diagnostic (CD) of Geweke (1992).¹⁷

One of the most common metrics examined to assess the efficiency of the MCMC sampler is to look at the autocorrelation function of the draws, which indicates how well the chain is mixing. Low autocorrelations are preferred to higher because the lower the autocorrelation, the closer the draws are to being independent and the higher the efficiency of the algorithm. The plots shown in the top panel of the Figure 4 correspond to the 10th and 50th order autocorrelations in the draws, and as can be seen, they indicate very low autocorrelation. In the case of the 50th order autocorrelation, except for a couple of them, most indicate correlation close to zero, and in the case of 10th order except for a few, most indicate correlation below 0.2.

The inefficiency factor related to the autocorrelation functions is the inverse of Geweke’s (1992) relative numerical efficiency measure (RNE). It is computed using the following formula, $(1 + 2 \sum_{i=1}^{\infty} \rho_i)$, where ρ_i refers to the $k - th$ order autocorrelation of the chain. The middle panel in Figure A1 plots the IF for the model parameters. The values lower than or close to 20 are considered desirable. As shown, in the case of the Base model, most of the IFs are below 20. (Note: IFs are computed using the default setting in LeSage’s toolbox: estimation of spectral density at frequency zero uses a tapered window of 4%.)

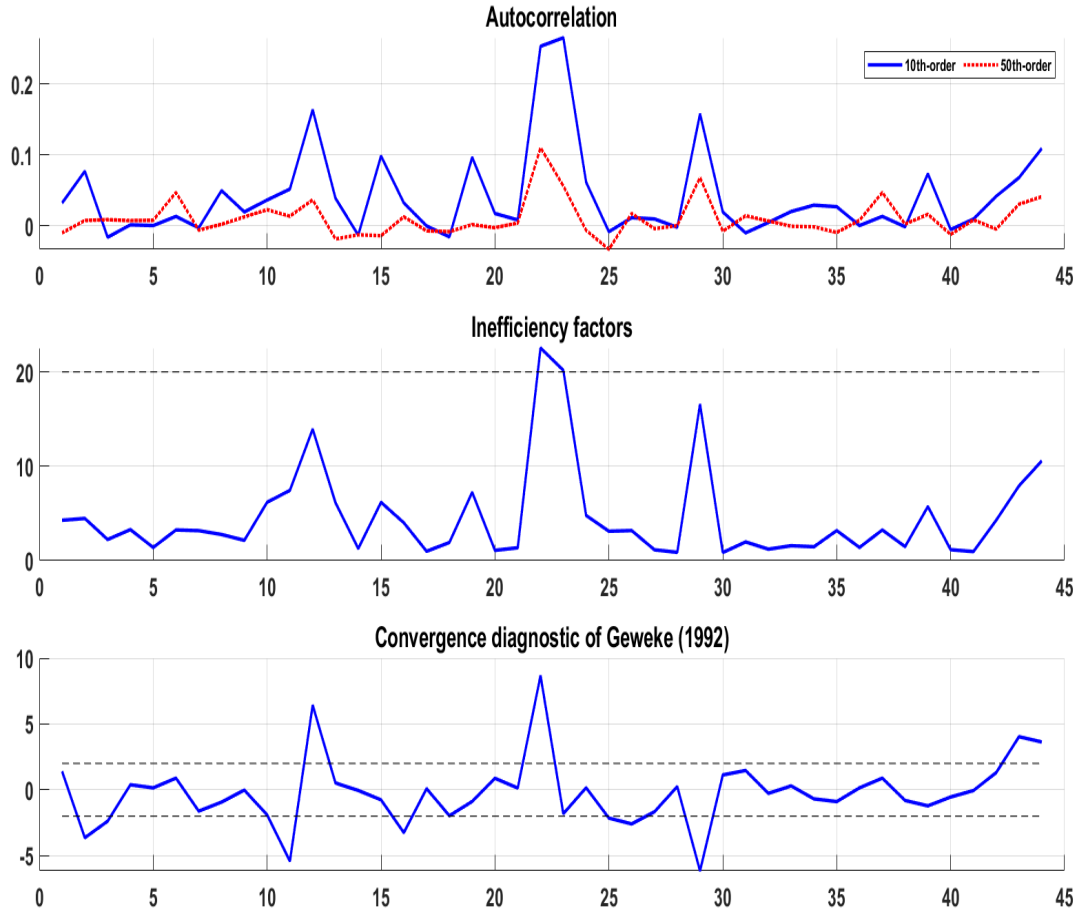
As discussed in Koop, Leon-Gonzalez, and Strachan (2010), to assess whether the MCMC sampler has converged, a rough rule of thumb is to look at the CDs and see whether 95% of them are less than 2. If they are, then convergence is likely achieved. Based on the plots in Figure A1 (third panel), most CDs are within +/- 2.

I also note that the results are fairly identical to the different initial conditions of the chain (picked randomly) and to a significantly lower number of simulations (and burn-in). For example, a run using 320K posterior draws with a burn-in of the first 300K and retaining all the remaining draws provides similar inference. However, the MCMC convergence properties favor higher simulations because it allows for a greater degree of thinning.

Overall, these diagnostic measures give me confidence in the good convergence properties of the MCMC algorithm developed for the Base model.

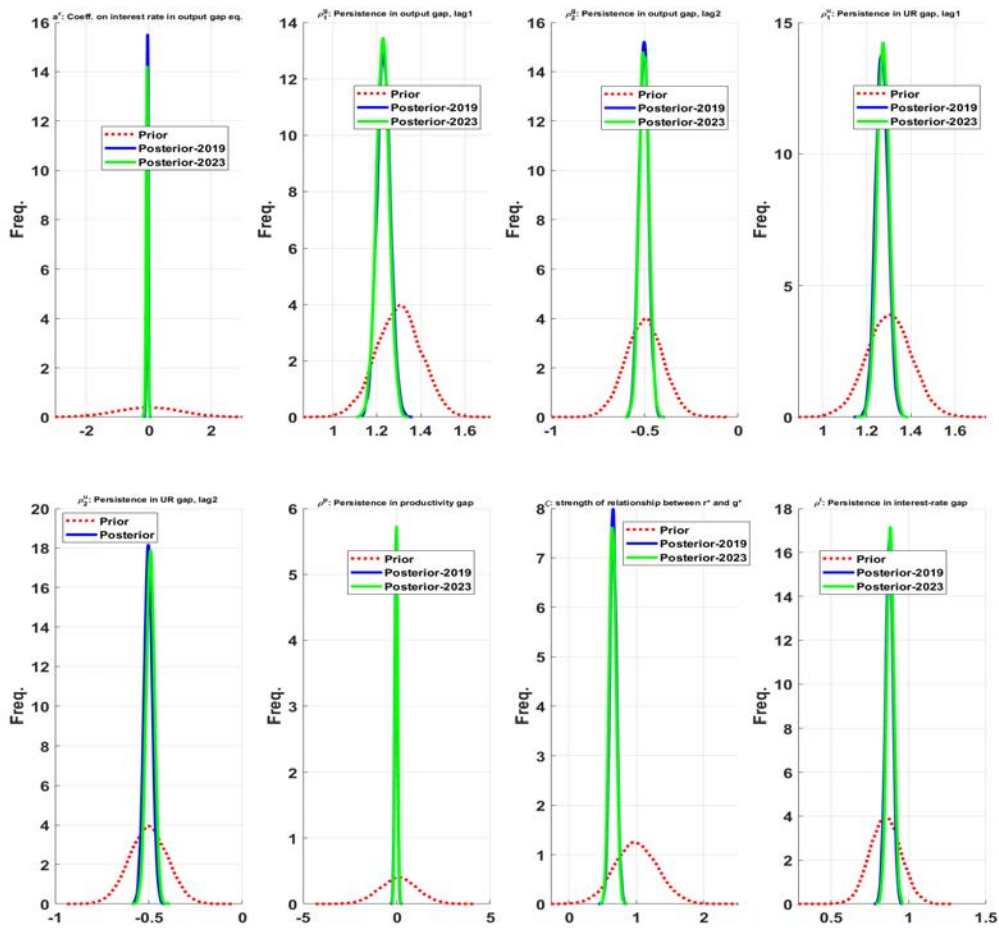
¹⁷In computing some of these metrics, I have benefitted from the Matlab toolbox developed by James P. LeSage. A detailed explanation, including intuition for these convergence diagnostics, is provided in Koop (2003; page 67-68) and Chan et al. (2019; page 209).

Figure 4: MCMC Diagnostics of Base Model



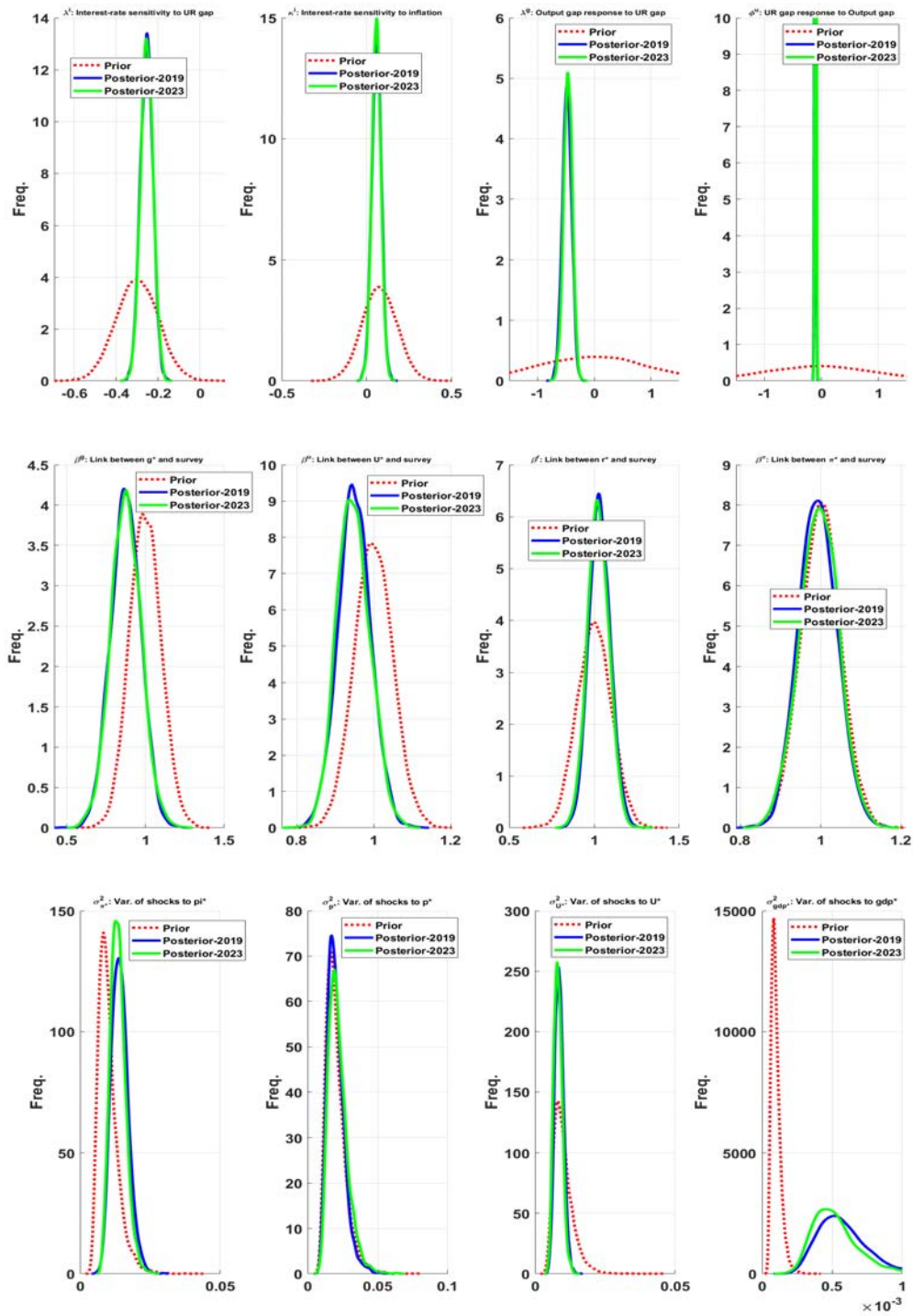
A9. Prior and Posterior Distributions of the Parameters: Base Model

Figure 5: Prior and Posterior Distributions of the Parameters: Base Model



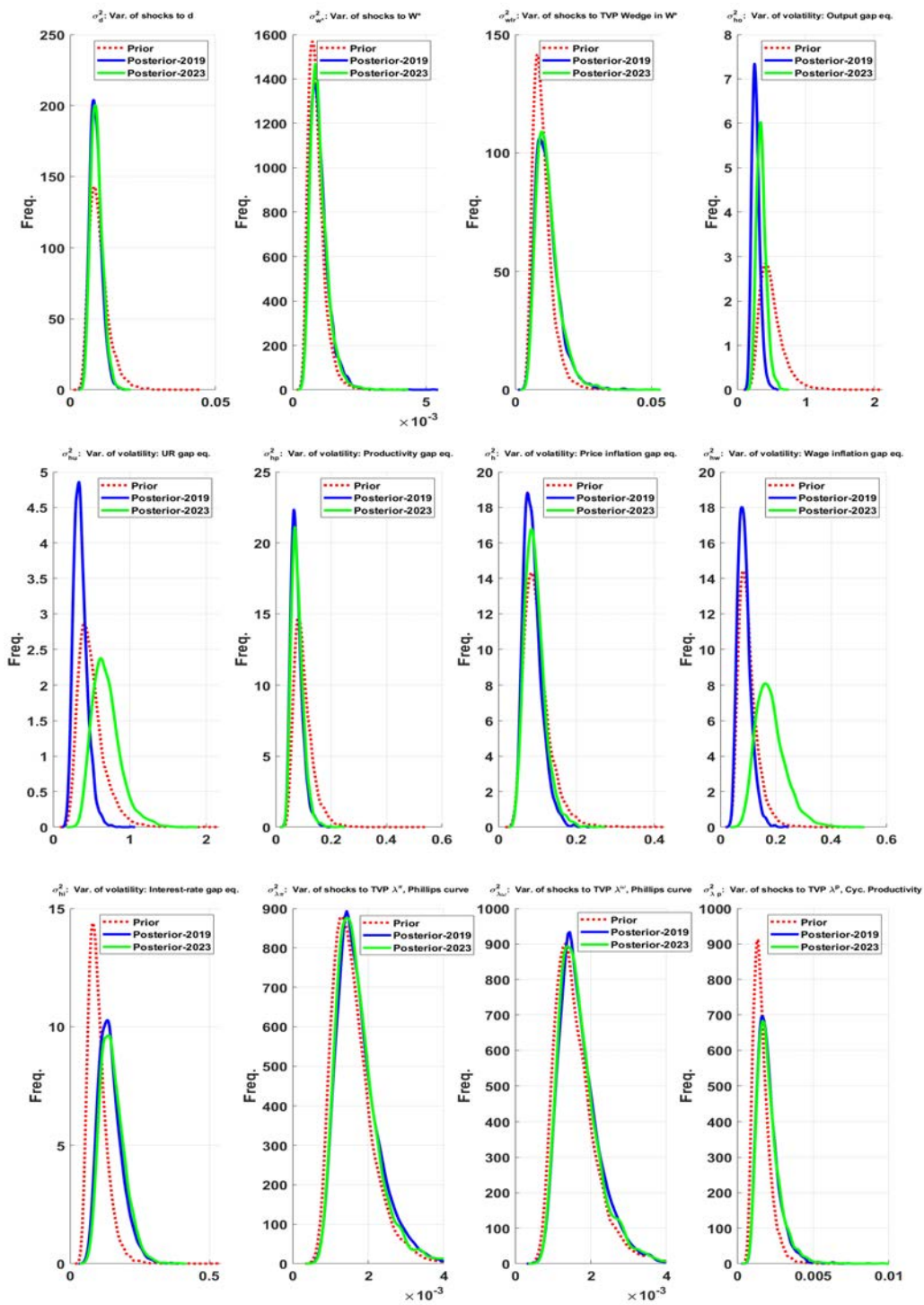
Note: Plotted in dotted red lines are the prior distributions, in blue are the posterior distributions based on estimating data from 1959Q4 through 2019Q4, and in green are the posterior distributions based on estimating data from 1959 through 2023Q3, which includes pandemic and post-pandemic data.

Figure 6: Prior and Posterior Distributions of the Parameters: Base Model, continued



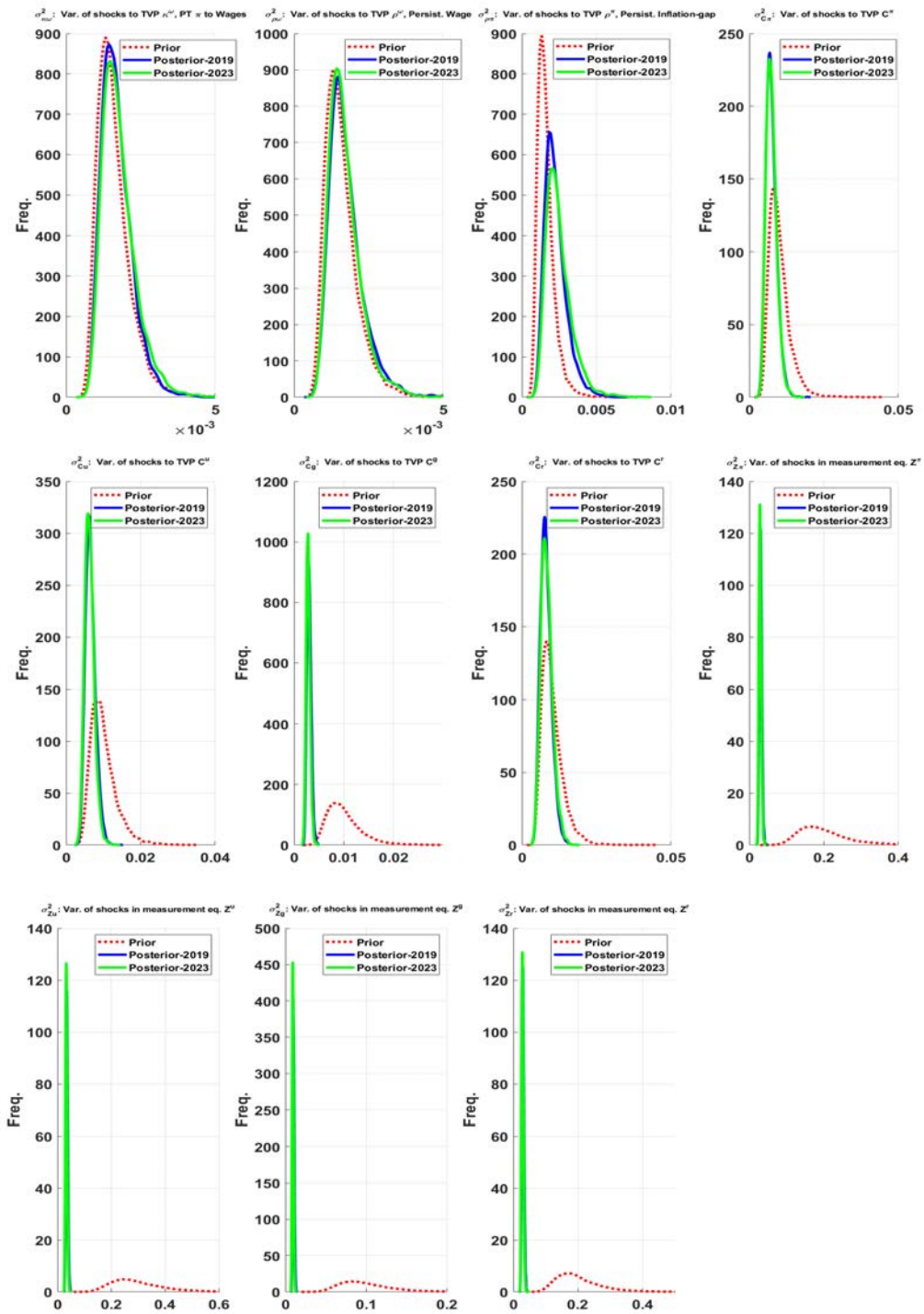
Note: Plotted in dotted red lines are the prior distributions, in blue are the posterior distributions based on estimating data from 1959Q4 through 2019Q4, and in green are the posterior distributions based on estimating data from 1959 through 2023Q3, which includes pandemic and post-pandemic data.

Figure 7: Prior and Posterior Distributions of the Parameters: Base Model, continued



Note: Plotted in dotted red lines are the prior distributions, in blue are the posterior distributions based on estimating data from 1959Q4 through 2019Q4, and in green are the posterior distributions based on estimating data from 1959 through 2023Q3, which includes pandemic and post-pandemic data.

Figure 8: Prior and Posterior Distributions of the Parameters: Base Model, continued



Note: Plotted in dotted red lines are the prior distributions, in blue are the posterior distributions based on estimating data from 1959Q4 through 2019Q4, and in green are the posterior distributions based on estimating data from 1959 through 2023Q3, which includes pandemic and post-pandemic data.

A10. Prior and Posterior Distributions: Deeper Dive

As is evident from the figures shown in the previous section, encouragingly, for most parameters, the data influence the posterior estimates, as evidenced by well-peaked posterior distributions and/or movements in posterior distributions away from prior distributions. For a select few parameters, the data appear to have only a trivial to no role. However, a deeper examination of some of these cases suggests this inference is misleading. I say this because, for a couple of the parameters, it just so happens that the default prior setting in the baseline model coincides (or is generally in line) with what the data would dictate, hence the similar prior and posterior distributions, as illustrated in the figure below. Put differently, if I change or loosen the prior significantly (new looser prior), the updated posterior mean shifts closer to the old posterior mean (which happens to match the old prior).

One of those parameters is β^π , which is the parameter linking survey expectations to the model star. For this parameter, the mean of the posterior distribution (0.995) coincides with the prior distribution (1.0). If I make the prior distribution for β^π looser (diffuse) by centering it at a lower mean value (0.8 instead of 1.0), the posterior mean shifts upward to 0.953 (which is closer to the original prior and posterior). If I make the prior distribution for β^π significantly looser (much more diffuse) by centering it at a lower mean value (0.5 instead of 1.0), the posterior mean shifts upward to 0.943 (which is again closer to the original prior and posterior). It is also to be noted that to get a sense of the relationship between survey expectations and the model-based star, one should look **at both** the β parameter and the variance of the innovation of the process governing the time-variation in the intercept C (and in turn the estimates of the time-varying C); see equation (2) in the main paper. For all four equations defining relationships between survey expectations and stars, the data influence the posterior of the intercept C (as evidenced by comparing the prior and posterior plots of parameters defining the variance of the innovations in equations defining Cs).

Figure 9, shown on the next page, plots prior and posterior distributions for the parameter β^π , which relates inflation survey expectations to model-based pi-star, for three different prior settings:

Panel (a): Baseline: prior mean = 1.0 (prior s.d. = 0.05) and posterior mean = .995

Panel (b): Loose prior: prior mean = 0.8 (prior s.d. = 0.3) and posterior mean = 0.953

Panel (c): Very loose prior: prior mean = 0.5 (prior s.d. = 0.4) and posterior mean = 0.943

As can be seen, no matter the prior setting, the posterior means of the β parameter are very similar. Not surprisingly, the corresponding estimates of the posterior mean of pi-star are identical (suggesting robustness to different priors), as evident from the plots shown in the top panel of Figure 10. The difference in the prior settings influences the precision of the pi-star, as seen in the bottom panel of Figure 10: Pi-star from the Base model is more precisely estimated in the first half of the sample and less precisely estimated in the latter part of the sample compared to specifications with looser priors. Bayesian model comparison metrics overwhelmingly support the default Base prior setting over the looser priors.

No matter the prior setting, the posterior means of β^π are very similar

Figure 9: Prior Sensitivity of Parameter, β^π

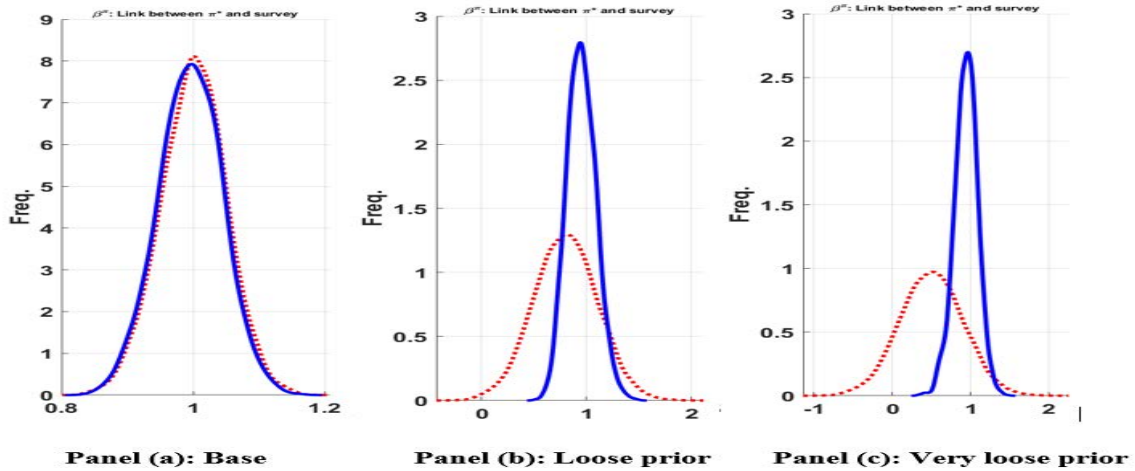
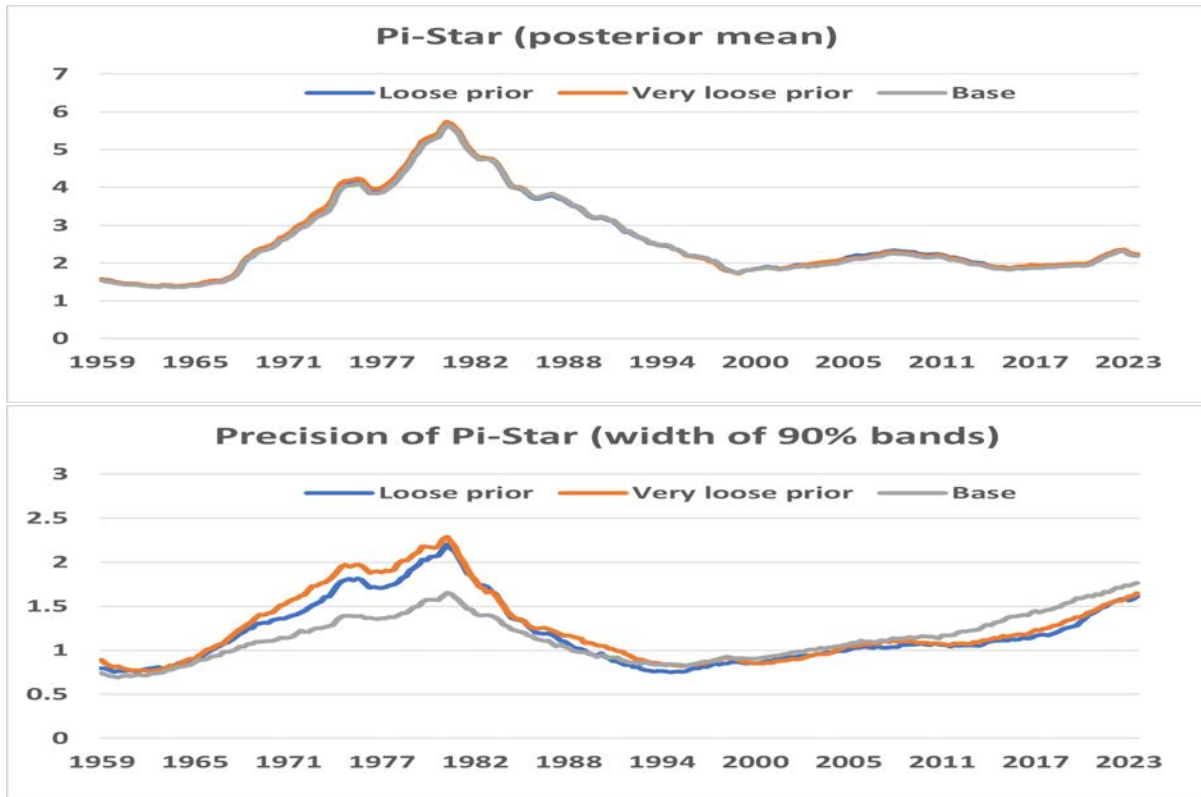
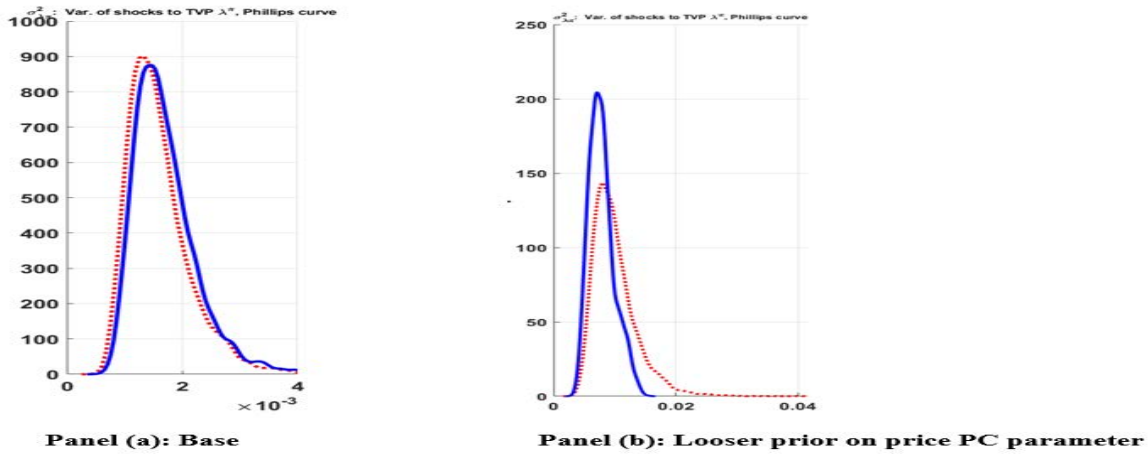


Figure 10: Prior Sensitivity of Parameter, β^π : Pi-star



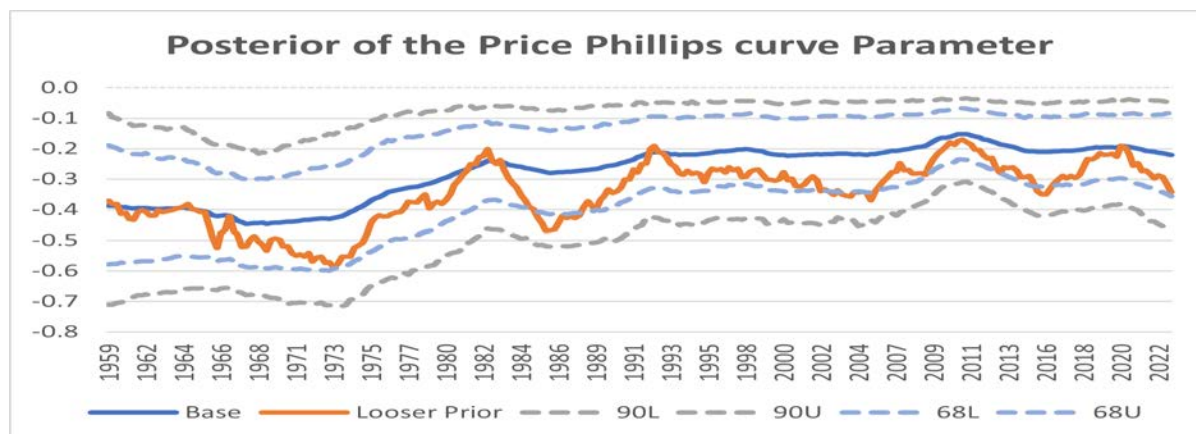
Another parameter that indicates a trivial difference in the prior and posterior distributions is the variance of the shocks to the parameter governing the evolution of the slope of the price Phillips curve (see panel (a) in Figure 9). Accordingly, I did a robustness check by significantly loosening the prior for this parameter while keeping priors for all other parameters the same as in the Baseline model. Doing so gives posterior a distribution that has a higher peak and is narrower than the prior distribution (panel (b), 9). As shown in Figure 10, loosening the prior on this parameter leads to a more volatile estimate of this parameter. However, the overall inference remains robust, as the posterior mean of the PC slope for the looser prior setting lies within the 68% (and 90%) credible intervals of the Baseline model's price PC slope parameter. The default (Base) prior for $\sigma_{\lambda\pi}^2$ is $IG(10, 0.04^2 \times 9)$, versus for the Looser Prior $\sigma_{\lambda\pi}^2$ is $IG(10, 0.1^2 \times 9)$.

Figure 11: Prior Sensitivity of Parameter, λ^π



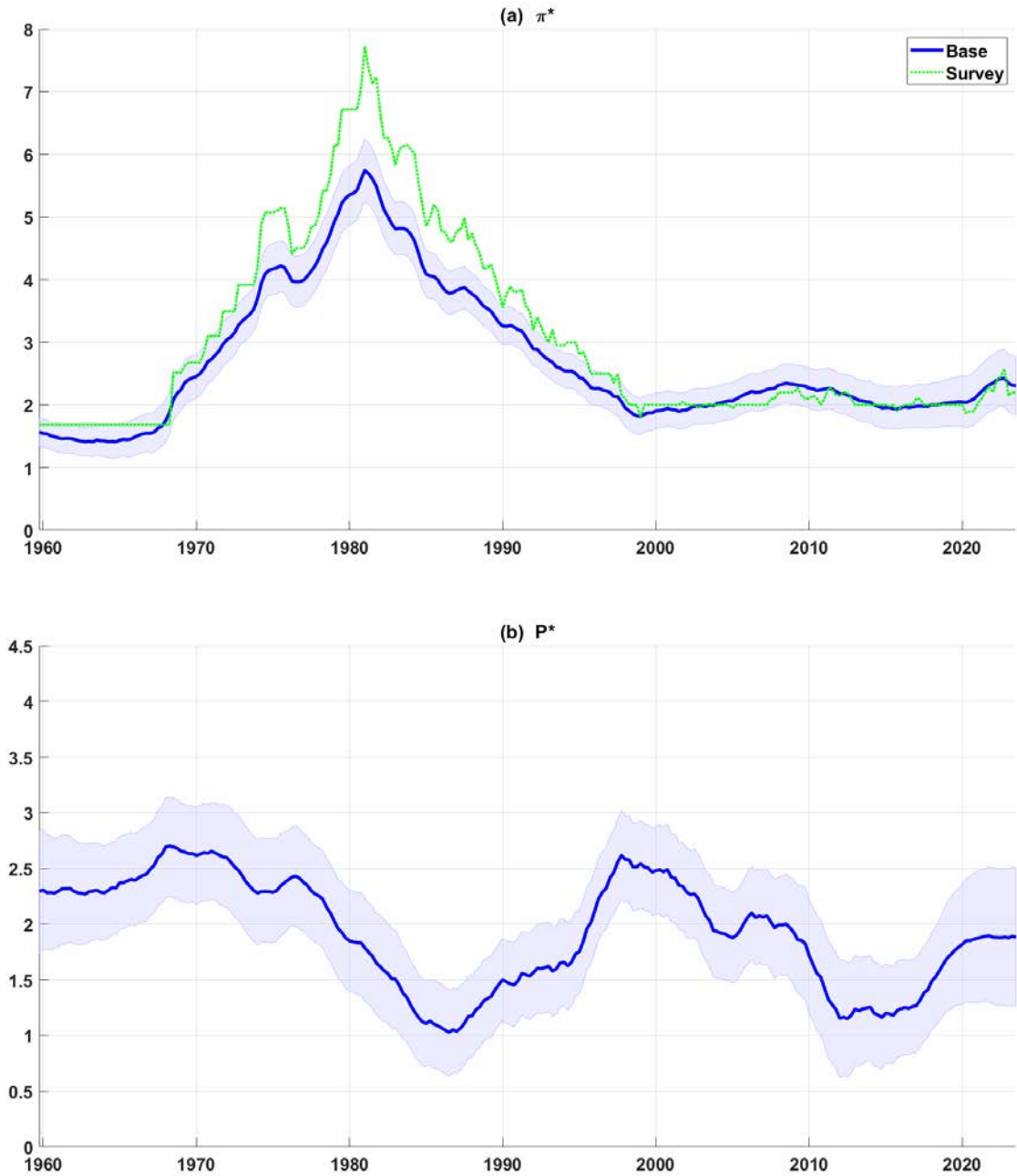
Robust Inference: posterior mean of PC slope for looser prior setting lies within the 68% credible intervals of the Baseline model's price PC slope parameter:

Figure 12: Time-varying estimate of parameter, λ^π



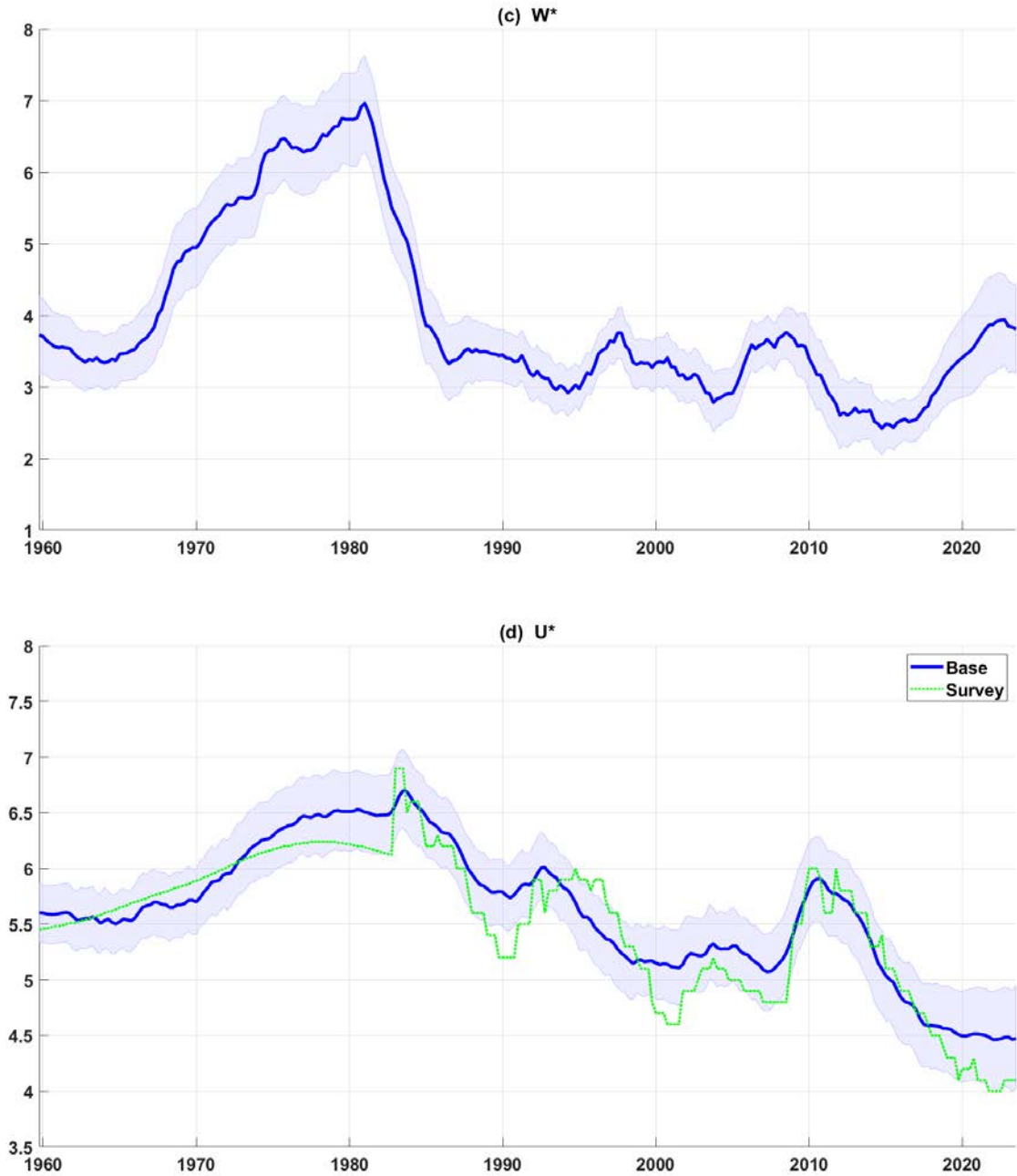
A11. Stars from Base Model: Zoomed In

Figure 13: Pi-star and P-star



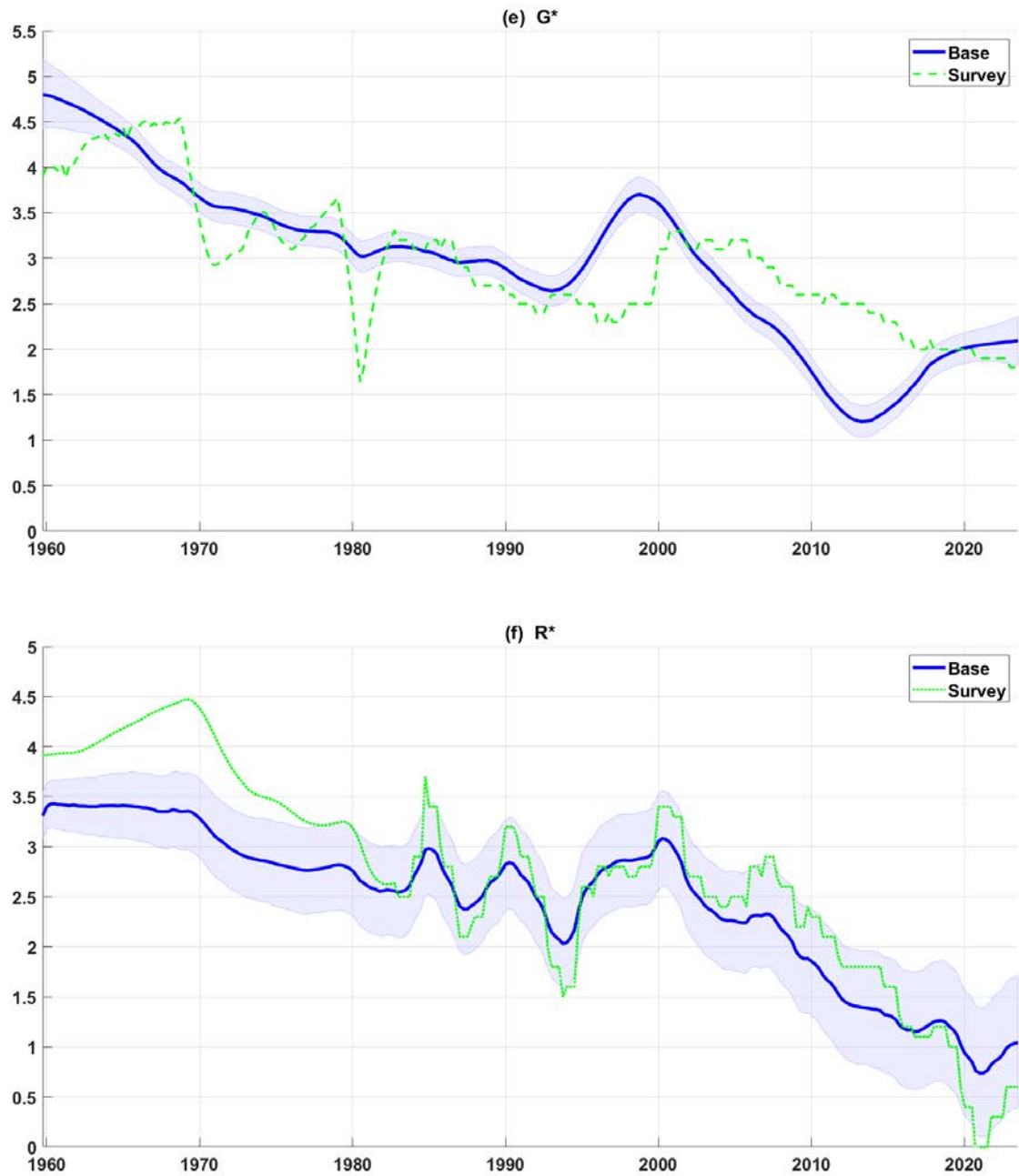
Note: The posterior estimates are based on the full sample (from 1959Q4 through 2023Q3). The dotted lines represent the 68% credible intervals.

Figure 14: W-star and U-star



Note: The posterior estimates are based on the full sample (from 1959Q4 through 2023Q3). The dotted lines represent the 68% credible intervals.

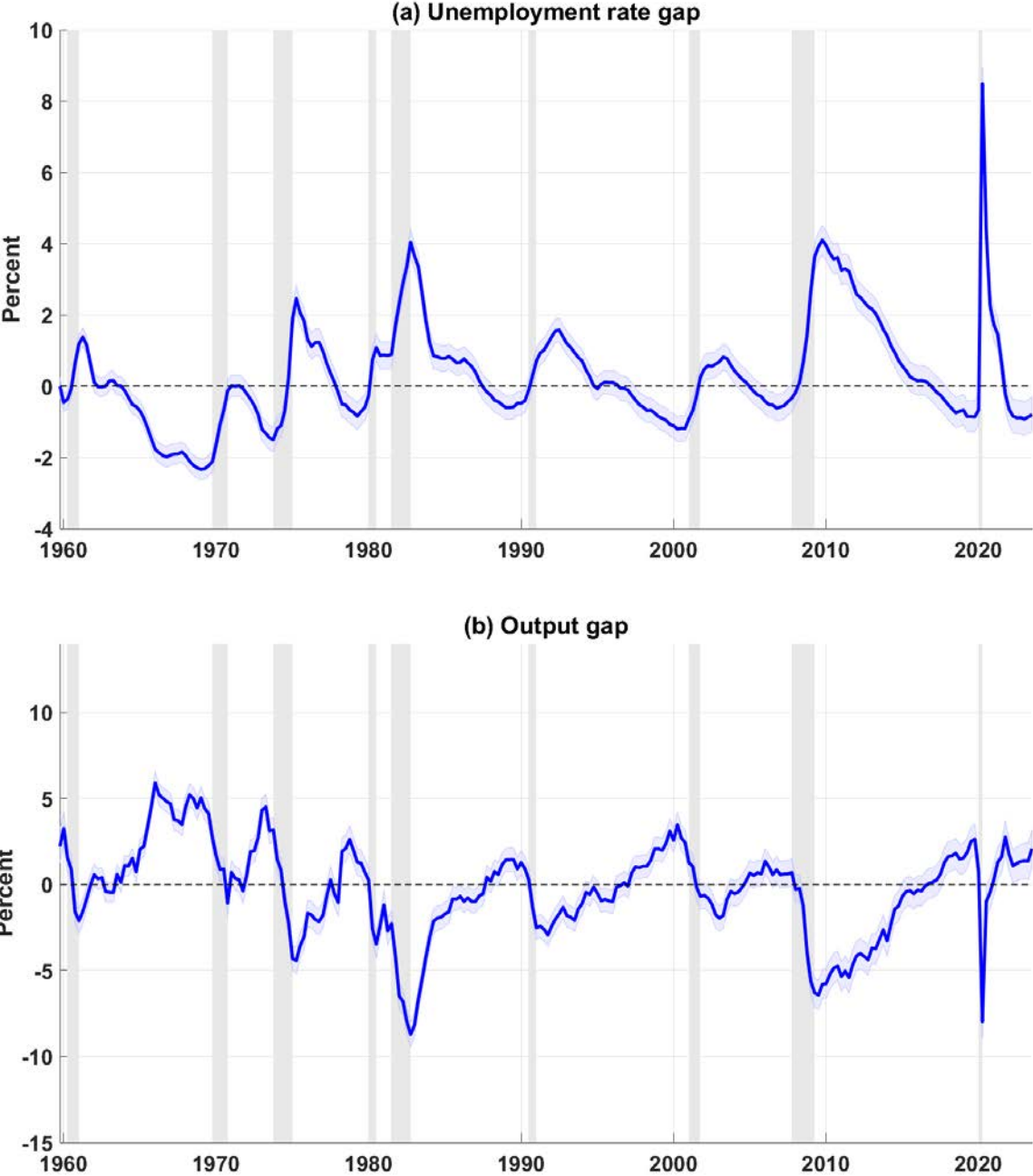
Figure 15: G-star and R-star



Note: The posterior estimates are based on the full sample (from 1959Q4 through 2023Q3). The dotted lines represent the 68% credible intervals.

A12. Base Model: Estimate of the Cyclical Unemployment Rate

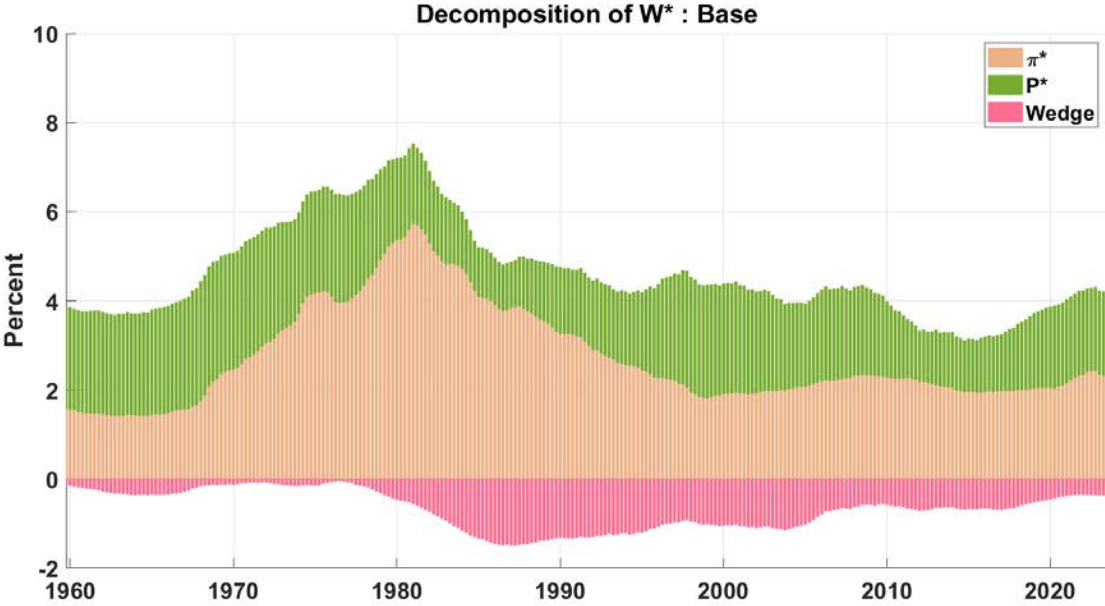
Figure 16: Unemployment Rate Gap and Output Gap



Note: Plotted are the posterior mean estimates based on estimating data from 1959Q4 through 2023Q3.

A13. W-star Decomposition: Base Model

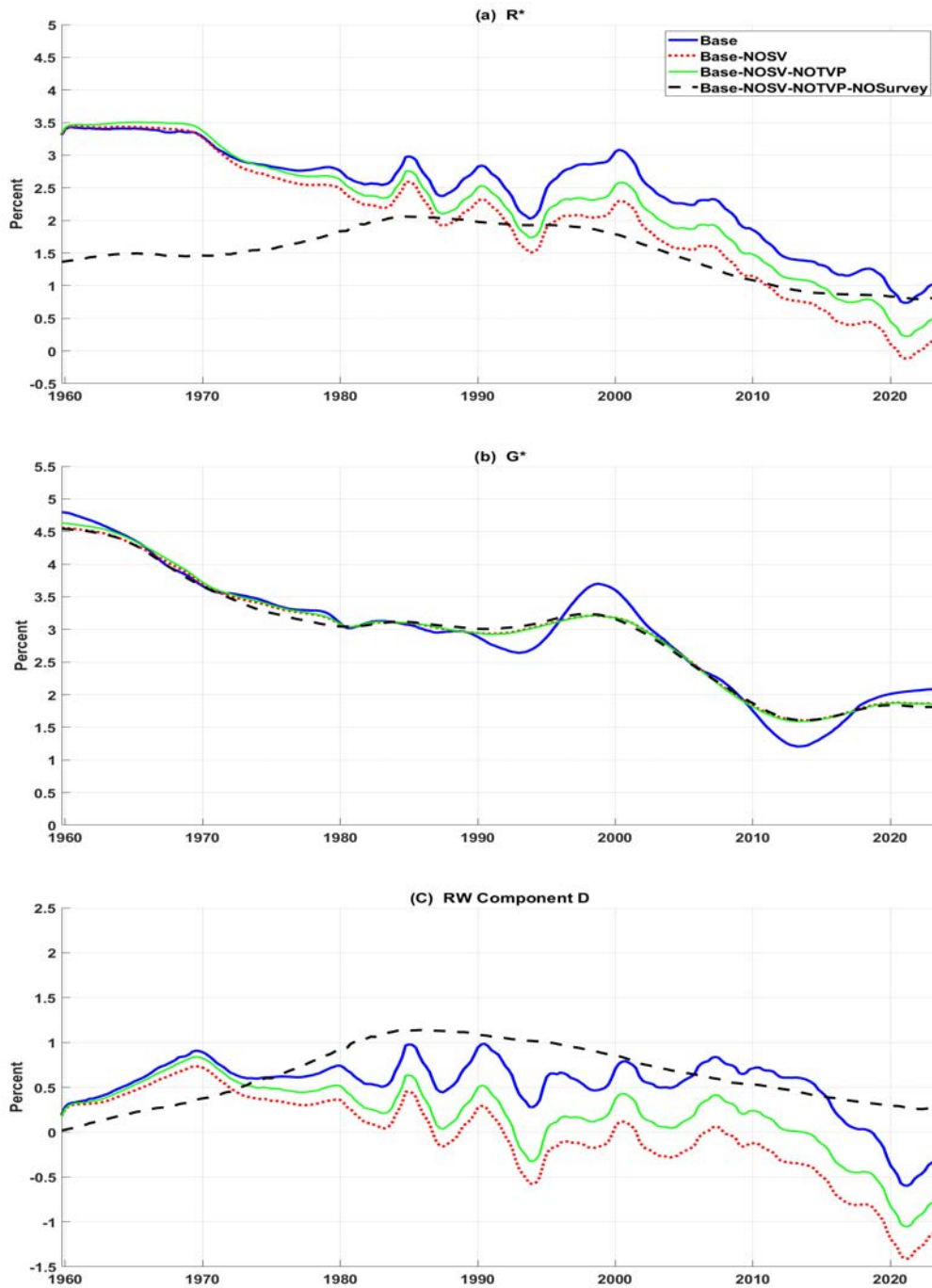
Figure 17: W*: Base Model



Note: Plotted are the posterior mean estimates based on estimating data from 1959Q4 through 2023Q3.

A14. R-star Decomposition: Base Model and Variants

Figure 18: Posterior Mean Estimates



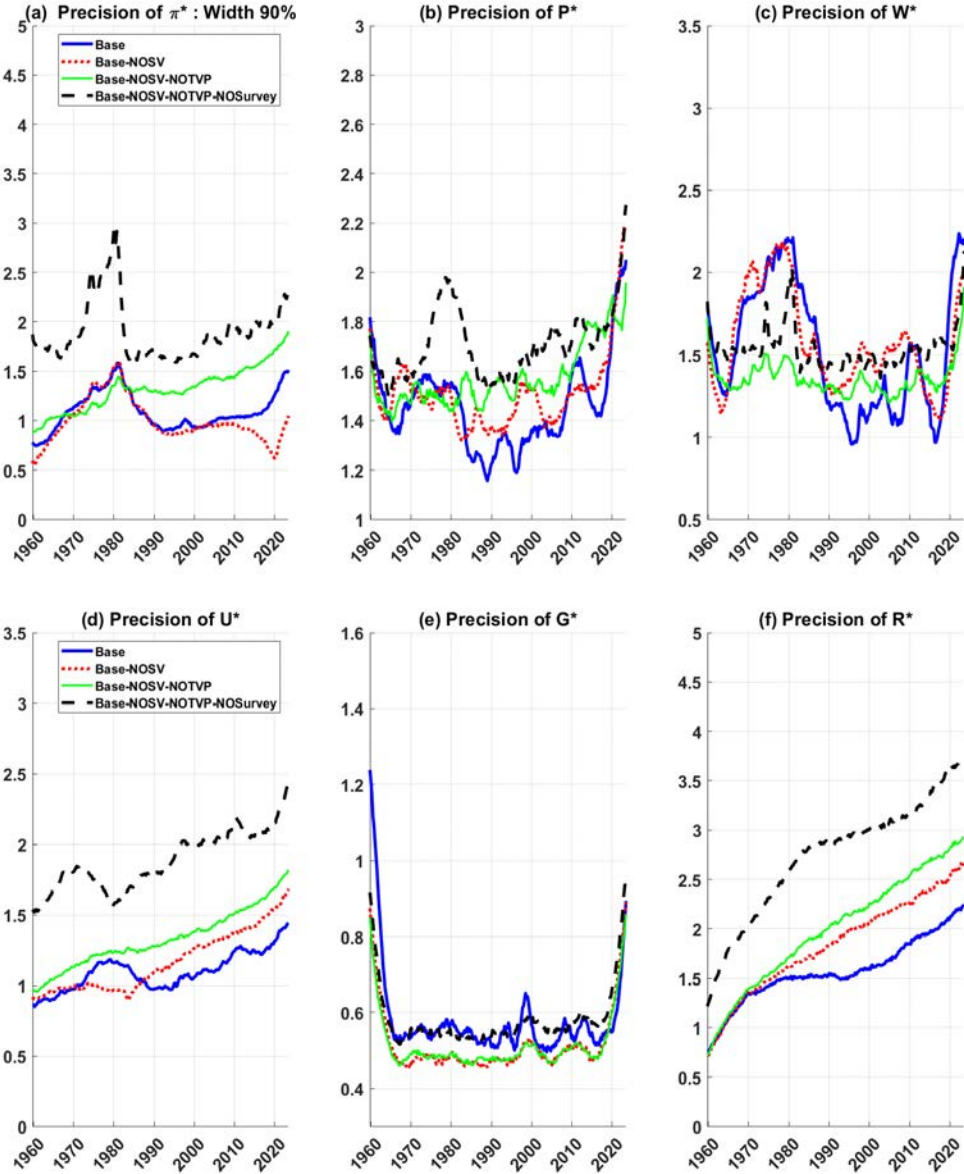
Note: Plotted are the posterior mean estimates based on the full sample from 1959Q4 through 2023Q3.

A15. Phillips curve slope (post-Pandemic): Base vs. External Studies

According to my baseline model's posterior mean estimates (with data through 2023Q3), the slope of the PC is estimated to be pretty much stable at -0.2 over the past three decades, which would be consistent with your assessment. I would point out that the finding in my paper (revised version) that the strength of the PC relationship has remained stable (and weak) since the onset of the pandemic is a new result and contrasts with some recent work (with simpler models than those developed in this paper) that evidence strengthening in this relationship, e.g., see Hobijn et al. (2023), and Cecchetti et al. (2023). These papers do not feature stochastic volatility when modeling inflation's dynamics and do not allow for endogenous changes to u -star (and, in turn, labor tightness); hence, most of the inflation surge during the 2021-2022 period is likely associated with a steeper slope in the PC relationship. However, in my model, because I have SV in the inflation gap, a majority of the inflation surge is seen as a large temporary spike in the idiosyncratic component. And because, in my model, u -star is allowed to respond to incoming data, the inferred unemployment gap widens (increased labor market tightness) to explain the remaining portion of the high inflation. Although the jury is still out, inflation has come down quickly without any significant movements in the unemployment rate (and the unemployment rate gap), suggesting the temporary nature of the inflation surge providing a validity check on my model's inference.

A16. Precision of Stars: Base Model vs. Variants of Base

Figure 19: Precision of Stars: Base model vs. Base specs



Note: Precision is measured as the width of 90% credible intervals. The sample spans 1959Q4 through 2023Q3.

A17. Base vs. External Models: Comparison of Stars

This subsection compares Base model estimates of stars with those produced by external sources, including small-scale UC models routinely used by Federal Reserve staff and featured in academic research. Figure 20 compares the smoothed estimates of pi-star (panel a), p-star (panel b), w-star (panel c), u-star (panel d), g-star (panel e), r-star (panel f), and the output gap (panel g) from the Base model and outside sources. To better highlight the differences and similarities in the estimates across models, the plots are shown to span the sample period from 1990 onward; however, Figure 21 shows a comparison over the full sample.

Beginning with pi-star, panel (a) plots posterior mean estimates of pi-star from the Base, the celebrated univariate UC model of Stock and Watson (2007) [SW], the bivariate UC model of Chan, Koop, and Potter (2016) [CKP], and the recently popularized bivariate UC model of Chan, Clark, and Koop (2018) [CCK]. The inflation block in the Base model combines many of the elements from these three models so they could be viewed as restricted variants of the Base model.

There are some interesting similarities and differences across the pi-star estimates. Whereas UCSV displays very volatile and erratic estimates, other models show a smoother evolution. From 1992 through 1998, CKP and CCK tracked each other closely, with a Base a few tenths higher (0.5 ppts higher in 1995). Since 1998 onward, CCK indicate a lower pi-star than others; from 1995 through 2020, it is almost a straight line at 1.6%. CKP and the Base tracked each other from 1998 through 2012, but thereafter, they diverged, with the Base remaining higher than CKP. Interestingly, except for SW, the other models indicate only modest increases in pi-star during the post-pandemic inflation surge. In contrast, the SW model attributes most of the pandemic surge to pi-star, as pi-star is estimated to increase to 7.1% by early 2022 (not shown because of the scale of the y-axis) compared to 2.3% in the Base and 1.8% in CKP and CCK. These differences in pi-star are arguably sizable for inflation targeting central banks, such as the Federal Reserve.

Panel (b) in Figure 20 plots the estimates of p-star from the Base model and three additional sources: univariate UC model of Stock and Watson applied to productivity data [UCSV-SW], the two-regime Markov-switching model of Kahn and Rich (2007) [KH], and smoothed estimate of the biweight filtered productivity data, where the source of the productivity data is John Fernald's series obtained from the San Francisco Fed's website [denoted SFFed-Fernald-BW].

A regime-switching framework (as in Kahn and Rich) [KR] allows for deterministic values of p-star, where the number of deterministic values equals the number of possible regimes. Accordingly, in the 2-regime setup of KR, the estimated p-star periodically alternates from a low productivity regime (p-star=1.3%) to a high productivity regime (p-star=3.0%). In contrast, the random walk assumption for p-star in the Base model allows for the possibility that p-star may be (slowly) changing in every period. This latter assumption implies that the possible values of p-star could equal the number of periods in the estimation sample. Because of the latter fact, the stochastic conception underlying the Base model is arguably more flexible

and informative than the KR model.

The flexibility of the Base over the KR model is evident in the following comparison. Over the period from 1995 through 2005, the KR model indicates a p-star at 3.0% (roughly similar to the univariate model) and almost a whole percentage point higher than the SFFed-Fernald-BW estimate of 2.1%. In contrast, the Base model, which in 1995 estimated a p-star similar to KH, has a p-star drifting lower over the period, reaching 1.7% by mid-2004, about 1.3 percentage points lower than Kahn and Rich, a sizable gap. The later model, eventually, with a delay of a couple of quarters, caught up with the Base model's assessment.

Following the Great Recession, except for SFFed-Fernald-BW, which has very gradual deceleration, others, including the Base model, have p-star falling sharply close to 1.0%, and remaining at that level until 2015. Since the pandemic's onset, the Base and the SFFed-Fernald-BW have been stable at 1.6%. In contrast, the UCSV-SW model displays volatility, as p-star falls initially and then rebounds, mirroring movements in the productivity data. Because the KR model had difficulties dealing with the extreme pandemic observations, the estimates of p-star are based on estimating the model with data through 2020Q1. Unsurprisingly, they cautioned about how much signal to take from their model's estimates. Specifically, they say, "We have been cautious about drawing strong conclusions from the model since the onset of the pandemic because of the extreme outliers in the data from 2020 to 2022."

Panel (c) in Figure 20 plots the estimates of w-star from the Base model and the univariate model of Stock and Watson applied to the nominal wage data. As indicated earlier, estimates of w-star are a novel aspect of this paper. A natural comparison for w-star is to compare it with the state-of-the-art univariate model of Stock and Watson that assumes an RW process for w-star. As the plots show, the w-star from the univariate model displays significant variation as it responds strongly to movements in nominal wages. In contrast, the estimate from the Base model is smoother even though it tracks the broad contours of the estimate from the univariate model. It is worth remembering that no survey data on wages are included in the model. But, because pi-star informs the w-star trajectory, survey data on inflation expectations indirectly influence w-star.

Panel (d) in Figure 20 plots the estimates of the u-star from the Base model, the CBO, the medium-scale UC model of Hasenzagl et al. (2022) [Hasenzagl], which does not feature SV or TVP, and the bivariate Phillips curve UC model of Chan, Koop, and Potter (2016) [CKP]. Over most of the sample period shown, there are notable differences in the estimates across the models. Both Hasenzagl and the Base models indicate similar u-star from 1990 through 1995, but they diverge significantly after that. The Hasenzagl model has u-star increasing from 5.5% to 6.7% from 1995 to 2010, whereas the Base model has u-star remaining steady for a good ten years and then in 2005 begins to move higher to reach a peak of 5.9% in 2010. Since 2015, the Base model has a u-star close to 4.5 percent, whereas Hasenzagl has a u-star fluctuating up and down randomly in a narrow range between 5.0 and 5.4%; a deeper dive reveals the model's difficulty in handling extreme pandemic-induced movements in the unemployment rate leading

to weird variations in u-star.

The u-star from the CKP model is smoother and significantly higher than the estimates from the Base and Hasenzagl. The CBO estimate indicates a steady decline in u-star from 5.7% to 4.4% over the sample. Between 1995 and 2000, and from 2015 onward, the CBO estimate is identical to the Base model, and both indicate u-star remaining stable from 2019 through 2023, suggesting that they attribute movements in the unemployment rate to be mostly of cyclical nature.

Panel (e) in Figure 20 plots the mean estimates of the g-star from the Base model, CBO, Laubach and Williams (2003) [LW] model, and the Grant and Chan (2017b) univariate model of real GDP. Panel (g) plots the corresponding estimates of the output gap. As can be seen, the inference about g-star from the univariate model over most of the sample period is notably different than others. Over an extended period, starting from the onset of the Great Recession and continuing through the onset of the pandemic recession, there are sizable differences in the g-star estimates between the Base and others, whereas immediately before the Great Recession, the Base model estimated a g-star of 2.3% (same as the univariate), and the CBO and LW indicate a much lower g-star of 1.6%. After that, estimates between the Base and others begin to diverge; as the univariate model stays steady at 2.3%, CBO and LW gradually drift higher, while the Base model trends lower. This diverging pattern continues until 2014. From thereon, the Base model has g-star steadily increasing and catching up with the others by 2022.

Like g-star, there are sizable differences in the output gap estimates implied from Grant and Chan's univariate model. For instance, the univariate model suggests a less dramatic fall in the output gap in the 2007-09 recession (and in the 1973-74 and 1981-82 recessions, as shown in Figure 21) but a steeper fall than others during the pandemic of 2020. In the mild 2001 recession, the univariate model estimates a positive output gap compared to others. Continuing with its pattern of opposing inference compared to others, as of 2023Q3, the output gap estimate remains negative, in sharp contrast to the other two models. The contrasting inference from the univariate model shouldn't be surprising given its univariate nature; it has an incomplete picture of the economic environment and arguably generates estimates of g-star and the output gap with less economic content. The formal Bayesian model comparison confirms the inferior fit of the univariate model to the GDP data compared to the Base model (Base: -255.3 vs. univariate of Grant and Chan: -410.6)

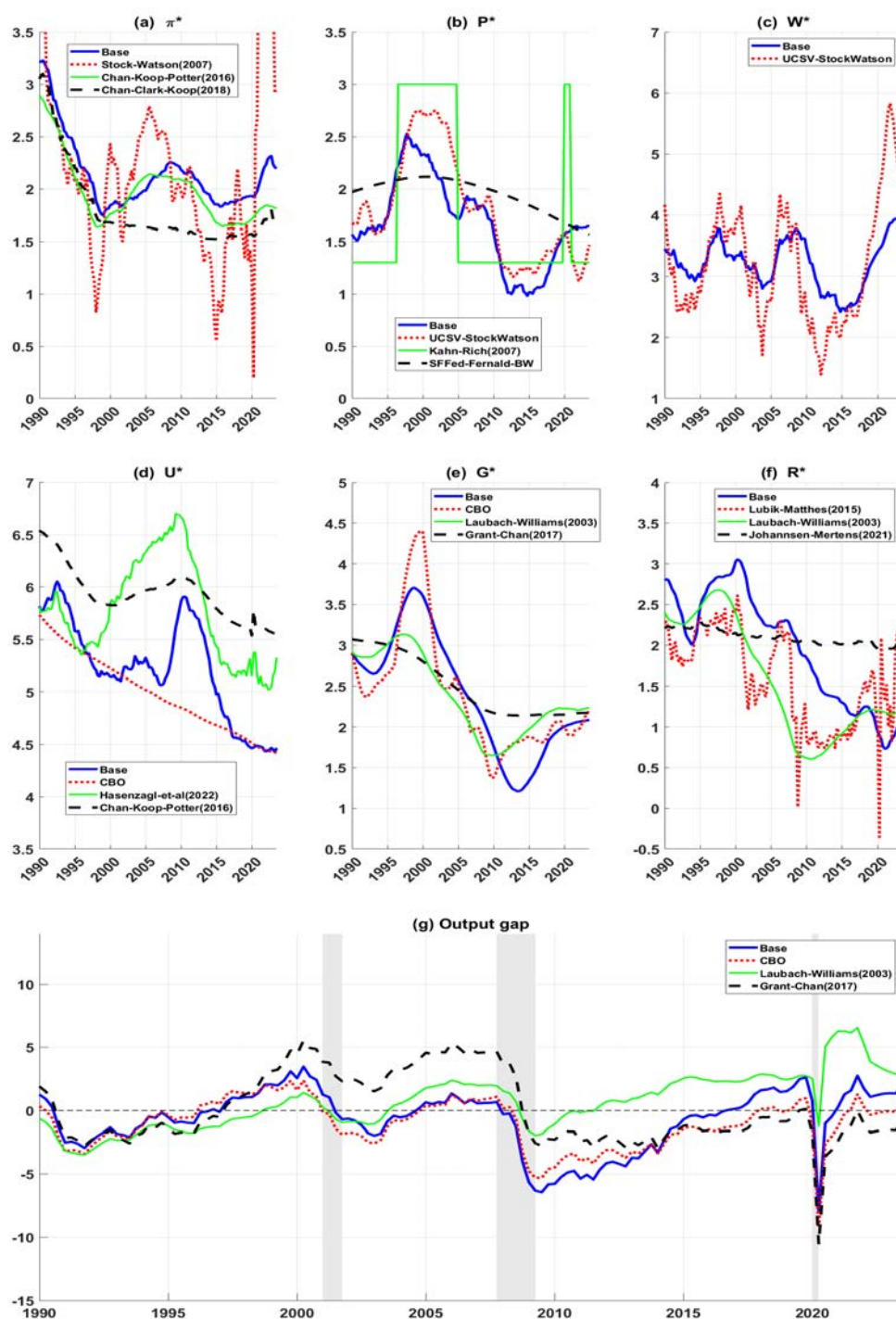
There have also been notable differences in the estimates between the Base and the LW models since the onset of the Great Recession. During the Great Recession and the pandemic recession, the output gap from LW turned only slightly negative. At the same time, the CBO and the Base model indicate a much sharper decline in the output gap (attributed to large transitory shocks). The slight negative gaps in the LW model reflect much bigger hits to the level of potential output (without affecting g-star much) than the Base and the CBO. As detailed in Holston et al. (2023), to capture the direct effects of the COVID pandemic, downward adjustment to the level of potential output is incorporated in 2020, 2021, and 2022

via an exogenous indicator in the LW model (i.e., a temporary supply shock that permanently lowers the level of potential output). This adjustment has direct implications for the estimates of the output gap. Given the significant hit to an estimated level of potential output in 2020 in the LW model, and with a strong recovery in actual output after that, the LW model implies a strongly positive output gap that is notably higher than the estimate from the Base model.

Panel (f) in Figure 20 plots the estimates of r-star from the Base model and three additional models widely used to inform estimates of the r-star. These models include Laubach and Williams (2003) [LW], Johanssen and Mertens (2021) [JM], and Lubik and Matthes (2015). The LW and JM models are small-scale UC models, whereas Lubik and Matthes model is a small-scale time-varying VAR with SV. LW, whose estimates are available to download from the New York Fed's website, paused the production of their estimates during the COVID pandemic because the model had difficulties dealing with the extreme volatility of the data. After making important adjustments to the model, LW resumed production of the estimates in the summer of 2023. Lubik and Matthes model, which is estimated with Bayesian methods, continued to provide estimates through the pandemic and afterward; however, recently, the authors assessed the need to re-calibrate some of the model parameters, and so the estimates shown are based on their updated model setting.

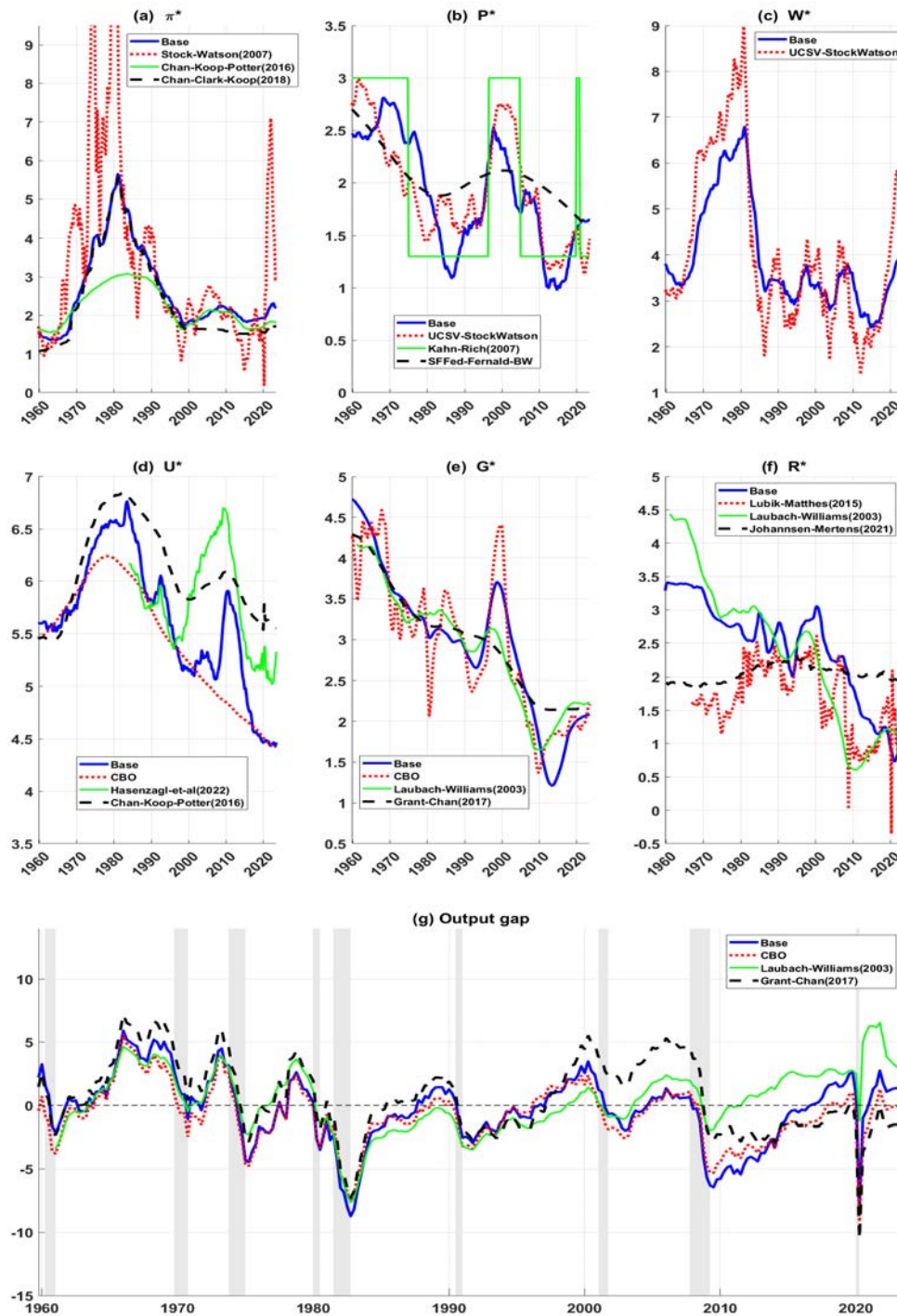
As can be seen, there are sizable differences in the estimates across the models. Lubik and Matthes model displays considerable volatility compared to the others, whereas JM, who model r-star as an RW, is essentially a straight line around 2%; from the 1990 to 2023, it inches down by only 0.3 ppts, from 2.3% to 2.0%. Although both LW and the Base show some similarity in the contours of r-star in that both have r-star declining over the sample shown, there are sizable differences between the estimates. At times, the difference between the estimates exceeds 200 basis points, e.g., in 2007. LW has r-star declining starting in early 2000, whereas in the Base model, the descent begins a year later and from a higher level. The two models provide contrasting inferences from 2009 to 2017, with the LW model estimating r-star gradually moving up and the Base model estimating r-star drifting lower. It is worth pointing out that the similarity in the contours of r-star between the two models mainly stems from the fact that in both models, g-star influences the r-star trajectory, with the influence stronger in the LW model than in the Base model; the estimate of the parameter capturing the strength of the relationship between g-star and r-star is 0.65 in the Base versus 1.13 in LW.

Figure 20: Estimates of Stars and Output Gap: Base model vs. Outside models, from 1990+



Note: Plotted are the (posterior) mean estimates that are computed using the full sample (from 1959Q4 through 2023Q3) but are shown for the period, 1990Q1 to 2023Q3.

Figure 21: Estimates of Stars and Output Gap: Base model vs. Outside models, from 1959+

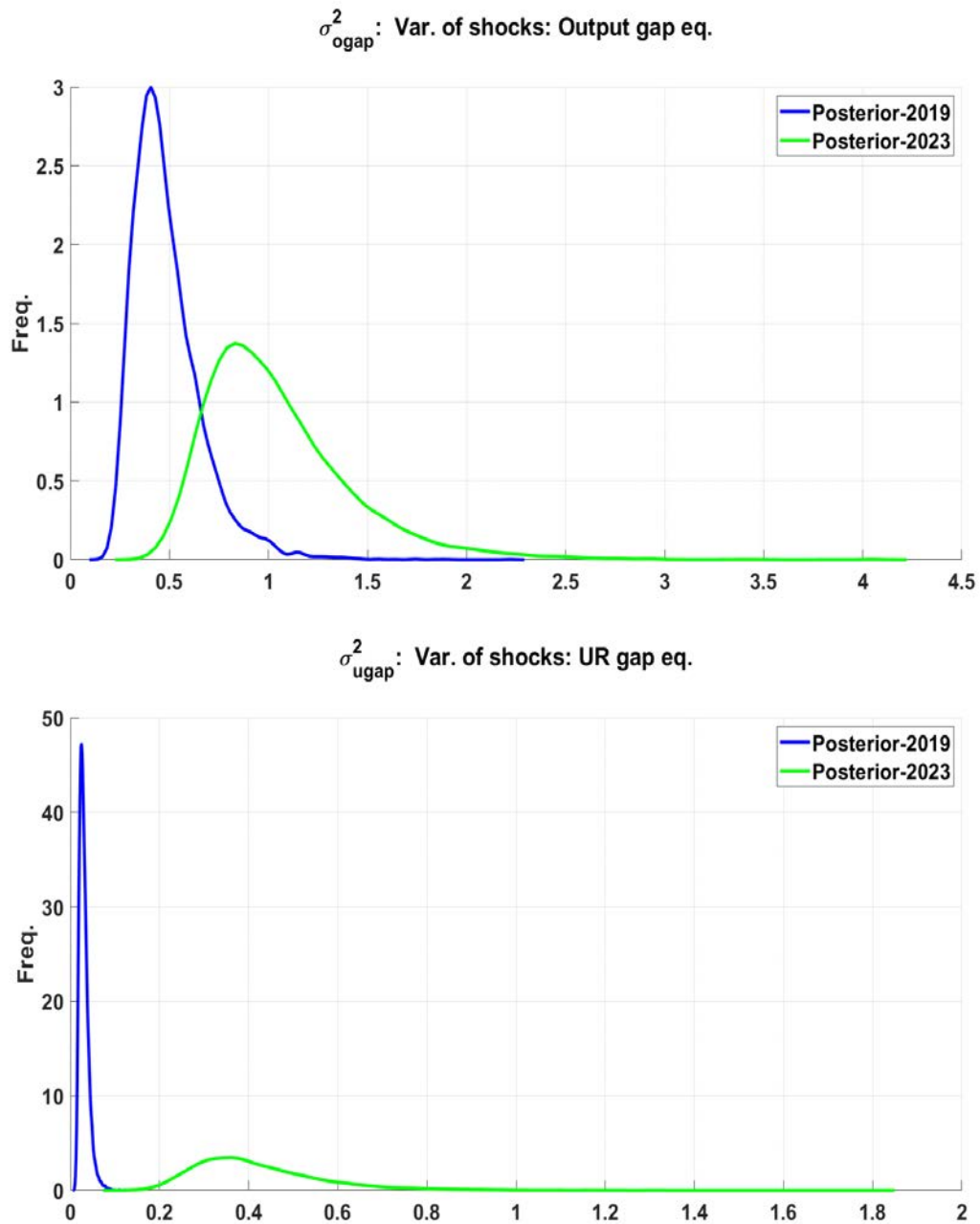


Note: Plotted are the (posterior) mean estimates that are computed using the full sample (from 1959Q4 through 2023Q3).

A18. COVID-19 Pandemic Effects on Variants of Base Model

Without SV, there is significant distortion in some of the parameter estimates from COVID outliers.

Figure 22: Base-NoSV Model



Without SV, there is significant distortion in some of the parameter estimates from COVID outliers.

Figure 23: Base-NoSV-NoTVP-NoSurvey Model

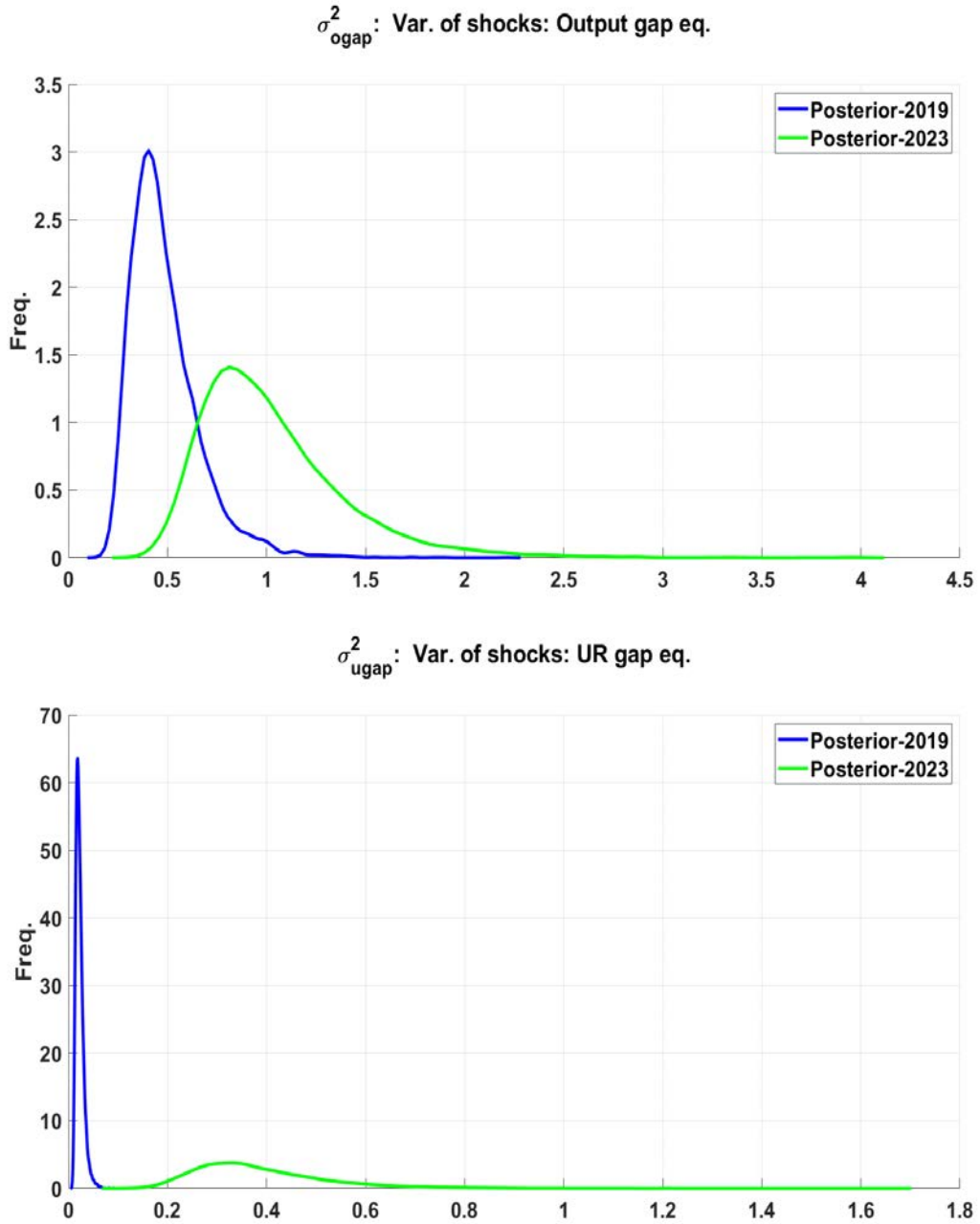
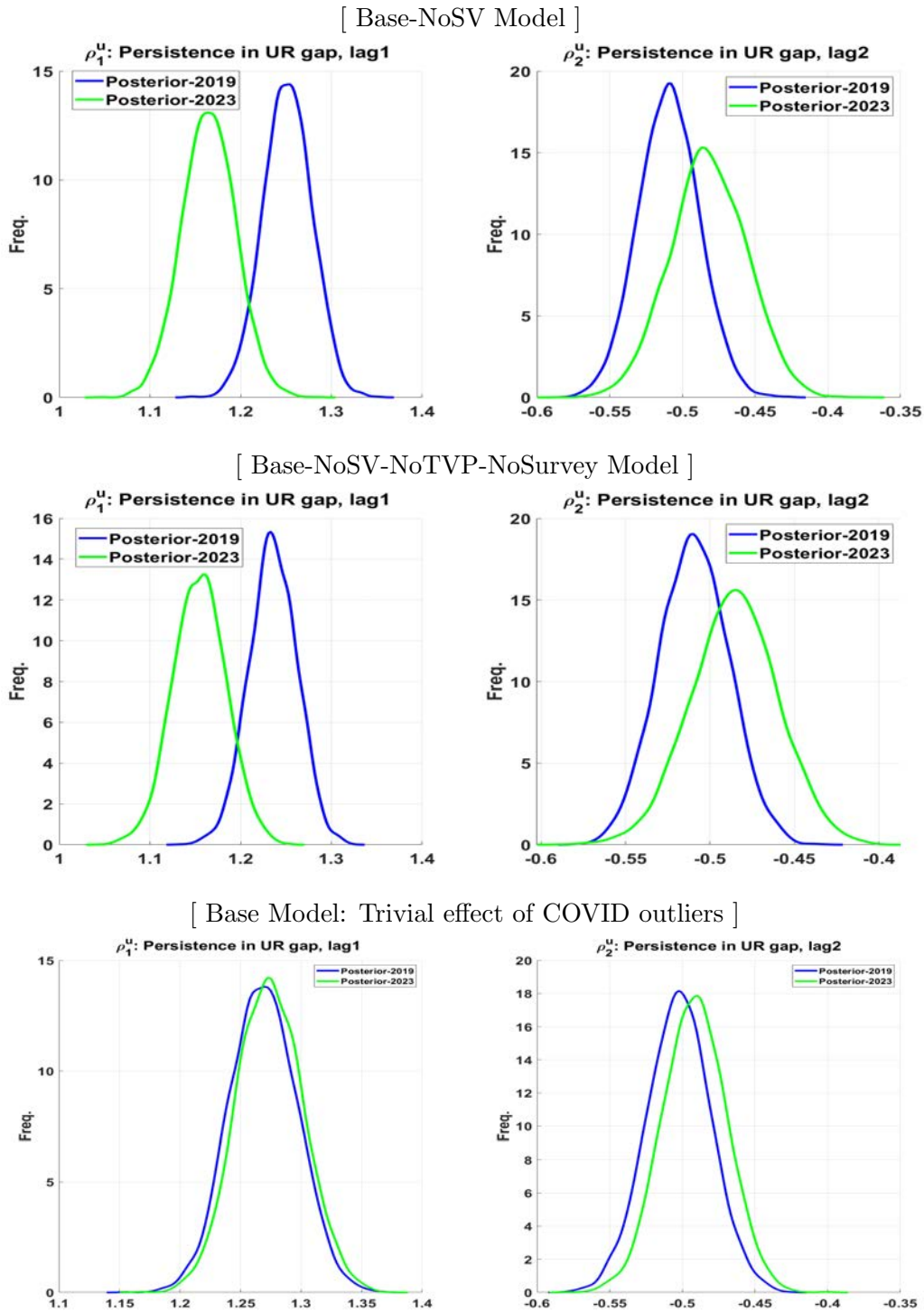
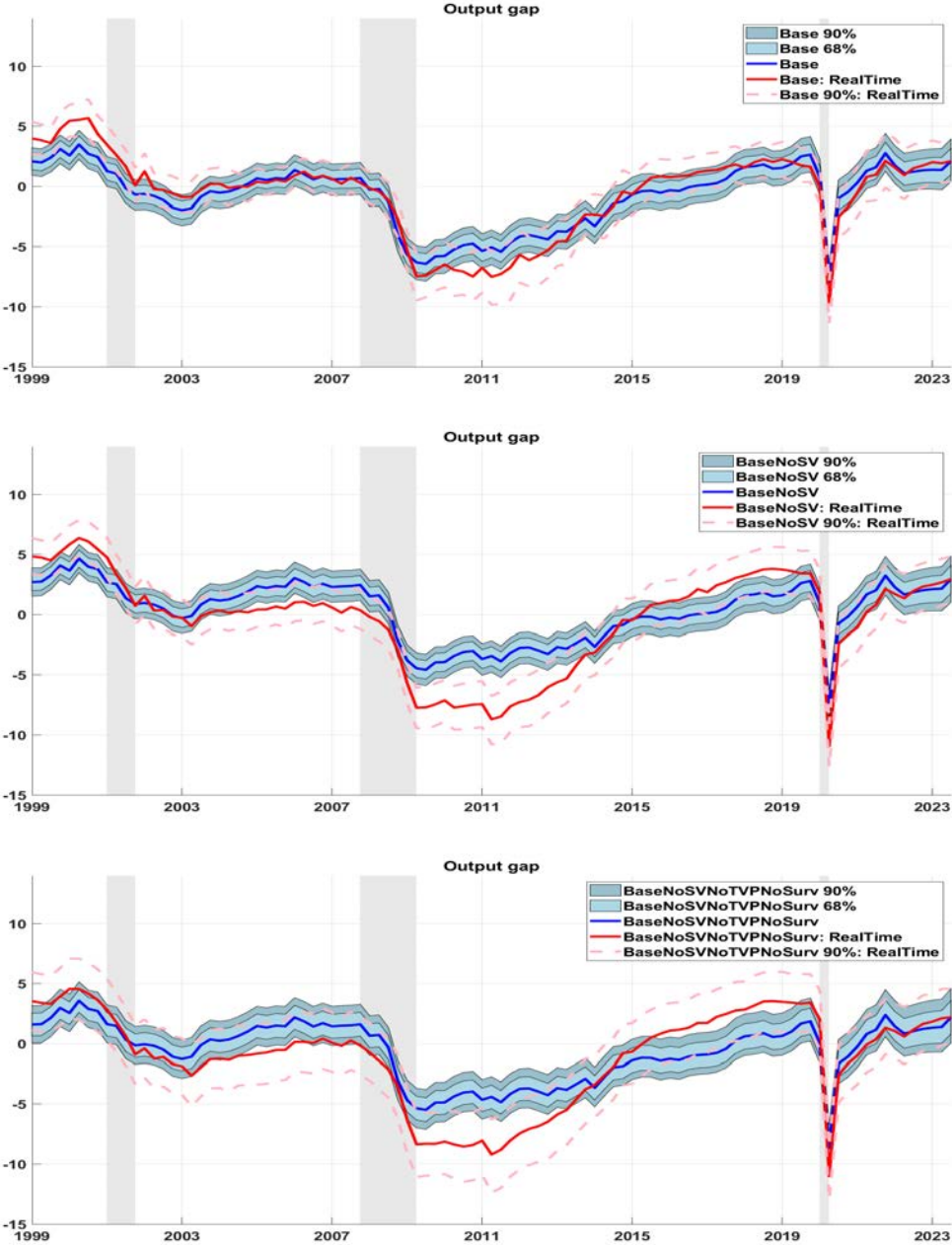


Figure 24: Base vs. Base variants without SV: COVID outliers effect on the persistence parameters in the equation defining the Unemployment Rate gap (the cyclical component)



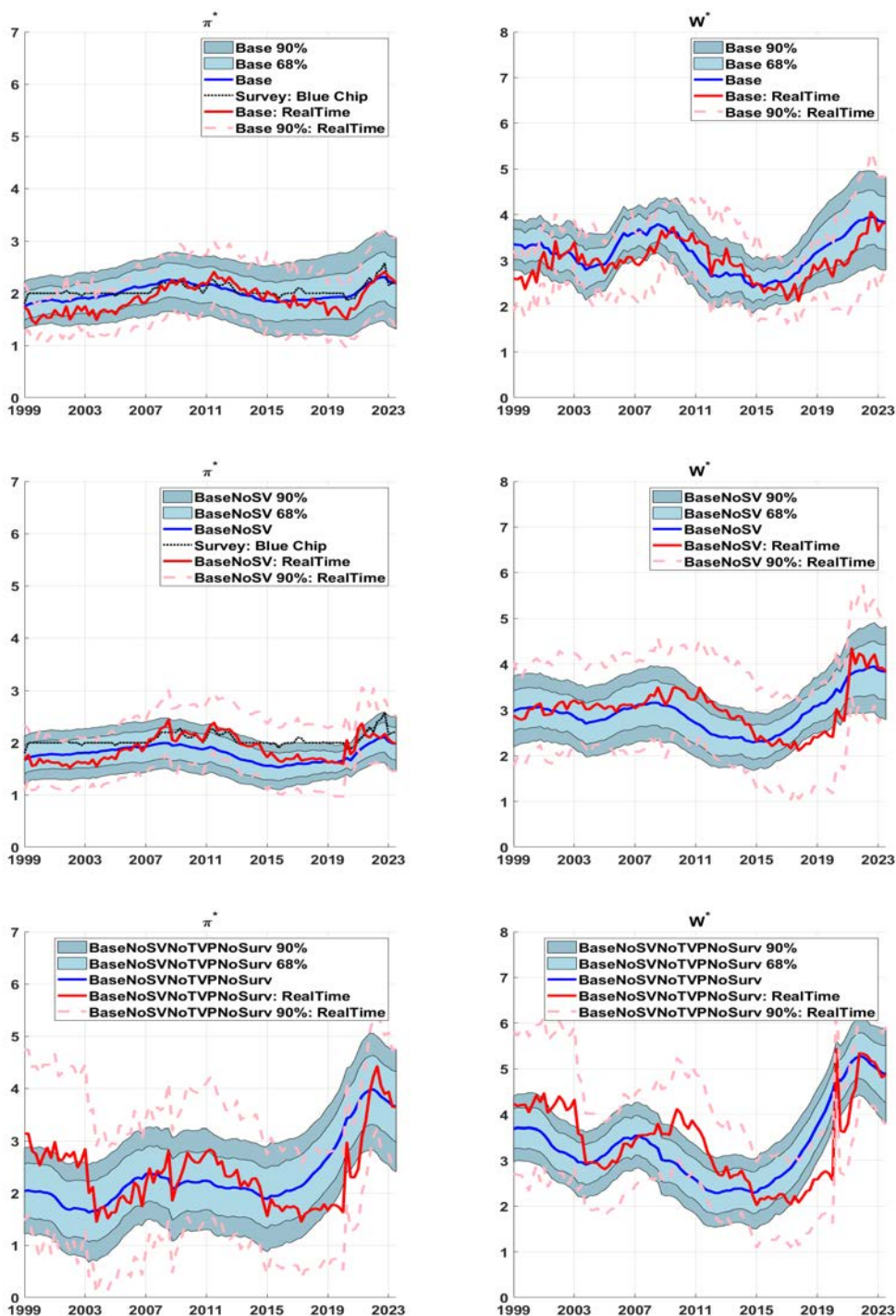
A19. Additional Real-Time Estimates of Stars

Figure 25: Real-Time Recursive Estimates vs. Smoothed: Output Gap



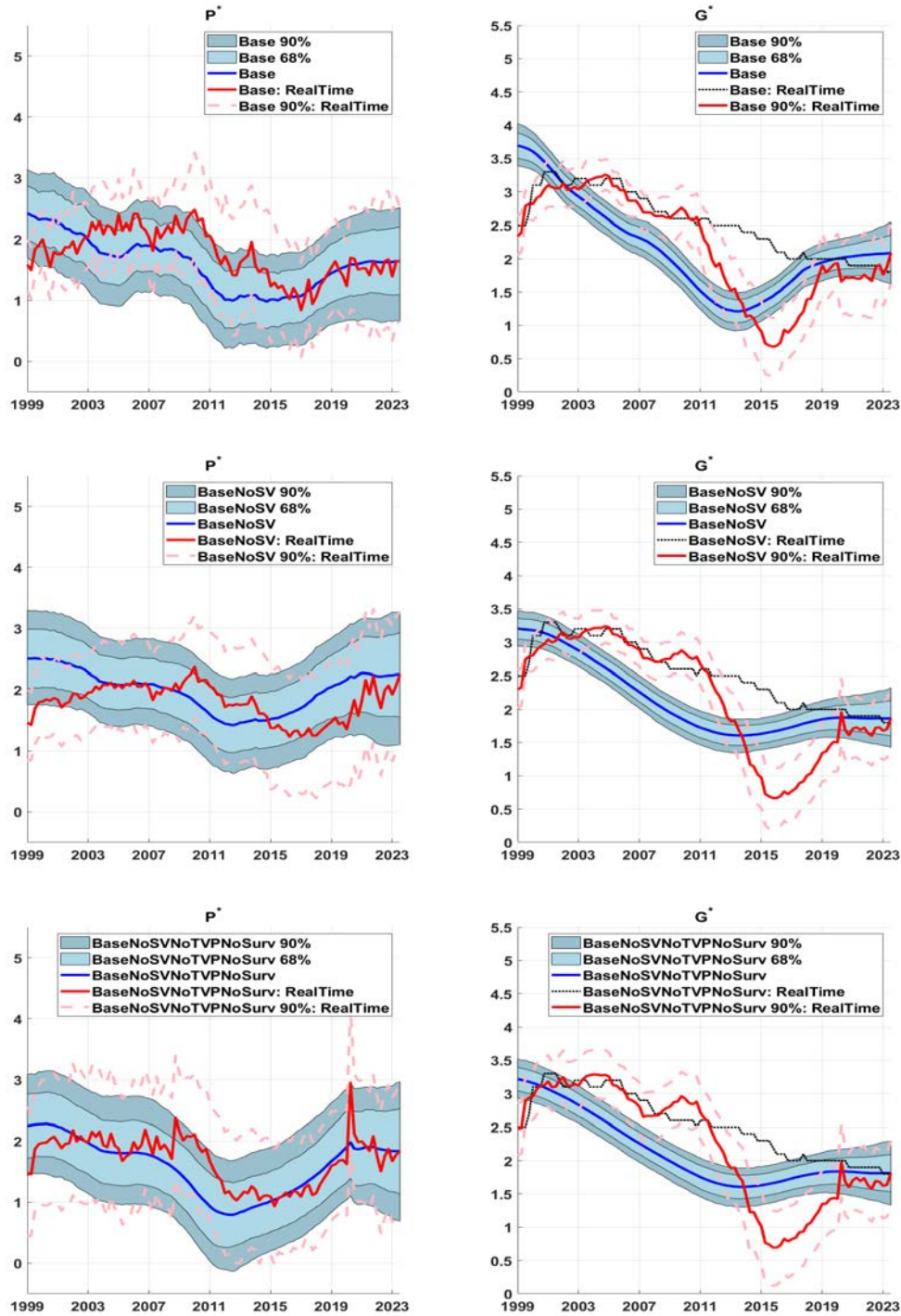
Notes: The first row plots estimates of the output gap from the Base model. The second and third rows plot the corresponding estimates from the models Base-NoSV and Base-NoSV-NoTVP-NoSurvey, respectively. The plots in blue correspond to estimates based on the full sample, i.e., 1959.Q4 through 2023.Q3. The plots in red correspond to real-time recursive estimates generated by estimating a given model at different points in time, specifically 1999.Q1 through 2023.Q3.

Figure 26: Real-Time Recursive Estimates of Stars vs. Smoothed Stars: pi-star and w-star



Notes: The first row plots pi-star and w-star estimates from the Base model. The second and third rows plot the corresponding estimates from the models Base-NoSV and Base-NoSV-NoTVP-NoSurvey, respectively. The plots in blue correspond to estimates based on the full sample, i.e., 1959.Q4 through 2023.Q3. The plots in red correspond to real-time recursive estimates generated by estimating a given model at different points in time, specifically 1999.Q1 through 2023.Q3.

Figure 27: Real-time Recursive Estimates of Stars vs. Smoothed Stars: p-star and g-star



Notes: The first row plots p-star and g-star estimates from the Base model. The second and third rows plot the corresponding estimates from the models Base-NoSV and Base-NoSV-NoTVP-NoSurvey, respectively. The plots in blue correspond to estimates based on the full sample information, i.e., 1959.Q4 through 2023.Q3. The plots in red correspond to real-time recursive estimates generated by estimating a given model at different points in time, specifically 1999.Q1 through 2023.Q3.

A20. Forecasting Results I: Base vs. Base Variants and Base vs. Benchmarks

Base vs. Base Variants

Table 4 presents the results comparing the out-of-sample point forecasting performance of the Base model to its variants over the forecast evaluation sample spanning 1999Q1 through 2019Q4. The forecast evaluation is based on real-time data vintages and uses a recursively expanding estimation window, where each recursive run uses an additional quarterly data point in the estimation sample.¹⁸ The forecast accuracy is computed from one-quarter ahead to 12 quarters out. Partly due to focus on the medium-term horizon and partly in the interest of space, I report accuracy metrics for 4, 6, 8, 10, and 12 quarters ahead. I evaluate the forecast accuracy using real-time data; specifically, I treat the “actual” as the *third* release of a given quarterly estimate.¹⁹ For instance, in the case of real GDP, the third estimate for 2018Q4 corresponds to the GDP data available in late 2019Q1. The point forecast accuracy is assessed using the root mean squared error (RMSE) metric, and the statistical significance of the forecast accuracy is gauged using the Diebold-Mariano and West test.

The numbers reported in the table correspond to relative RMSE –RMSE Base relative to RMSE of the Base variant. Hence, numbers less than one suggest that the point forecast accuracy of the Base forecast is more accurate on average than the comparative Base variant.

As is evident by the numbers reported in the table, the evidence generally favors the Base model as more accurate than any of the variants.

¹⁸Going back in time means that relatively fewer observations are being used to estimate model(s). As is commonly done when performing real-time forecasting using multivariate UC models, I impose tighter priors on the shocks’ variances driving the latent components (see, for instance, Barbarino et al., 2020). Accordingly, I devise a systematic approach to adjusting the prior on the scale parameters of the inverse gamma distributions defining the variances of the stars. I multiply the scale parameter with the $factor = (\frac{2T}{N} - 1) * (\frac{T}{N+5(N-T)})$, where N is the total sample size from 1959Q4 through 2019Q4, and T refers to the number of data points in a given data vintage. At the end of the sample, the $factor = 1$ because $T = N$.

¹⁹Results are qualitatively similar if I instead use the revised data (2020Q1 vintage data) as the actual values in the forecast evaluation exercises.

Table 4: Real-Time Point Forecasting Accuracy: Base vs. Base Variants

Panel A: Base vs. Base-NoSV (Recursive evaluation: 1999.Q1-2019.Q4)

Relative RMSE: RMSE Base / RMSE BaseNoSV					
	h=4Q	h=6Q	h=8Q	h=10Q	h=12Q
Real GDP	0.95*	0.98*	0.97*	0.96*	0.98*
PCE Inflation	0.99	0.99	0.97	0.98	0.99
Productivity	0.98*	1.00	1.00	0.99	0.99*
Nominal Wage (AHE)	0.88	0.86	0.84	0.82	0.83
Unemployment Rate	0.99	1.00	0.99	0.99	0.99
Shadow FFR	0.94*	0.94*	0.94*	0.95	0.95

Panel B: Base vs. Base-NoTVP (Recursive evaluation: 1999.Q1-2019.Q4)

Relative RMSE: RMSE Base / RMSE BaseNoTVP					
	h=4Q	h=6Q	h=8Q	h=10Q	h=12Q
Real GDP	0.99*	0.99*	0.98*	0.99	0.98
PCE Inflation	0.96*	0.97*	0.98	1.01	1.01*
Productivity	0.98*	0.98*	0.98*	0.99	0.98*
Nominal Wage (AHE)	1.04	1.05*	1.00	0.97	0.98
Unemployment Rate	0.98*	0.98*	0.98*	0.98	0.97
Shadow FFR	1.01	1.02	1.03*	1.03	1.03

Panel C: Base vs. Base-NoSurv (Recursive evaluation: 1999.Q1-2019.Q4)

Relative RMSE: RMSE Base / RMSE BaseNoSurv					
	h=4Q	h=6Q	h=8Q	h=10Q	h=12Q
Real GDP	1.02	0.98*	0.99	0.99*	1.00
PCE Inflation	0.96	0.92*	0.93*	0.91*	0.90
Productivity	0.99	1.01	1.01	1.01	0.98*
Nominal Wage (AHE)	0.98	0.94*	0.90*	0.92*	0.93*
Unemployment Rate	1.02	1.02	1.01	1.00	0.98
Shadow FFR	1.05	1.07*	1.11*	1.13*	1.14*

Panel D: Base vs. Base-NoSVNoTVPNoSurv (Recursive evaluation: 1999.Q1-2019.Q4)

Relative RMSE: RMSE Base / RMSE BaseNoSVNoTVPNoSurv					
	h=4Q	h=6Q	h=8Q	h=10Q	h=12Q
Real GDP	0.99	0.98	0.97*	0.97	0.98
PCE Inflation	0.90*	0.87*	0.87	0.87	0.91
Productivity	0.98	0.98	0.98	0.96*	0.96*
Nominal Wage (AHE)	0.80*	0.79*	0.73*	0.72	0.73
Unemployment Rate	1.02	1.01	1.00	0.98	0.97*
Shadow FFR	0.95	0.95	0.94	0.94	0.94

Notes: Numbers less than 1 indicate that the Base model is more accurate on average than the variant. The table reports statistical significance based on the Diebold-Mariano and West test (with the lag $h - 1$ truncation parameter of the HAC variance estimator) for the point forecast accuracy. The test statistics use two-sided standard normal critical values for horizons less than or equal to 8 quarters, and two-sided t-statistics for horizons greater than 8 quarters. *up to 10% significance level.

Base vs. Benchmarks In this section I compare the real-time forecasting performance of the Base model to the outside benchmark models, which the forecasting literature has shown to be useful forecasting devices. Specifically, I compare the accuracy of the inflation forecasts from the Base model to the following three models: UCSV of Stock and Watson (2007) [UCSV], Chan et al. (2016) [CKP], and Chan et al. (2018) [CCK]. I compare the accuracy of the unemployment rate forecasts from the Base model to the CKP, and the accuracy of the nominal wage inflation from the Base model to the UCSV model applied to the nominal wage inflation – motivated by Knotek II (2015).

Table 5 presents the forecast evaluation results for headline PCE inflation, nominal wage inflation, and the unemployment rate. These results indicate the following three observations. First, in terms of point forecast accuracy, inflation forecasts from all four models considered are competitive with each other. There is some statistically significant evidence that the Base model is more accurate than UCSV at $h=12Q$. Regarding the density forecast accuracy, the Base model is more accurate than the UCSV but inferior to CCK, as the latter produces more precise intervals than the Base model. Second, in the case of nominal wage inflation, the Base model generates more accurate forecasts (both point and density) than UCSV, and the gains are statistically significant for the most part.

Third, the accuracy of the unemployment forecasts from the Base model is competitive with the CKP model statistically speaking, even though the relative numbers favor CKP. A closer inspection of the forecast errors reveals that the Base model, which incorporates survey forecasts of the unemployment rate, experienced significantly bigger misses than the CKP model around the Great Recession period. Outside of this period, the Base model is slightly more accurate than the CKP, and when combined with the Great Recession period, on the net, the much bigger misses of the Base model result in overall slightly higher RMSE.

As illustrated in Tallman and Zaman (2020), just before and at the onset of the Great Recession, survey participants projected relatively upbeat long-run forecasts of unemployment, which indicated a declining natural rate of unemployment. It was not until a few months into the recession that survey participants recognized the extent of the labor market damage and began to revise their estimates of the long-run unemployment rate higher. Hence, models such as the Base model that take signals from the survey forecasts experienced big misses.

To sum up, I view these forecasting results as providing evidence supporting the Base model's competitive forecasting properties.

Table 5: Out-of-Sample Forecasting Performance: **Base vs. Benchmarks**

Full Sample (Recursive evaluation: 1999.Q1-2019.Q4)									
	Point forecasting				Density forecasting				
	4Q	8Q	12Q	20Q	4Q	8Q	12Q	20Q	
PCE Inflation									
Relative RMSE					Relative Log Score				
Base/UCSV	0.96	0.96	0.93*	0.95	Base - UCSV	0.012*	0.022*	0.027*	0.025*
Base/CCK	1.02	1.04*	1.02	1.02	Base - CCK	-0.018*	-0.032*	-0.048*	-0.076*
Base/CKP	1.00	0.98	0.98	1.00	Base - CKP	0.001	-0.001	-0.004*	-0.024*
Nominal Wage									
Relative RMSE					Relative Log Score				
Base/UCSV	0.88*	0.78*	0.80*	0.50	Base - UCSV	0.017*	0.035*	0.031*	0.010
Unemployment Rate									
Relative MSE					Relative Log Score				
Base/CKP	1.01	1.03	1.05	1.06	Base - CKP	0.115*	0.025	-0.019	-0.059*

Notes: For variables PCE inflation and nominal wage (i.e., average hourly earnings), the forecasts and associated accuracy correspond to the quarterly annualized rate. **Base** forecast is defined as the Steady-State (SS) VAR forecast in which the steady states are assumed to be the estimates of the stars from the Base model. **UCSV** forecast corresponds to the forecast from the univariate unobserved component stochastic volatility model similar to Stock and Watson (2007). The model is used to construct forecasts of PCE inflation and nominal wage inflation. **CCK** forecast corresponds to the forecast from the bivariate unobserved component stochastic volatility model of Chan, Clark and Koop (2018). **CKP** forecast corresponds to the forecast from the bivariate unobserved component stochastic volatility model of Chan, Koop and Potter (2016), with the bounds on u-star fixed to values identical to the Base model. The left panel reports results for the point forecast accuracy (relative root mean squared errors) and the right panel reports the corresponding density forecast accuracy (mean of the relative log predictive score). The table reports statistical significance based on the Diebold-Mariano and West test with the lag $h - 1$ truncation parameter of the HAC variance estimator and adjusts the test statistic for the finite sample correction proposed by Harvey, Leybourne, and Newbold (1997); *up to 10% significance level. The test statistics use two-sided standard normal critical values for horizons less than or equal to 8 quarters, and two-sided t-statistics for horizons greater than 8 quarters.

A21. Forecasting Results II: SSBVAR, Base Stars vs. Survey

In macroeconomic forecasting, research by Wright (2013) and Tallman and Zaman (2020), among others, using workhorse Bayesian VAR models shows that the predictive performance boils down to good starting conditions (i.e., nowcasts) and terminal conditions (i.e., steady states proxied by stars). Survey forecasts provide both nowcasts and long-run projections, whose accuracy has been shown by past research to be quite good. Wright (2019) emphasizes the desirable forecasting properties of the survey forecasts and highlights that econometric approaches utilizing survey projections are at the forecasting frontier, especially in inflation forecasting. Most empirical research on forecasting has focused on proposing methods to improve the accuracy of the nowcast estimates relative to survey nowcasts' accuracy, but only little effort has been dedicated to improving estimates of long-run projections. Hence, this paper raises a natural curiosity about the usefulness of the stars' estimates from this paper's modeling framework for macroeconomic forecasting using Bayesian VARs (via the imposition of steady states).

To assess the efficacy of the Base model's stars' estimates for the external VAR models, I perform a real-time out-of-sample forecasting evaluation similar to Wright (2013) and Tallman and Zaman (2020). These studies informed the time-varying steady states for the steady-state (SS) BVAR using long-run survey projections and found that doing so leads to significant gains in accuracy. Accordingly, the design of the forecasting examination is as follows. I take the SSBVAR from Tallman and Zaman (2020) and perform two sets of recursive real-time out-of-sample forecasting runs. In the first run, I inform the steady states for real GDP growth, PCE inflation, core PCE inflation, the unemployment rate, nominal wage inflation, and labor productivity growth using long-run survey projections. For the latter two variables, I use the survey expectations from the SPF.²⁰ The forecasts from this run are denoted 'Survey' in Table 6. In the second run, I repeat the exercise, but this time inform the steady-states using the real-time estimates of the stars from the Base model, denoted 'Base'.

Each of the two forecasting runs is based on estimating the SSBVAR with a recursively expanding sample, i.e., the recursive execution uses an additional quarterly data point in the estimation. The SSBVAR is estimated with quarterly data beginning 1959Q2. The model consists of ten variables: (1) real GDP growth; (2) real consumption expenditures; (3) headline PCE inflation; (4) core PCE inflation; (5) labor productivity growth; (6) growth in average hourly earnings; (7) growth in payroll employment; (8) the unemployment rate; (9) the shadow federal funds rate; and (10) the risk spread, defined as the difference between the yield on the 10-year Treasury bond and yield on BAA-rated bond. The out-of-sample forecasting period spans 1999Q1 through 2019Q4. The forecast accuracy (point and density) is computed from one-quarter-ahead to 20 quarters out. Partly due to the focus on the medium-term horizon and partly in the interest of space, I report accuracy metrics for 4, 8, 12, and 20 quarters ahead.

²⁰In the case of nominal wage inflation, I construct an implied survey projection by adding the survey expectation of PCE inflation and productivity, both of which are obtained from the SPF.

I evaluate the forecast accuracy using real-time data; specifically, I treat the “actual” as the third quarterly estimate. For instance, in the case of real GDP, the third estimate for 2018Q4 corresponds to the GDP data available in late 2019Q1. The point forecast accuracy is assessed using the root mean squared error (RMSE) metric, and the density forecast accuracy is assessed using the continuous ranked probability score (CRPS). Forecasts with lower RMSE and CRPS are preferred. The statistical significance of the point and density forecast accuracy is gauged using the Diebold-Mariano and West test. The description of these tests is listed in the notes accompanying the tables reporting forecast accuracy.

Table 6 reports forecast evaluation results corresponding to this exercise. The left panel reports the point forecast accuracy results, while the right panel reports results for the density forecast accuracy. I evaluate and compare the point and density forecast accuracies of the two forecasting runs in a pairwise fashion. For each variable, the row reports the relative RMSE (Base relative to Survey) for point forecast accuracy and the relative CRPS for density forecast accuracy. A model with lower values of RMSE and CRPS is preferred to a model with higher values. These relative metrics indicate the competitive accuracy of the stars’ estimates from the Base model compared to Survey.

In the case of nominal wage inflation and the unemployment rate, the SSBVAR with steady states informed by the Base model generates forecasts that are substantially more accurate than Survey on average. The gains are statistically significant for the most part.

Overall, these forecasting results lend credibility to Base model’s stars’ estimates in their use to inform steady states for VAR forecasting models. I also note that the results in this section lend support to the survey projections in their use as proxies for stars, something also documented by Tallman and Zaman (2020), among others. However, the preference is for forecasts (or estimates of stars) obtained using a single multivariate model because the resulting forecasts will be coherent and allow for a credible narrative in a systematic manner.

Table 6: Out-of-Sample Forecasting Performance: **Steady-State BVAR**

Full Sample (Recursive evaluation: 1999.Q1-2019.Q4)									
Point forecasting					Density forecasting				
	4Q	8Q	12Q	20Q		4Q	8Q	12Q	20Q
Real GDP									
Relative RMSE					Relative CRPS				
Base/Survey	0.96	1.00	1.03	1.01	Base - Survey	-0.05	0.02	0.04	0.02
PCE Inflation									
Relative RMSE					Relative CRPS				
Base/Survey	0.98	1.00	1.02	1.01	Base - Survey	-0.02*	0.01	0.03	0.02
Productivity									
Relative RMSE					Relative CRPS				
Base/Survey	1.03	1.04	1.04	1.01*	Base - Survey	0.02	0.04	0.04	0.01*
Nominal Wage									
Relative RMSE					Relative CRPS				
Base/Survey	0.71*	0.68*	0.67*	0.71*	Base - Survey	-0.09*	-0.13*	-0.18*	-0.26*
Unemployment Rate									
Relative MSE					Relative CRPS				
Base/Survey	0.93*	0.91*	0.90	0.92	Base - Survey	-0.04	-0.12	-0.16	-0.12
Shadow FFR									
Relative RMSE					Relative CRPS				
Base/Survey	0.99	0.97	0.96	0.95*	Base - Survey	-0.01	-0.07	-0.13	0.16*

Notes: For the variables real GDP, PCE inflation, productivity, nominal wage (i.e., average hourly earnings), the forecasts and the associated accuracy correspond to the quarterly annualized rate. Base forecast is defined as the Steady-State (SS) VAR forecast in which the steady states are assumed to be the estimates of the stars from the Base model. The left panel reports results for the point forecast accuracy (relative root mean squared errors) and the right panel reports the corresponding density forecast accuracy (mean of the relative continuous ranked probability score). The table reports statistical significance based on the Diebold-Mariano and West test with the lag $h - 1$ truncation parameter of the HAC variance estimator and adjusts the test statistic for the finite sample correction proposed by Harvey, Leybourne, and Newbold (1997); *up to 10% significance level. The test statistics use two-sided standard normal critical values for horizons less than or equal to 8 quarters, and two-sided t-statistics for horizons greater than 8 quarters.

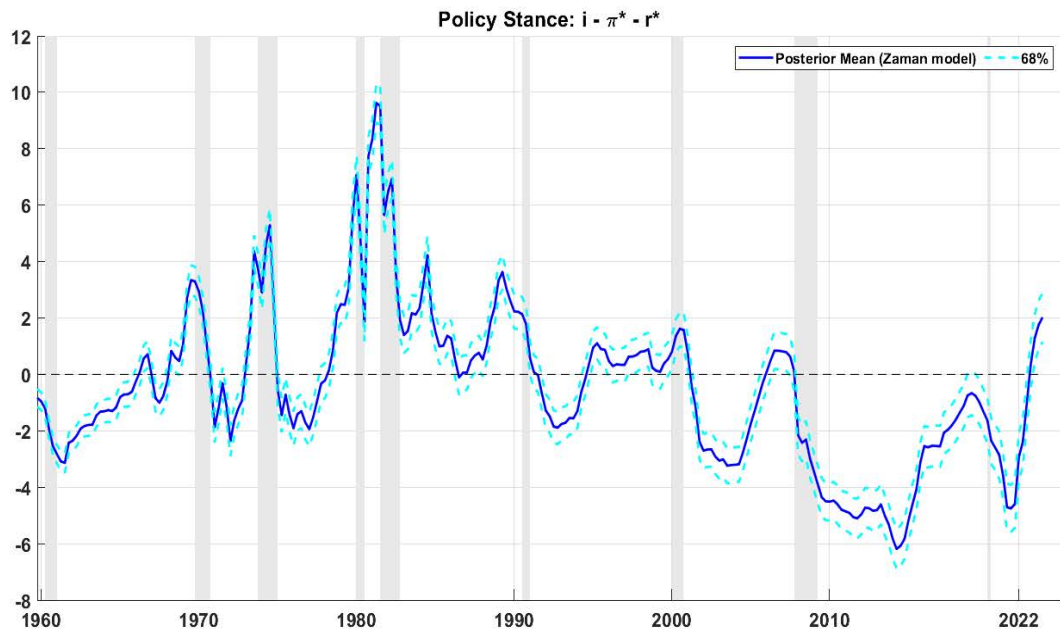
A22. Assessment of Policy Stance: Base Model

Figure 28 provides an assessment of the stance of monetary policy, defined as the deviation of the short-term nominal interest rate from the implied long-run nominal neutral rate of interest (sum of r^* and π^*) – this is the interest rate gap from the Taylor-rule equation. A positive interest rate gap characterizes a restrictive monetary policy stance, and a negative interest rate gap implies a stimulative stance. The solid line corresponds to the posterior mean estimate of the policy stance inferred from the Base model and the dashed lines are the 68% credible bands.

According to the Base model estimates, after remaining quite accommodative following the COVID pandemic shock, the policy stance turned restrictive at the end of 2022, and as of 2023Q3 is more restrictive than anytime prior to 1990. However, in comparison to the early 1980s (when inflation was in double digits), the stance is significantly less restrictive. The stance was slightly restrictive before the Great Recession, but at the onset of the Great Recession, the policy stance immediately turned accommodative. It remained very accommodative (reflecting the effects of unconventional monetary policy) until late 2015, after which the degree of accommodation gradually declined (i.e., the interest rate gap became less negative), such that, by the end of 2019, it edged closer to the neutral threshold. Soon after, the COVID-19 pandemic shock happened, and in response the stance turned very accommodative yet again.

A closer inspection of the figure reveals an interesting insight. Since 1990, both the degree and the duration of policy accommodation in response to the recession have been more significant than in the previous recession, with the COVID-19 pandemic as an exception. For instance, the monetary policy stance was more accommodative in terms of both level and duration following the 2001 recession than following the 1990-1991 recession. Similarly, during the Great Recession and afterward, the policy stance, in terms of level and duration, was more significant than following the 2001 recession. This reflects the fact that each subsequent recession was more severe than the previous one. In the case of the COVID recession, although the stance was more accommodative than in 1990-91 and 2001 recessions, due to its shorter duration than the Great Recession, the stance was relatively less accommodative than post-Great Recession.

Figure 28: Policy Stance



Notes: Plotted are the posterior mean estimates based on estimation using the full sample (from 1959Q4 through 2023Q3).

References

- Antolin-Diaz, Juan, Thomas Drechsel, and Ivan Petrella (2017). “Tracking the slowdown in long-run GDP growth.” *The Review of Economics and Statistics*, 99(2), pp. 343–356. doi:10.1162/REST_a-00646.
- Bañbura, Marta and Elena Bobeica (2020). “Does the Phillips curve help to forecast euro area inflation?” Working Paper 2471, European Central Bank. doi:10.2866/61538.
- Barbarino, Alessandro, Travis J. Berge, Han Chen, and Andrea Stella (2020). “Which output gap estimates are stable in real time and why?” Technical Report 2020-101, Board of Governors of the Federal Reserve System. doi:10.17016/FEDS.2020.102.
- Bauer, Michael D. and Glenn D. Rudebusch (2020). “Interest rates under falling stars.” *American Economic Review*, 110(5), pp. 1316–1354. doi:10.1257/aer.20171822.
- Berger, Tino, Gerdie Everaert, and Hauke Vierke (2016). “Testing for time variation in an unobserved components model for the U.S. economy.” *Journal of Economic Dynamics and Control*, 69, pp. 179–208. doi:10.1016/j.jedc.2016.05.017.
- Brand, Claus and Falk Mazelis (2019). “Taylor-rule consistent estimates of the natural rate of interest.” Working Paper 2257, European Central Bank. doi:10.2866/44361.
- Carriero, Andrea, Todd E. Clark, and Massimiliano Marcellino (2019). “Large Bayesian vector autoregressions with stochastic volatility and non-conjugate priors.” *Journal of Econometrics*, 212(1), pp. 137–154. doi:10.1016/j.jeconom.2019.04.024.
- Cecchetti, S., M. Feroli, P. Hooper, F. S. Mishkin, and K. L. Schoenholtz (2023). “Managing disinflations.” Discussion Paper DP18068, CEPR.
- Chan, Joshua C. C. (2013). “Moving average stochastic volatility models with application to inflation forecast.” *Journal of Econometrics*, 176(2), pp. 162–172. doi:10.1016/j.jeconom.2013.05.003.
- Chan, Joshua C. C. (2017). “The stochastic volatility in mean model with time-varying parameters: An application to inflation modeling.” *Journal of Business & Economic Statistics*, 35(1), pp. 17–28. doi:10.1080/07350015.2015.1052459.
- Chan, Joshua C. C. (2019). “Large hybrid time-varying parameter VARs.” Technical Report 2019-77, Centre for Applied Macroeconomic Analysis, Crawford School of Public Policy, The Australian National University.
- Chan, Joshua C. C., Todd E. Clark, and Gary Koop (2018). “A new model of inflation, trend inflation, and long-run inflation expectations.” *Journal of Money, Credit and Banking*, 50(1), pp. 5–53. doi:10.1111/jmcb.12452.

- Chan, Joshua C. C. and Eric Eisenstat (2018a). “Bayesian model comparison for time-varying parameter VARs with stochastic volatility.” *Journal of Applied Econometrics*, 33(4), pp. 509–532. doi:10.1002/jae.2617.
- Chan, Joshua C. C. and Eric Eisenstat (2018b). “Comparing hybrid time-varying parameter VARs.” *Economics Letters*, 171, pp. 1–5. doi:10.1016/j.econlet.2018.06.031.
- Chan, Joshua C. C., Gary Koop, and Simon M. Potter (2013). “A new model of trend inflation.” *Journal of Business & Economic Statistics*, 31(1), pp. 94–106. doi:10.1080/07350015.2012.741549.
- Chan, Joshua C. C., Gary Koop, and Simon M. Potter (2016). “A bounded model of time variation in trend inflation, Nairu and the Phillips curve.” *Journal of Applied Econometrics*, 31(3), pp. 551–565. doi:10.1002/jae.2442.
- Clark, Peter K. (1987). “The cyclical component of U.S. economic activity.” *The Quarterly Journal of Economics*, 102(4), p. 797. doi:10.2307/1884282.
- Clark, Todd E. and Sharon Kozicki (2005). “Estimating equilibrium real interest rates in real time.” *The North American Journal of Economics and Finance*, 16(3), pp. 395–413. doi:10.1016/j.najef.2005.04.002.
- Cogley, Timothy, Giorgio E. Primiceri, and Thomas J. Sargent (2010). “Inflation-gap persistence in the US.” *American Economic Journal: Macroeconomics*, 2(1), pp. 43–69. doi:10.1257/mac.2.1.43.
- Cogley, Timothy and Argia M Sbordone (2008). “Trend inflation, indexation, and inflation persistence in the New Keynesian Phillips Curve.” *The American Economic Review*, 98(5), pp. 2101–2126. doi:10.1257/aer.98.5.2101.
- Coibion, Olivier, Yuriy Gorodnichenko, and Mauricio Ulate (2018). “The cyclical sensitivity in estimates of potential output.” *Brookings Papers on Economic Activity*, 2018(2), pp. 343–441. doi:10.1353/eca.2018.0020.
- Crump, Richard, Stefano Eusepi, Marc Giannoni, and Ayşegül Şahin (2019). “A unified approach to measuring u^* .” Working Paper 25930, National Bureau of Economic Research. doi:10.3386/w25930.
- Del Negro, Marco, Domenico Giannone, Marc P. Giannoni, and Andrea Tambalotti (2017). “Safety, liquidity, and the natural rate of interest.” *Brookings Papers on Economic Activity*, 2017(1), pp. 235–316. doi:10.1353/eca.2017.0003.
- Del Negro, Marco, Michele Lenza, Giorgio Primiceri, and Andrea Tambalotti (2020). “What’s up with the Phillips Curve?” Working Paper 27003, National Bureau of Economic Research. doi:10.3386/w27003.

- Fernald, John G. and J. Christina Wang (2016). “Why Has the Cyclical-ity of Productivity Changed? What Does It Mean?” *Annual Review of Economics*, 8(1), pp. 465–496. doi:10.1146/annurev-economics-080315-015018.
- Feunou, Bruno and Jean-Sébastien Fontaine (2023). “Secular Economic Changes and Bond Yields.” *The Review of Economics and Statistics*, pp. 1–17. doi:10.1162/rest_a_01034.
- Fleischman, Charles A. and John M. Roberts (2011). “From Many Series, One Cycle: Improved Estimates of the Business Cycle from a Multivariate Unobserved Components Model.” Technical Report 2011-46, Board of Governors of the Federal Reserve System.
- Galí, Jordi (2011). “The return of the wage Phillips curve.” *Journal of the European Economic Association*, 9(3), pp. 436–461. doi:10.1111/j.1542-4774.2011.01023.x.
- Galí, Jordi and Luca Gambetti (2019). “Has the U.S. wage Phillips curve flattened? A semi-structural exploration.” Working Paper 25476, National Bureau of Economic Research. doi:10.3386/w25476.
- Galí, Jordi and Thijs van Rens (2021). “The vanishing procyclicality of labour productivity.” *The Economic Journal*, 131(633), pp. 302–326. doi:10.1093/ej/ueaa065.
- González-Astudillo, Manuel and Jean-Philippe Laforte (2020). “Estimates of r^* Consistent with a Supply-Side Structure and a Monetary Policy Rule for the U.S. Economy.” Technical Report 2020-085, Board of Governors of the Federal Reserve System. doi:10.17016/FEDS.2020.085.
- Grant, Angelia L. and Joshua C. C. Chan (2017a). “A Bayesian Model Comparison for Trend-Cycle Decompositions of Output.” *Journal of Money, Credit and Banking*, 49(2-3), pp. 525–552. doi:10.1111/jmcb.12388.
- Grant, Angelia L. and Joshua C. C. Chan (2017b). “Reconciling output gaps: Unobserved components model and Hodrick–Prescott filter.” *Journal of Economic Dynamics and Control*, 75, pp. 114–121. doi:10.1016/j.jedc.2016.12.004.
- Hasenzagl, Thomas, Filippo Pellegrino, Lucrezia Reichlin, and Giovanni Ricco (2022). “A Model of the Fed’s View on Inflation.” *The Review of Economics and Statistics*, 104(4), pp. 686–704. doi:10.1162/rest_a_00974.
- Hobijn, Bart, Russell Miles, James Royal, and Jing Zhang (2023). “The recent steepening of phillips curves.” Economic Letter 475, Chicago Fed Letter.
- Holston, Kathryn, Thomas Laubach, and John C. Williams (2023). “Measuring the natural rate of interest after covid-19.” *Federal Reserve Bank of New York Staff Reports*, no 1063.
- Jacobs, Jan P.A.M. and Simon van Norden (2016). “Why are initial estimates of productivity growth so unreliable?” *Journal of Macroeconomics*, 47, pp. 200–213. doi:10.1016/j.jmacro.2015.11.004.

- Johannsen, Benjamin K. and Elmar Mertens (2021). “A time-series model of interest rates with the effective lower bound.” *Journal of Money, Credit and Banking*, 53(5), pp. 1005–1046. doi:10.1111/jmcb.12771.
- Jones, Callum J., Mariano Kulish, and James Morley (2021). “A Structural Measure of the Shadow Federal Funds Rate.” *Finance and Economics Discussion Series*, 2021(064), pp. 1–40. doi:10.17016/FEDS.2021.064.
- Kahn, James A. and Robert W. Rich (2007). “Tracking the new economy: Using growth theory to detect changes in trend productivity.” *Journal of Monetary Economics*, 54(6), pp. 1670–1701. doi:10.1016/j.jmoneco.2006.07.008.
- Kiley, Michael T. (2020). “What can the data tell us about the equilibrium real interest rate?” *International Journal of Central Banking*, 16(3), pp. 181–209.
- Knotek II, Edward S. (2007). “How useful is Okun’s law?” *Economic Review*, 92(Q IV), pp. 73–103.
- Knotek II, Edward S. (2015). “Difficulties forecasting wage growth.” *Economic Trends*.
- Knotek II, Edward S. and Saeed Zaman (2014). “On the relationships between wages, prices, and economic activity.” *Economic Commentary (Federal Reserve Bank of Cleveland)*, pp. 1–6. doi:10.26509/frbc-ec-201414.
- Koop, Gary and Dimitris Korobilis (2010). “Bayesian multivariate time series methods for empirical macroeconomics.” *Foundations and Trends(R) in Econometrics*, 3(4), pp. 267–358. doi:10.1561/08000000013.
- Kozicki, Sharon and P. A. Tinsley (2012). “Effective use of survey information in estimating the evolution of expected inflation.” *Journal of Money, Credit and Banking*, 44(1), pp. 145–169. doi:10.1111/j.1538-4616.2011.00471.x.
- Laubach, Thomas and John C. Williams (2003). “Measuring the Natural Rate of Interest.” *Review of Economics and Statistics*, 85(4), pp. 1063–1070. doi:10.1162/003465303772815934.
- Laubach, Thomas and John C. Williams (2016). “Measuring the natural rate of interest redux.” *Business Economics*, 51(2), pp. 57–67. doi:10.1057/be.2016.23.
- Lee, Jaejoon and Charles R. Nelson (2007). “Expectation horizon and the Phillips curve: The solution to an empirical puzzle.” *Journal of Applied Econometrics*, 22(1), pp. 161–178. doi:10.1002/jae.928.
- Lewis, Kurt F. and Francisco Vazquez-Grande (2019). “Measuring the natural rate of interest: A note on transitory shocks.” *Journal of Applied Econometrics*, 34(3), pp. 425–436. doi:10.1002/jae.2671.

- Lubik, Thomas A. and Christian Matthes (2015). “Calculating the natural rate of interest: A comparison of two alternative approaches.” *Richmond Fed Economic Brief*, (Oct).
- Mertens, Elmar (2014). “On the Reliability of Output Gap Estimates in Real Time.”
- Mertens, Elmar (2016). “Measuring the Level and Uncertainty of Trend Inflation.” *The Review of Economics and Statistics*, 98(5), pp. 950–967. doi:10.1162/REST_a_00549.
- Mertens, Elmar and James M. Nason (2020). “Inflation and professional forecast dynamics: An evaluation of stickiness, persistence, and volatility.” *Quantitative Economics*, 11(4), pp. 1485–1520. doi:10.3982/QE980.
- Morley, James C., Charles R. Nelson, and Eric Zivot (2003). “Why are the Beveridge-Nelson and unobserved-components decompositions of GDP so different?” *Review of Economics and Statistics*, 85(2), pp. 235–243. doi:10.1162/003465303765299765.
- Morley, James C. and Benjamin Wong (2020). “Estimating and accounting for the output gap with large Bayesian vector autoregressions.” *Journal of Applied Econometrics*, 35(1), pp. 1–18. doi:10.1002/jae.2733.
- Peneva, Ekaterina V. and Jeremy B. Rudd (2017). “The Passthrough of Labor Costs to Price Inflation.” *Journal of Money, Credit and Banking*, 49(8), pp. 1777–1802. doi:10.1111/jmcb.12449.
- Pescatori, Andrea and Jarkko Turunen (2016). “Lower for Longer: Neutral Rate in the U.S.” *IMF Economic Review*, 64(4), pp. 708–731. doi:10.1057/s41308-016-0017-x.
- Primiceri, Giorgio E. (2005). “Time varying structural vector autoregressions and monetary policy.” *The Review of Economic Studies*, 72(3), pp. 821–852. doi:10.1111/j.1467-937X.2005.00353.x.
- Proietti, Tommaso (1995). “The beveridge-nelson decomposition: Properties and extensions.” *Journal of the Italian Statistical Society*, 4(1), pp. 101–124. doi:10.1007/BF02589061.
- Roberts, John M. (2001). “Estimates of the productivity trend using time-varying parameter techniques.” *The BE Journal of Macroeconomics*, 1(1), p. 153460051,014. doi:10.2202/1534-6005.1014.
- Sinclair, Tara M. (2009). “The relationships between permanent and transitory movements in U.S. output and the unemployment rate.” *Journal of Money, Credit and Banking*, 41(2-3), pp. 529–542. doi:10.1111/j.1538-4616.2009.00220.x.
- Stella, Andrea and James H. Stock (2015). “A state-dependent model for inflation forecasting.” In Siem Jan Koopman and Neil Shephard, editors, *Unobserved Components and Time Series Econometrics*, pp. 14–29. Oxford University Press. doi:10.1093/acprof:oso/9780199683666.003.0003.

- Stock, James H. and Mark W. Watson (2007). “Why Has U.S. Inflation Become Harder to Forecast?” *Journal of Money, Credit and Banking*, 39, pp. 3–33. doi:10.1111/j.1538-4616.2007.00014.x.
- Tallman, Ellis W. and Saeed Zaman (2017). “Forecasting inflation: Phillips curve effects on services price measures.” *International Journal of Forecasting*, 33(2), pp. 442–457. doi:10.1016/j.ijforecast.2016.10.004.
- Tallman, Ellis W. and Saeed Zaman (2020). “Combining survey long-run forecasts and nowcasts with BVAR forecasts using relative entropy.” *International Journal of Forecasting*, 36(2), pp. 373–398. doi:10.1016/j.ijforecast.2019.04.024.
- Taylor, John B. (2001). “A historical analysis of monetary policy rules.” In John B. Taylor, editor, *Monetary Policy Rules*, volume 31 of *Studies in Business Cycles*, pp. 319–347. University of Chicago Press.
- Wright, Jonathan H. (2013). “Evaluating real-time VAR forecasts with an informative democratic prior.” *Journal of Applied Econometrics*, 28(5), pp. 762–776. doi:10.1002/jae.2268.
- Wu, Jing Cynthia and Fan Dora Xia (2016). “Measuring the macroeconomic impact of monetary policy at the zero lower bound.” *Journal of Money, Credit and Banking*, 48(2-3), pp. 253–291. doi:10.1111/jmcb.12300.